HUMAN EYE DETECTION SYSTEM FOR RECOGNIZE EYE DISEASES USING IMAGE PROCESSING

Thesis submitted to College of Engineering and Technology of Srinivas University in fulfillment of the requirements for the Degree of

DOCTOR OF SCIENCE
IN
ELECTRONICS AND COMMUNICATION ENGINEERING

By

NANDHAGOPAL N

Reg. No. 19SUDSCS01

SRINIVAS UNIVERSITY

MUKKA, MANGALURU - 574 146, KARNATAKA STATE, INDIA

JULY – 2019

BONAFIDE CERTIFICATE

This is to certify that the Thesis Entitled "**HUMAN EYE DETECTION SYSTEM FOR RECOGNIZE EYE DISEASES USING IMAGE PROCESSING**" Submitted to Srinivas University, Mukka, Mangaluru, Karnataka State, India by **NANDHAGOPAL. N** for the Award of the Degree **Doctor of Science** in Electronics and Communication Engineering is a bonafide research work carried out by him. The Thesis has reached the Standard of the regulation for the degree and it has not been formed the basis for the award of any Degree, Diploma, Associate ship, fellowship are any other similar title to the candidate or any other Person(s).

Signature of the Director –Research
Dr.B.M.Praveen
Director –Research,
College of Engineering and Technology,
Srinivas University,
Mukka, Mangaluru 574 146
Karnataka State, India

ACKNOWLEDGEMENT

I wish to acknowledge several individuals who provided me with immeasurable help in the completion of this Thesis and degree. First of all, I derive immense pleasure in placing on record my deep sense of appreciation, gratitude and indebtedness to Prof. **Dr. P.Sreeramana Aithal**, Vice Chancellor, Srinivas University, Mukka, Mangaluru, for his all-round help in suggesting the problem, sustaining the interest, motivating, inspiring and extending valuable guidance for the successful completion of the present investigation. Also, numerous discussions I had with him have increased my knowledge.

I am happy for the love and support I have had from **Premadevi.R.**, my wife and **P.N. Lalithkishor.,** my son through the years of dreams, and making life truly exciting. I would like to thank my **parents** who have blessed me with great tolerance.

I would like to thank **Dr.B.M.Praveen,** Director – Research and Innovation Council of Srinivas University and Chief Coordinator of College of Engineering and Technology for his continuous support and motivation for completing my research work

Without you all, things would have so much harder. I am wholeheartedly grateful to **Sri. CA. A. Raghavendra Rao**, President, A. Shama Rao Foundation, Mangalore and also Chancellor, Srinivas University, Mukka, Mangalore, for encouraging me by providing all facilities to carry out this work. I wish to express my sincere thanks to **Dr. P. Srinivas Rao,** Vice- president, A. Shama Rao Foundation, Mangalore and also Pro-Chancellor, Srinivas University, Mukka, Mangalore, for their support.

Last but not the least; I thank the **Almighty**, who has made my life blissful. May his name be exalted, honored and glorified.

NANDHAGOPAL N

TABLE OF CONTENTS

LIST OF TABLES

LIST OF FIGURES

LIST OF ABBREVIATIONS

2D	-	Two-Dimensional
AHE	-	Adaptive histogram equalization
ASIC	-	Application Specific Integrated Circuit
CHT	-	Circular Hough Transform
CLAHE	-	Contrast limited histogram equalization
COG	-	Center of Gravity
CPU	-	Central Processing Unit
CT	-	Computer Tomography
EDA	-	Electronic Design Automation
EOG	-	Electrooculography
FIFO	-	First In, First Out
FPGA	-	Field Programmable Gate Array Gaussian Filter
GUI	-	Graphical User Interface
HDL	-	Hardware Description Language
HE	-	Histogram Equalization
HT	-	Hough Transform
IDO	-	Integro-Differential Operator
LoG	-	Laplacian of Gaussian
NIR	-	Near Infrared
NIR	-	Near infrared version
NMS	-	Non-maximum suppression
PC	-	Personal Computer
PET	-	Positron Emission Tomography
PLL	-	Phase Locked Loop
RANSAC	-	Random sample consensus
RED	-	Ridge Energy Detection

ROI	-	Regions of Interest
ROM	-	Read Only Memory
RTL	-	register transfer Level
SDRAM	-	Synchronous Dynamic RAM
USB	-	Universal Serial Bus
VOG	-	Videooculography
VW	-	Visible Wavelength

ABSTRACT

An implementation of a real-time system on an FPGA board to detect a human eye is the main motive of this work. This proposal is a process, to identify the eye position in the given image. Eye detection is one in all the applications in image process. This is very important in human identification and it will improve today's identification technique that solely involves the eye detection to spot individuals. This technology is still new, only few domains are applying this technology as their medical system. This system is focus on four major parts of preprocessing phase which are image enhancement using median, Gaussian filtering, threshold process, morphology dilation and the sobel filter to detect eye region. This system used in medical image database. Original image is filtered by median filter to remove noises present in original image. Proper threshold is applied on filtered image to separate the pupil region. Here I used threshold value is 30. Dilation process is involved to remove extra eyelashes and eyelids. Finally Sobel filter has given clear pupil region. Finally, the graphical user interfaces is designed to display the output image in Matlab. The proposed hardware architecture is designed using Verilog HDL and implemented on an Altera development board for prototyping and logic utilizations are compared with Existing work. The overall setup included Cyclone II FPGA, image processing algorithm, pupil region computation. Experimental results proved the accuracy and effectiveness of the hardware real-time implementation as the algorithm was able to manage various types of input video resolutions. All calculation was performed in real time.

CHAPTER 1

INTRODUCTION TO HUMAN EYE DETECTION SYSTEM

This chapter discusses the overview of Human Eye structure, different Eye Tracking technique, objective and scope of the work.

The eye detection or eye tracker is the sensor technology to permit the machine to know distinctly the focus of our eyes and regulates our consciousness, drowsiness, attention, presence and other fatigue states. This intelligence shall be used for acquiring the deep accurate and understanding in to consumer behavior or to model the new interfaces across diverse devices. When comes to eye tracking in the real world the three factors comes to our mind that is construe the human behavior, allows hand free interplay, and user experiences of the humanized user interfaces. By adjoining the eye tracking (Katarzyna Harezlak, A. et al., 2014) with other input modules, for instance keyboard, mouse, and voice. Employing the eyes as a pointer at a screen the methods of eye tracking facilitates interoperation with nodes and other gadgets when the user unable to resort their hands as a input form.

1.1 BIOMETRIC TECHNOLOGY

It is a measurement and statistical determination of identifying people's distinct physical and behavioral traits. The biometric technology (K.W. Bowyer et al 2008) is utilized for recognition, controlled accessing and to sense the individuals when they are under surveillance. The bare ground of biometric authentication is that each person can be precisely sensed by his or her unique behavioral factors. The term Biometric is originated from the Greek work where Bio is human and Metric is to measurements. The two important types of

biometric technology identifiers are depend on either physiological factors or attitude characteristics. The Biometric technology works by the factor of authentication by biometric verification which turns in to increasingly regular in corporate organizations. Some biometric methods such as quantifying a person's gaze (Ryo Takahashi et al., 2018) which can drive with indirect contact with the person is being authenticated. The components of biometric devices include,

a) The gadgets for reading or scanning device to store the biometric factor being authenticated.

b) To convert the scanned data in to regularized digital format and to compare the actual points which are observed and stored data.

c) Considering the database for securely storing the biometric data for the usage and comparison in future.

The Biometric data can be possessed in a centralized database though new biometric implementations often relies on procuring biometric data locally and according to that the biometric data is cryptographically hashed as a result so the authentication and identification could be attained without open access to the biometric data itself . Figure 1.1 displays authentication of an eye.

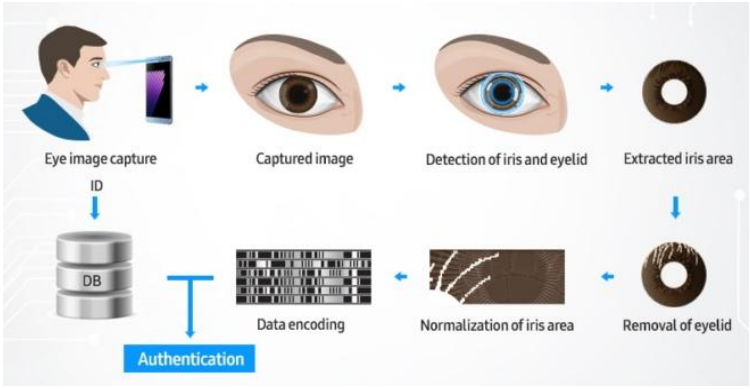

Figure 1.1 Detection and Authentication of an Eye

In the recent years, the field of automation to identify humans multiplied with emergence of diverse types of biometric systems, viz hand, iris, face, tone, fingerprint that use pattern recognition, processing of image, sensors, and PC [Faundez-Zanuy, 2006], [Jain and Kumar, 2012]. The above mentioned structure certify and validate those through their biometric features (physiological or behavioral) for safety measures and to control access. The validation or verification systems stand on biometrics locates the user's uniqueness on the fundamental that several behavioral or physiological characteristics are eccentric for every person and consequently, validate absolutely. For instance, the iris-patterns of an individual vary from person to person even for the like twins; also, irises in both left and right side of the eye of the same person are different. Besides, the iris arrangement remains sturdy throughout the life unless a damage occur to the eye. On contrary of biometric system, conventional procedure of validating individuals are subject to be biased as the document carried like identification card, license for driving, and other authorization documents can be lost, stolen or forged ; and (b) login credentials of a managed system are unsecured techniques as it may be forged, lost or difficult to recall from memory. Biometric automated system like iris

recognition or fingerprint are with success utilized in many widespread applications, increasing dependableness, comfort for users and safety [Jain and Kumar, 2012]. Iris recognition system is a cybernated system to facilitate the identification of individual on the basis of iris arrangement by comparing the iris-patterns [Ross, 2010]. Being the most secured and reliable technology, the iris recognition is deployed in the areas high level security, likely countering terrorism or control information admittance among the users. In the course of iris recognition, the region of iris is extracted by the iris segmentation system from the eye picture. In addition, the iris portion obtained is further removed in a rectangular chunk with steady sizes. Finally, the feature extraction method extracts iris features to program the exclusive pattern of the iris in the form of biometric template. The iris model produced is referred to earlier iris templates to detect a counterpart on the basis of match threshold.

Figure 1.2 exhibits the two major operations implicated in the use of biometric systems.

(a) Admission or conscription step and (b) endorsement step (verification). The first step is a process of constructing and storing the biometric models in the model store (database), whereas the assessment process (template matching) is done in second step apart from template creation. A client can enroll only on one occasion while acknowledgment is made every time as a safety check.

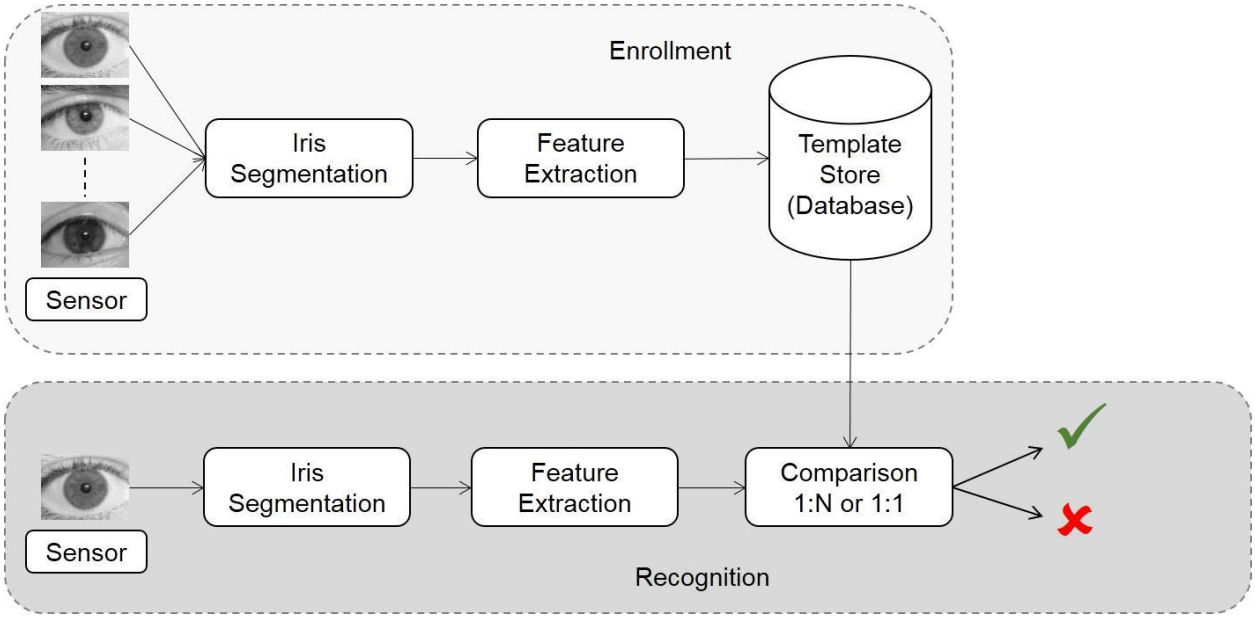

Figure 1.2 Operations in an Iris-biometric system

Biometric systems perform two types of detection tasks [Faundez-Zanuy, 2006], [Bowyer et al., 2008], [Liu-Jimenez et al., 2011]: (a) recognition; and (b) validation. These recognition tasks are treated as basic approach of operation in biometry. Without providing the user credentials (example, identification number), the biometric system explores the user from existing models in identification task. The keyed in biometric data is judged against with *N* models saved in biometric database. As a contradiction to recognition task, authenticate mode compares the input biometric data consisting of ID number (refers to the model in biometric database) with the biometric database. The authentication process in a biometric system can be either (a) online or (b) offline [Liu- Jimenez et al., 2011]. On-stream authentication entails contact with central databases to way in biometric data. While in offline, biometrics stored with special biometric identity numbers. The on-stream authentication technique transacts with serious protection and privacy matters, as the system and the central database disseminate with each other. The risk of attack,

stealing or altering in the system is more in online authentication. Henceforth, offline systems are advocated, as the data is secured through personal biometric token.

1.2 HUMAN IRIS

The Iris in human being eyes is a thin circular arrangement responsible in limiting the diameter and the pupil size to control the luminance towards reaching the retina. The iris color is either blue or brown whereas the pupil in the centre is circular black spot and enclosed by the white sclera. The cornea is utterly clear so it is invisible except the gloss luster it gives the eye. The iris determines the eye color and it comprises of two layers the front and the beneath the front layer is pigmented fibro vascular also termed as stroma and the underneath layer is pigmented epithelial cells. The Iris is bifurcated as two regions,

a) The border of the Pupillary area figures the border line of the pupil.

b) The ciliary area is the outer region which prolongs to the source in the ciliary body.

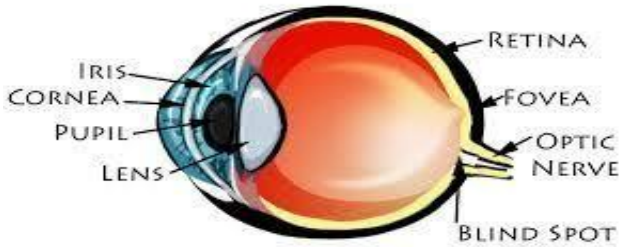

Figure 1.3 Human Iris

In humans the color of iris is commonly blue or brown whereas the pupil is encompassed by the white sclera with a circular black spot in the middle. The cornea is utterly clear so it is invisible except the gloss luster it gives the eye. Figure 1.3 shows the human Iris..

1.2.1 Structure of an Eye

The importance of an iris based automatic identification process is well understandable if the iris structure is perceived clearly. Figure 1.4 shows the iris portion in a captured eye picture. The iris encircled by pupil, eyelashes, sclera, and eyelids, is planted between pupillary and limbic boundaries.

Figure 1.5 illustrates the ball-like architecture of human eye. The sclera, an outer coat of Human eye, is enclosed by a layer known as conjunctiva. Cornea, the frontage part of the eye, is transparent and iris is at the rear part of cornea. Being the colored portion of the eye, the iris holds the pupil with a hole at its center. The iris plays significant role in human being eye as the muscle in the iris controls the dimension of the pupil region.

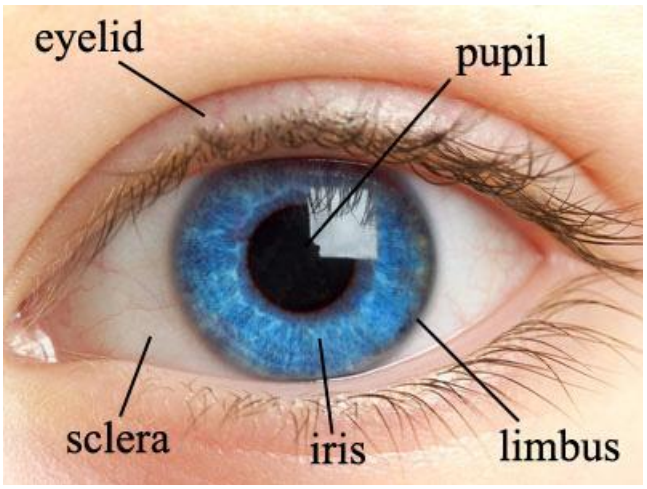

Figure 1.4 Parts of a Human eye image

The pupil size determines the brightness of light entering into the eye. The pupil size expands and shrinks during the dim and brilliant light, respectively. The light passing through the lens aids to spotlight the image/sunshine. The light passes through cornea, pupil and lens and then falls on back wall of the eye called retina. The sensitive high-density cells termed as macula are located in the retina. The transformation of light into electrical signals is carried out by photoreceptor cells in the retina and these signals pass through optic nerve for image formation in the brain.

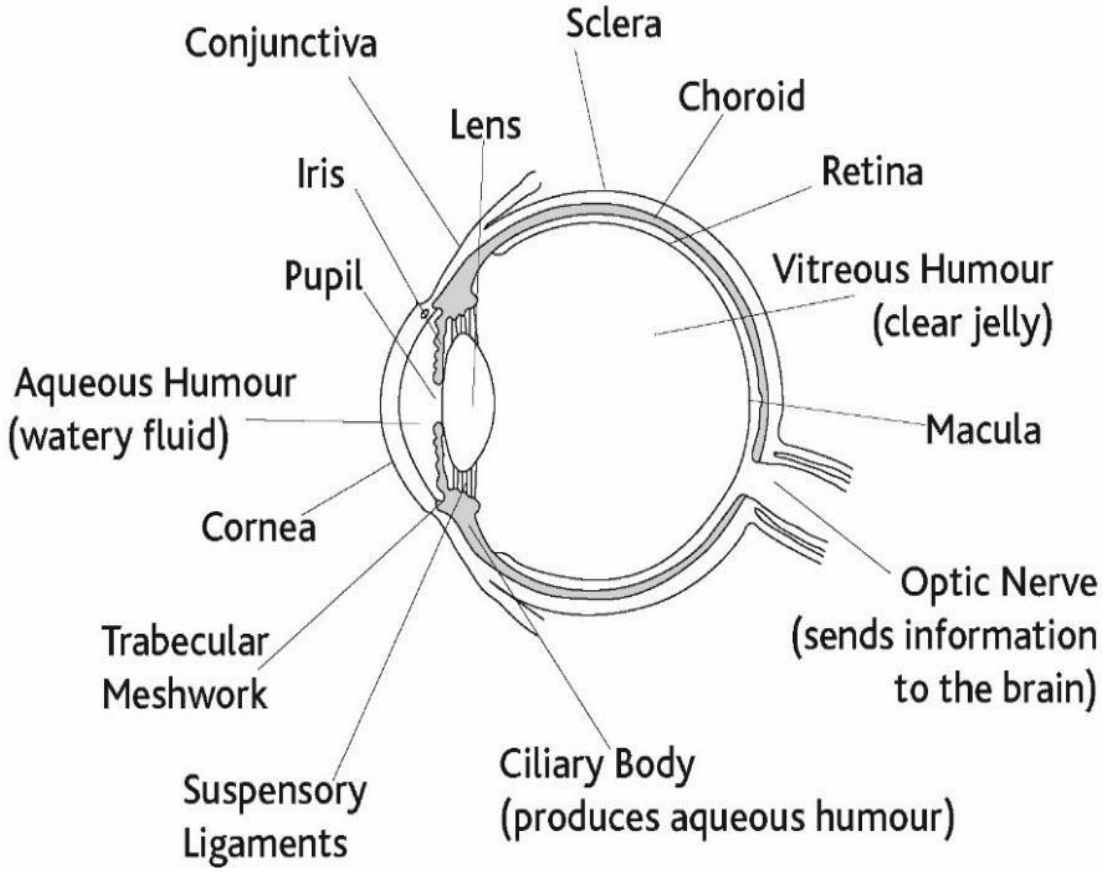

Figure 1.5 Architecture of Human Eye

The vitreous humour is present between the retina and lens in the course of which the light passes to the retina. The aqueous humour formed by

ciliary body determines the pressure of eye and fills up the region between cornea and the lens. The choroid region beneath the retina supply blood to the retina cells.

1.2.2 Evident Features of Iris

The lossely woven soft muscle, stroma [Muron and Pospisil, 2000] and its density decides the color of the iris. The apparent pattern of the iris shows different characteristics. Figure 1.6 depicts the iris separated into the pupillary area and the ciliary area. The collarette is the zigzag border line from the pupillary portion to ciliary area that is dense in nature. Figure 1.7 shows few noticeable features of human iris in identifying a person. These features control pupil size, collarette and pigment frill.

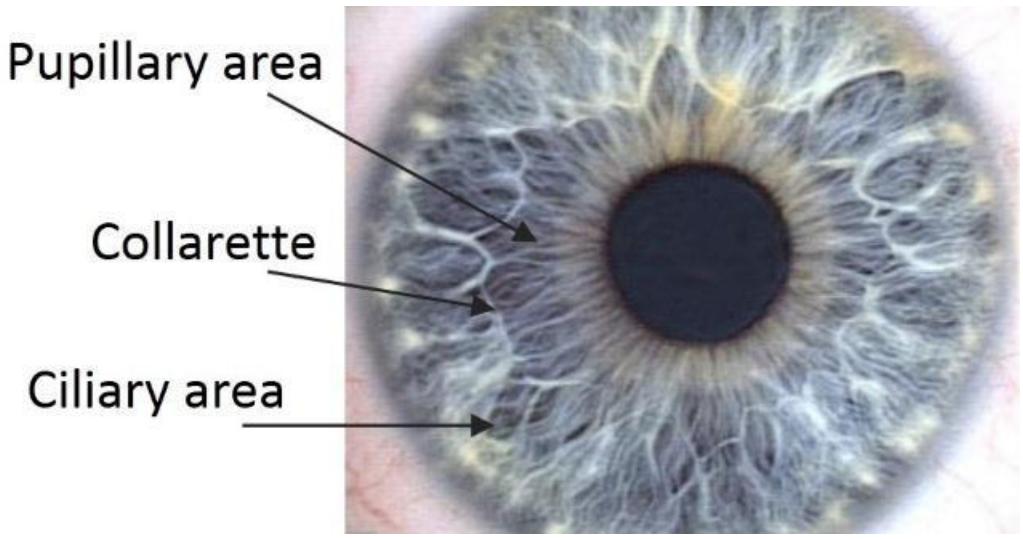

Figure 1.6 Picture of human iris

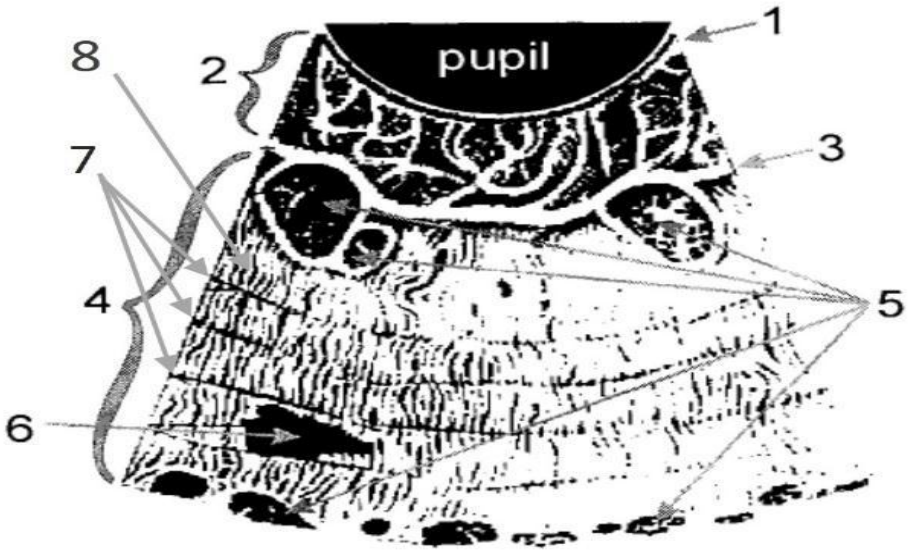

Figure 1.7 Noticeable features on surface of the human iris

1) Pigment frill, 2) Pupillary area, 3) Collarette, 4) Ciliary area, 5) Crypts,

6) Pigment spot, 7)Concentric furrows, 8) Radial furrows.

The pigment allied features appear as crypts and pigment spots. The dark colored crypts show up as sharply demarcated excavations close to the collarette or/and the periphery of the iris. The iris region in the crypts is thin. The pigment spots termed as moles and freckles that come out in the ciliary portion are (nearer to) black colored random concentrations of pigment cells. [Muron and Pospisil, 2000].

The contraction furrows which direct the pupil size are radial and concentric. The radial furrows originate nearby the pupil end up in the ciliary portion through the collarette. The circular emerge between the ciliary portion and near the periphery of the iris. The border between the pupil and the iris is the pigment frill. The iris color (ranging from blue to black) is determined by the quantity of pigment and the dense of the iris muscle .

1.3 IRIS RECOGNITION

The biometric identification in iris recognition system deploys mathematical pattern techniques to explore the iris structures. There are many algorithms based on iris pattern recognition techniques proposed by authors in that the author John Daugman, 2002 evolved and obtained patent for the algorithm to conduct a iris recognition. The classification of algorithms based on two factors.

a) Visible wavelength.

b) Near infrared (NIR).

The concentric furrows are circular and concentric with the pupil shown in Figure 1.8.

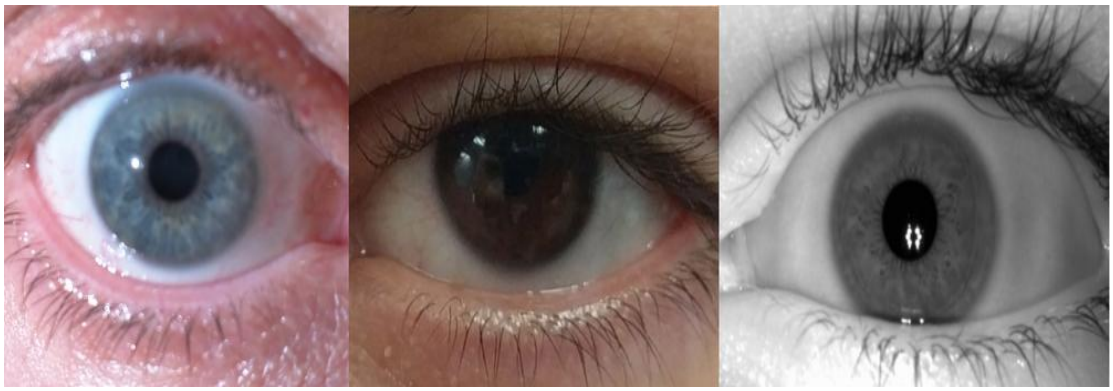

Figure 1.8 Iris Recognition

1.3.1 Advantages And Disadvantages of Iris Scan

The dominance of iris scanning is the reliability and accuracy. The prediction of accuracy and reliability is to be ten times accuracy than fingerprinting which poses around 1 in 100,000. The fingerprints are consistently exposing and conformable to the damage and the pupil around the

eye is intrinsically guarded by the cornea (the transparent eyes in the front layer) and the model seems to sustain integrally remains same for decades. Unlike pattern recognition the fingerprint scanners also need direct touch and requires transparency. To scan the iris the method of processing should be done hygienically and securely at a little farther from the eye. The disadvantage of scanning the iris includes more preliminary cost.

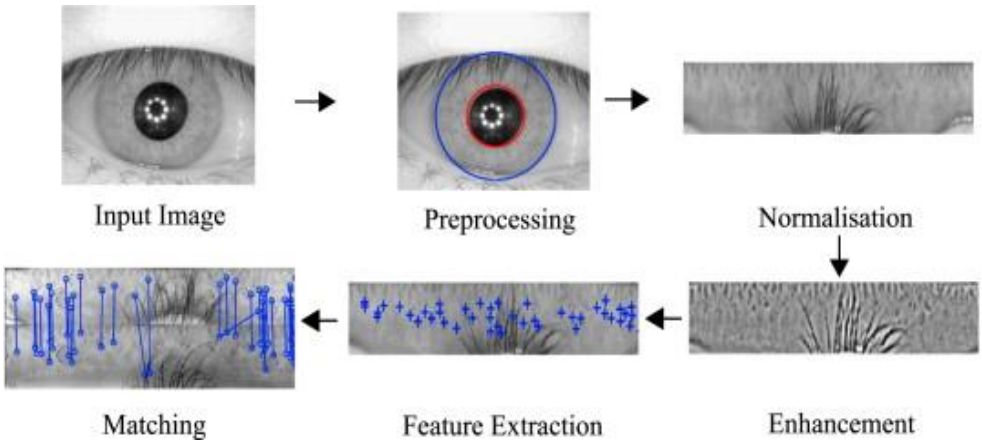

Figure 1.9 Steps of Processing using Iris Scanner

Figure 1.9 shows the steps involved in iris scanning. A digital camera acts as the iris scanner. Iris scanning employs both infrared and visible light to snap a high quality contrast picture of persons pupil around the eye. In the short infrared light when look at the person's pupil in the eye is black and it facilitates the system to separate the pupil and iris. The rear end of camera in the scanner automatically focuses or resort the mirror in the computer to ensure that the eyes are positioned exactly. The eyes are kept 3 to 10 inches away from the camera. An image while clicked using a mobile the system resides are,

a) Pupil edge

b) Eyelids and eyelashes

c) Pupil center

d) Iris edge

1.4 EYE TRACKING APPROACHES:

The research in tracking the eye position (R. Jacob,1995) and some eye movements has implied in the article (A. Duchowski,2002)which are mostly in psychology shown in Figure 1.10. Though pursuant to the evolvement of eye tracking techniques, during the past decades, the broader exploitation of eye tracking methods and its characteristics has turned viable (Leng Donga et al., 2016). For over the period of time the methods of such information gathering have been influentially changed. In fact the most precise or exact and at the same time the invasive methods are depends on a contact lens furnished with images. The visual activity sheds off rapidly from the retina to the visual periphery. The optimal visual activity has found in a parafoveally area of 1-5 degrees from the fovea.

In order to process the visual eye I shall shift the eye balls such that I aim it in such a way that I procure the highest resolution which is in the fovea. The anatomy of the individual person's eye ball movement relies on the eye muscles.

a) Muscles of the Inferior rectus

b) Muscles of the Lateral rectus which lies opposite symmetrically.

c) Muscles of the Superior rectus.

d) Inferior oblique muscle that is adapted from the movement of eye balls. Typically an eye fixation takes time about .5 seconds commonly

the eye processes all visual data driven during a fixation and started the execution of the any action. In case any execution required. When more data is present then another fixation is required. The techniques of eye tracking are,

e) Electrooculography (EOG)

f) Contact lens techniques

g) Limbus tracker

h) Video based pupil

i) Corneal Reflection

Figure 1.10 Eye Image Recorded with and without IR Filter

Table 1.1 depicts eye-tracking variables which consider a fixation duration, saccade duration and relative pupil detection

Table 1.1 Measures in Eye-tracking

Variable	**Description** (measurements are in milliseconds)
Fixation duration	Eye fixation duration
Saccade duration	Saccade Duration
Relative pupil dilation	Comparative change in diameter of the pupil region

Table 1.2 Eye-tracking Technique Characteristics

Technique	**Comments**
Contact lens	Very intrusive, but accurate and fast
Limbus tracking	Depends on the camera and vertical accuracy is low
Pupil tracking	Depends on the camera and recognition of the pupil region is hard
Depend on Image	Depends on the camera and requires training
Pupil-glint	Depends on the camera and tolerates head motion

Table 1.2 shows the traditional different Eye tracking Techniques which are Contact lens, Pupil and Limbus tracking, Image-based and Pupil-glint.

1.4.1 Electrooculography

The Electrooculography is one among the techniques of eye tracking methods (Amer Al-Rahayfeh et al., 2013). Figure 1.11 shows the electrooculography and it exploits the corneo-retinal method which exists amidst front and rear of human eye. The corneo-retinal quantified with the exploitation of physical electrodes presented in the surrounding of the eye. While the eye spin towards the person or any things it will turns in to more positive on the other side the rotation in reverse direction becomes partial negative. The electrooculography method is view as connectively cumbersome and inopportune for the entities.

Disadvantage

The restriction of this use solely for the laboratory essays application without the viability on a day-to-day basis and gadgets scenarios.

Principle

The eye operates as a dipole - anterior and posterior poles which are positive and negative, respectively. (Dan Witzner et al 2010).

Left Gaze: Cornea move towards the electrode which are far outer canthus of the eye in left that results in negative trending transition in the stored potential variance.

Right Gaze: Cornea move towards the electrode which are far from inner canthus of the eye in left that results in positive trending transition in the stored potential variance.

Figure : 1.11 Electrooculography

1.4.2 Contact Lens

The most precise and most intrusive techniques of eye tracking are contact lens which provided with mirrors. It is being embedded in the eye a slim copper wire is presented in the annulus of the silicon and the contact lens is associated with optical device, similar to a magnetic coil that scales the difference of the electromagnetic field while an individual spins the eye balls. Though the complexness of method scales the experiment to be restricted to 20 minutes during the unconsciousness of eye curbs the employment of method.

The method that comprises identifying one or more patterns on the modeled contact lens on the eye of the individual person. The direction of the eye ball in the person's eye is evaluated based on the detection of the one or more pattern elements. The modeled elements could be detected using a single pixel sensor. The pattern which contains for an instance the pattern may be having a different form of colors.

Advantages

The advantage of availing contact lens for tracking the eye and viewing the information of 3D in that they are more pragmatic that is miniature, small

weight, and portable. When compared to other peripheral devices the contact lens is mainly employing for 3D viewing information.

a) Furthermore the contact lenses can accord highly precise tracking eye information in moderate cost. For an instance when using contact lenses for the eye gazing or tracking the performance function will be good than the one that can be accomplished along with based on camera eye tracking methods.

b) When compared to camera based solutions which entails established high resolution cameras, contact lenses facilitates for giving at low cost solutions which make them more appropriate for customer products.

c) In the diverse embodiments, a amalgamation of marker and marker less based eye tracking methods availing contact lenses furnish interoperate with entities such as video game, projected virtualized user interface. And augmented reality user interface.

d) In one embodiment the person can be outfitted with a magnetized contact lens which may be captured by one or more electromagnetic sensors positioned for a video game console.

1.4.3 Contact Lens Techniques

There are two types of techniques employing in contact lens which are as follows.

a) Sclera coil

(b) Sclera Mirror

a) Sclera Coil

The sclera search coil is relied on the current flow through induction loop and it is a fine temporal resolution (J.R. Parker and A.Q. Duong et al 2009) In sclera the supreme spatial resolution is less than 10arcsec which is not comfortable as well as easily adapted for the animal research.

The sclera lens also called sclera contact lens and it is a colossal contact lens which rest on the sclera and poses s tear filled vault over the cornea.

The sclera lens are designed for to handle a diverse of eye situations most of which do not reciprocate to other forms of treatment. Figure 1.12 depicts the modern sclera lens are built up of a highly oxygen permeable polymer which are special in their framework such that they suits on to and are assisted by the sclera portion. The reason of the exclusive positioning typically relates to a particular patient whose pupil can be much sensitive to assist the lens instantly. While comparing to corneal contact lenses the sclera coil swell outward more. The area between the cornea and the lens is replenished with artificial tears. The semi liquid which is formed in a tiny elastic reservoir, complies with the inconsistencies of the deformed cornea which empowers vision to be retained suitably.

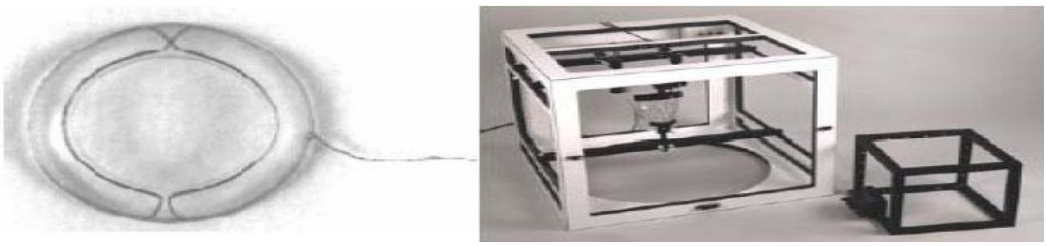

Figure 1.12 Sclera Search Coil

b) Sclera Mirror

It is a suction cup mounted mirror that reflects optical reference beam. The important inertial mass better the good temporal solution the moderate spatial accuracy is 1 degree which is exquisitely inopportune requires anesthesia and the detailed sampling epochs solely head immobilization required. Sclera mirror is a prototypical lens dated back early 1880's. These sclera lenses are modeled by using a substance to make a mold of the eye. The contact lenses will be shaped to comply with the mould. In previous sclera's were not contain oxygen preamble which gravely limited the amount of oxygen imparted to the cornea of the wearer.

The sclera of contact lens yields surged again after oxygen permeable things. It was firstly exploited in rigid gas permeable in short RGP lenses turned in to available for other users. The latest evolvement of digital imaging methods has permitted some providers to estimate and testify the fitness of great accuracy. A multitude of sclera fabrications has also posed contact lens include sclera lenses with practiced points of adjustment available. So that every lens could be adapted through a lathe to be better match the contours of the single eye.

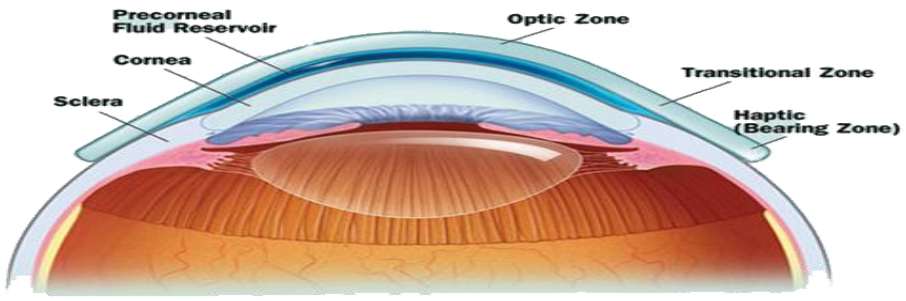

Figure 1.13 Sclera Mirror

The Figure 1.13 Sclera mirror shows a prototypical lens dated back early 1880's. These sclera lenses are modeled by using a substance to make a mold of the eye. The contact lenses will be shaped to comply with the mould. In previous sclera's were not contain oxygen preamble which gravely limited the amount of oxygen imparted to the cornea of the wearer.

1.4.4 Limbus Tracker

Limbus tracker depends up on the differential reflectance of sclera and the iris and it is a high temporal resolution which is less than 1000Hz, exhibits poor spatial accuracy and it has a very limited operating range that is 10 degree and horizontal EM's only. In limbus tracking there are two bare approaches for POG computation (Kenneth Holmqvist et al 2011). The first is relied on 3D model of the rotations of eye ball and calculation of ray emission from eye's central point. Then, POG is computed as ray's dividend. The limbus tracking comprises of three common steps performed on each eye image frame which are as follows,

a) Image preprocessing

b) Feature detection

c) Ellipse fitting

a) Processing an Image

In image processing filtering each frame is essential so that blur or noise in the image is alleviated while restoring as much as viable. As like Starburst algorithm (Dongheng Li et al 2005) the process of eye image in the camera along with Gaussian filter embark to mitigate the blurred portions of image. The Gaussian filters are beneficial in mitigating noise sensitive to any

algorithm that exploits gradient information. In addition the dividable nature of 2D Gaussian allows effective implementation. Mostly the noise in video or image begets using OTS cameras is because of lossy compression. The lossy compression algorithm shall be anticipated to pose some sensitive artifacts in the motion video. As number of artifacts is empowered the videos could turn in to more compressed. The algorithms I have used here specifically became to permit artifacts as long as they just simply noticeable. It is commonly known as merely noticeable difference.

The image processing methods are typically much sensitive to the artifacts than the human eye.in most shortened schemes bifurcate the image in to tiny blocks and perform a conversion of each block separately. The elements within the block are rounded. As adjacent blocks are different Iare left with borders with small edges. There are inopportune borders poses wise gradients that cover the sharp gradients with the edges of the desirable factors. The Gaussian filter smoothens the picture removing highly localized gradients the gradients which are wiser are blurred but not ousted. In starburst the complete gradient picture has not profiteered instead calculated during traits detection. It was conceived that processing a mitigated computation. Though gradient assessing is barely a driven one which is analogous to Gaussian smoothing and evolves with the derivative of the Gaussian. I have chosen to facilitate implementation by computing the gradient.

b) Feature Detection

In limbus tracker, two steps are carried out for feature detection. Identical to starburst algorithm, the points borne by the features in first step comes from the starting seed doing and ends the ray as it comes out from a dark region. In the second step the feature detection method is iterated with rays

back out from the side features towards the seed point. It tends to surge the multitude of feature points on the pupil around the eye. The light continues until the gradient length equals with the ray bearing fixed threshold transcends.

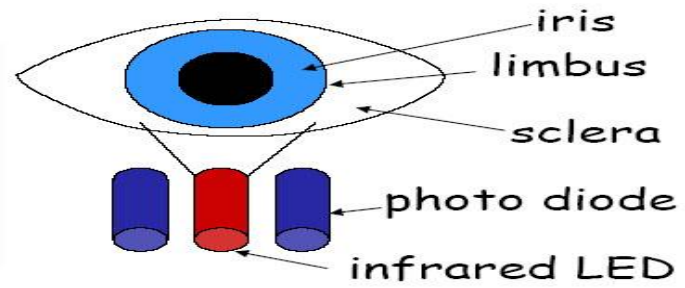

Figure 1.14 Feature Detection

Figure 1.14 feature detection methods are somewhat effective in fewer lighting conditions but its sensitivity during specific (chosen) fixed threshold is quite setback. Recognizing a perfect threshold is amazing as thresholds when increased are quite useful for gleaming light in the lower thresholds in dark light.

c) Fitting the Ellipse

The starburst algorithm exploits the random sample consensus (RANSAC) model to suite the ellipses to the feature points. It was selected because of the tolerance of the outliers. The outliers are typical in the witnessed feature sets. Here random ellipses are created in a same manner but instead of assessing it based up on the factors of real image. The proposed algorithm that is starburst is accomplished using the ellipse fitting. The starburst ellipse fitting is inadddtion becomes bottleneck to distinguish ellipses that unbiased the span of pupil. The feature points could be divided in to one of two similar sized bins.

The feature point dividing permits the creation of ellipses in to two sets which are,

a) One relates to either iris or sclera limbus

b) The next relates to either pupil or iris boundary

An eye tracker which permits the use of calibration coefficients between sessions instead of recalibrate the every session is preferable.

1.4.5 Determining The Eye Positioning

A group of eye archives procured from an eye tracker in context to the latest image processing techniques is aimed to evaluate the successive positions of the eye and the direction of look or gaze (L. Young and D. Sheena, 1975). The image based eye identification and sensing is a wide subject and variance methods are evolved to abstract pupil from an eye image. In the literature it is divided as appearance and feature based.

i) Appearance Based Identification Method

In appearance based method the factors are computed directly based on the occurrence of eye imagery and assesses the points of gaze by exploiting a functional mapping to the region of groups.

ii) Feature Based Methods

The feature based methods may review an image of an eye to analyze its traits e.g. the pixels of dense black portion that relates to pupil region or iris. Figure 1.15 shows the eye movements in the infrared light application makes possible the process since it augments the contrast between the two elements of an eye. Many of this kind of methods avail an image segmentation during that

processing an image has been translated in to grayscale image and then to threshold to accomplish an evident image wherein the pupil around the eye is implied by a dense region. A suitable threshold value abstracts the portion pertained the pupil. The center of dark area is assessed middle point of the iris.

Figure 1.15 Variance of Eye Movement

The process in which the dark region is ascertained in to white one may also detect. Sometimes when a picture encounters poor resolution and more contrast , the standardization of the histogram image is employed. This process augments the differences from the determined image by permitting the distinguishable details slightly apparent. The various approaches are presented by the Timm and Barth (2012) availed the snap gradients and a derivational function of the vector field permitting to model the connection between the determination of relative position of an image gradients and center of the eye. It is relevant to locate where almost all gradients vectors touch.

1.5 VIDEO BASED PUPIL

One among the most popular methods in tracking an eye is tracking the pupil of an eye based on video, shortly known as (VOG) which records the eye rotations in terms of digital video cameras shown in the figure 1.16. The

process of eye tracking captures consequent images. The eye locations and rotations are decided by utilizing the images captured. In addition the position of the eye camera determines clarity in the recording.

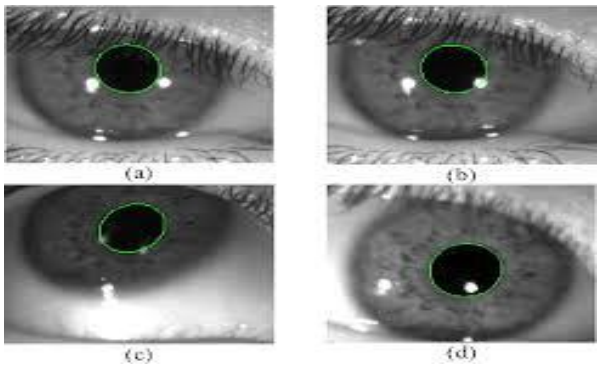

Figure 1.16 Video Based Pupil

The VOG eye detectors are less invasive as don't entail direct contact with eyes. However this method has a bottleneck and is very expensive as many algorithms that evolved in image processing, and feature detection has turned out to be accordable for the broader research fraternity. The resolutions of images determine the accuracy of detecting the eye.

1.6 CORNEAL REFLECTION TECHNIQUE

Figure 1.17 corneal reflection technique is relies on the real time image processing to identify and localize pupil around the eye and corneal reflection. The corneal reflection technique required the IR Illuminator which is to sense the data happening in the ambience. The temporal resolution relies on the eye camera frame rate such as 60, 120, 240, 500 HZ). The corneal reflection moderates the spatial accuracy which is less than 1 degree. Here the bright pupil is bit robust versus dark pupil around the eye in the daylight. In corneal reflection technique there are two factors which are as follows,

a) Head mounted

b) Remote optics

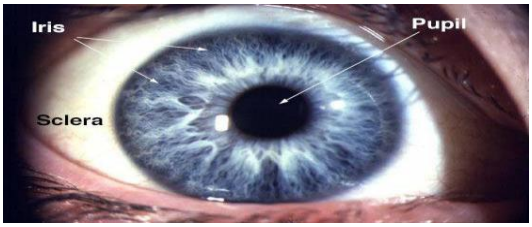

Figure 1.17 Corneal Reflection

1.7 APPLICATIONS OF EYE TRACKING

To track an eye, position of an eye is recorded and movements ries on optical detecting of video based analysis or corneal reflections so that creating the examination of eye movements and gaze gestures or positions in both 2D and 3D ambience viable. The eye tracking assists to review the human processing of visual data for interplay and diagnostic applications. The eye trackers were earlier the vast and cumbersome. Eye trackers scale attention, interest which poses a great method for human behavior research. The following eye tracking applications are most typically used which are as follows,

a) Academic and scientific research

b) Market research

c) Psychology research

d) Medical research

e) Usability research

f) Packaging research

g) Pc and gaming research

h) Human factors and simulation

Figure 1.18 Application of Eye Tracking

The image enhancement stage includes resolution and contrast enhancement. These images suppress speckle and imaging of spectral parameters. Thus the medical image is reborn into a typical image ignoring noise film artifacts and labels. Preprocessing of an image signifies that an equivalent texture sort might need images of exceptional signal intensities for various applications of eye tracking shown in Figure 1.18.

1.8 PREPROCESSING OF EYE IMAGE

In preprocessing and enhancement stage, the quality and information content of image is improved by manipulating contrast, reducing noise in the image, background removal, sharpening the edge and filtering processes. Before the ultimate image generation, some additional techniques medical image process of coherent echo- signals. Preprocessing functions are those

operations before the most knowledge analysis and data extraction, and are categorized as radiometric and geometric corrections.

Image process and improvement stage is that the simplest classes of medical image process. This stage is employed to reduce noise in images, to highlight edges, or to display digitized images. Further certain additional techniques are deployed to process medical images using coherent echo signals before generating the image.

Image enhancement methods inquire about the improvement in visual appearance of images from Positron Emission Tomography (PET), Computer Tomography (CT) scan, Magnetic Resonance Image (MRI). The improvement activities require label and film artifacts to be removed, image filtering. This part enhances the evenness towards piecewise-homogeneous area as well as reduces the outcome of edge-blurring. The Traditional Enhancement techniques use filters of kind viz Prewitt edge-finding, Gaussian, Gabor, Median, and Low pass.

1.8.1 Segmentation

The demarcation of a picture separates the image into meager regions of comparable attribute. The intention of slicing the picture to smaller images is to extract necessary options like outline, interpretation from the picture by the machine in an exceptional way. The demarcation of brain tumour from resonance pictures is a crucial and overwhelming task of the medical examiners. In brief, segmentation determines the ROI (ROIs)- mark the pixels of affected area in an image.

In digital image processing numerous segmentation strategies are adapted. The most common being : (i) region-growing segmentation, (ii)

template matching, (iii) texture segmentation and (iv) amplitude Thresholding. It is important to detect edema and necrotic tissues in brain tumors. Such algorithms divide the brain pictures into 3 classes (i) constituent primarily based (ii) Texture based and (iii) Structural based.

Natural pictures encompass an amazing variety of visual models generated by terribly various random methods in nature. The goal of image understanding is to analyse degree of association between the input image and its constituent models or patterns. Depending on the kind of patterns that a task is inquisitive about, the parsing problem is resolved respectively

1) Image segmentation - to process colored, grey and texture regions.

2) sensor activity grouping - to process point, curve, and general graph

3) Object recognition - to analyze text and objects.

In other way, segmentation is the method of separating a digitalized image into slices of various sets of pixels. The aim of eye demarcation is to alter and/or modify the illustration of a picture as one thing with lot of significance and accessible picture to investigate. Image segmentation is usually familiarized to identify objects and restrictions (lines, curves, etc.) in images. The effect of image segmentation may be a band of regions so as to conjointly band together to form the complete image, or a collection of contours taken out from the segmented image. All of the pixels in every region is analogous with several feature like texture, intensity, or color. Segmentation algorithms perform hinges on any one of the following properties on intensity values.

Discontinuity: Partitioning a picture supporting the changes in intensity including edges

Similarity: Partitioning a picture into group identical with a collection of criteria defined previously.

Four common methods for intensity pictures (i.e. those represented by point-wise intensity concentrations) are: threshold methods, which construct decisions backed indigenous element information, are efficient when object intensity concentrations drop squarely outside the background level range.As spacial data is unnoticed, blurred area boundaries create chaos. Edge-based strategies focus on contour detection but they may fail if blurred images are present.

A technique based on region typically return as : the image is detached into associated regions by lining up neighboring pixels of comparable intensities. Adjacent regions are then amalgamated depending on homogeneity of area boundaries. While over demanding criteria produce fragments soft ones over merge and overlook. Hybrid techniques employ a mixture of strategies higher than in style. An active contour model of segmentation technique that preserves connectivity was proposed recently. The major plan is to initiate with some boundary form painted within the type of spline curves, and modifies repeatedly by applying varied contraction /expansion operations with energy function. Though energy minimizing model is familiar, coupling it with the “elastic"” contour model offers a remarkable turn. Unlike other such methods, the risk of getting trapped into a local minimum makes the task hard.

1.8.2 Edge Detector

An edge is observed at an area wherever the picture features a sturdy intensity distinction.

Edges might even be painted by a distinction in color, without distinction in intensity. Wherever a powerful intensity distinction appears there square measure an exception exists doesn't exemplify a foothold. A zero crossing detector is utilized as a feature detector instead of a selected edge detection method.

The edge detection process is vital within the domain of ophthalmology or eye care. The perimeter of a picture, referred as Edges helps to segment and for visual perception. Depending on the intensity of a picture, they exhibit the shadows in addition to distinct modifications for the given picture. The detection of edges may be a elementary of level image process. The problem is that generally edge detectors behave terribly poor. In general, the adaptability of edge detectors in unique situations is weak. The quality of detected edge is very captivated with solidity of edges in the scene, lighting conditions, noise, and the presence of objects of comparable intensities. Although these issues are adjusted by the edge detector based on the so called foothold values, the fact is that there is no ideal method to set these values systematically and it requires human intervention whenever this process encounters such data. Since edge detectors {different|totally completely different|completely different} function higher underneath unusual conditions, the algorithm used should make use of multiple edge detectors, as it can apply each one when such data is encountered for its technique of detection. To make such a technique, it is obligatory to know about edge detectors and its performance in various conditions which is the aim of our project. In this

project , four edge detectors are studied based on the techniques used for detecting edges and a comparative study on their results are used to analyze the efficiency and identify the most preferred detector well suited under different sets of criteria. This information help produce a multi-edge-detector system, which evaluates the scene and spot the edge detector suitable for the existing set of data. The 2 alternative ways to implement are, one exploitation based on intensity solely and also the different exploitation color data.

1.9 METHODOLOGIES

The Pupil detector receives the image from the different data standard iris database and detects pupil on the image. Here I used 640*480 resolutions for pupil detection. After received the clear image, image processing algorithm is to be applied. Median filter lessen the salt and pepper noise meanwhile Gaussian filter smoothen the image. Then proper threshold is applied to convert black and white image. So that easily can detect black region in an image. Spatial and temporal filters are used to find out the exact pupil regions in an eye. Finally centroid is calculated to track the pupil in moving conditions.

1.9.1 Objective

The iris recognition systems work in as both stationary devices and portable devices. The high-performance serial microprocessors that work in the GHz range acts as a catalyst for implementing iris recognition algorithms. The executions of these complex algorithms are rapid due to the state-of-the-art built-in architecture with high speed communication buses. The cost of the system and microprocessor along with greater power consumption obstructs the implementation process. Embedded biometric systems are systems that can be merged with electronic gadgets for the ultimate safe and security reasons. Due

to the intricacy of computational tasks the usage of such embedded systems is considered as a problem. [Grabowski and Napieralski, 2011].

The affordability of the devices accessible directly affects the pace of the algorithm which at times needs exhaustive computations. For instance, ARM922 T, an iris recognition algorithm which runs at 160 MHz is 80 times slow on a microprocessor with high-performance [Lopez et al., 2011]. Such high speed data is processed effectively through a dedicated hardware. For instance, underneath sure conditions, a picture improvement routine that utilizes fingerprint recognition rule is processed in dedicated hardware works 30 times more than on a Pentium [Lopez et al., 2011]. Further, the velocity relies on the architecture and the cost of the chip. A out-and-out hardware solution need not be valid reply for a problem always, as it depends upon the operations involved in a problem.

The FPGA embedded iris recognition systems, play a major role in developing an ideal, inexpensive, feasible, reconfigurable and easily marketable embedded iris recognition system to answer the issues discussed above.

1.10 OBJECTIVES AND SCOPE

This work enables

1. To detect human eye pupil region with limited computational complexity.
2. To remove noises using Gaussian filter and Median filter
3. To find center of pupil region using centroid computation by Morphological operators

4. To implement in an FPGA with low area resources.

This method shortens the false edges dramatically in the edge-mapping for obsolete and rapid pupil detection. The Field programmable logic array (FPGA) oriented hardware or software execution suggested can be employed in the iris and pupil localization system as an application of FPGA oriented techniques.

1.11 ORGANIZATION OF THE THESIS

The flow the thesis under six labels, namely introduction, Literature review, basic concepts of Image Enhancement using Gaussian & Median filters , morphological Operators and Edge detection with hardware implementation, results and finally Conclusion. The concepts of pupil detection and its implementation done in Altera quartus II tool. The project is systematized as:

Chapter 1 Discusses the overview of Human Eye structure, different Eye Tracking technique, objective and the scope.

Chapter 2 deals with Literature survey of various pupil detection methods and image processing techniques involved in this chapter in detail.

Chapter 3 explains about Image enhancement using Gaussian filter and Median filter with its hardware implementation. EDA tool specification is as well discussed in this chapter.

Chapter 4 confers about the Morphological operations with image enhancement for identifying pupil region in an iris image. The equations are optimized for digital implementation.

Chapter 5 shows the results are presented in their sub-modules and then all the modules are incorporated to give the final output.

Chapter 6 consist conclusion, limitation along with further improvement of this work.

CHAPTER 2

REVIEW OF LITERATURE WORK

2.1 SURVEY OF THE HUMAN EYE PUPIL DETECTION USING INTENSITY VALUES WITH EDGE DETECTION

2.1.1 Introduction

Eye tracking is the visual process to spot the gazing point correctly and non-intrusively. As the investigation of gazing is gaining momentum, the point of saccade selection and monitoring process are achieved and they act as input data for Human Computer Interaction. Eye movements are of four kinds namely, saccades, VOR, Smooth pursuit and Vengeance movement. Consequently, the motion of pupil center acts pivotal for gaze tracking(Su Yeong Gwon et al., 2013) and the method of its extraction strikes the accuracy and precision of this tracking system. Eye tracking mentions the movement of eye and points of gaze positions during the vision of human eyes. There are immense numbers of research focusing eye tracking to study human behaviour. The precision of the eye gaze tracking technology is improvised by adopting an innovative pupil detection algorithm stand on intensity level with canny edge detection technique is presented (N.Nandhagopal et al 2019).

2.1.2 Canny Edge Detection Method

In this detection technique, the initial process is image smoothing extricates the gradients to focus on regions of higher spatial derivatives. Further, the algorithm (J. Canny,1986) marks and suppresses the pixels which

are not maximum (if found) by trailing along these regions (non maximum suppression). The gradient array additionally reduces as it consists of remaining unsuppressed pixels. Hysteresis employs two thresholds and if the value of significance is between the two thresholds, it is non edge. If the value of significance is on top of the high threshold, it is an edge. And it is an non edge only if there exists a track between this pixel to a pixel with a gradient above second threshold.

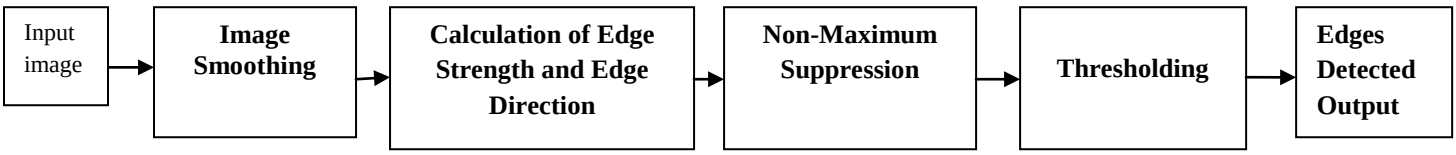

Figure 2.1 Phases in canny edge detector.

Figure 2.1 depicts diagram of the smart edge detection algorithmic program. The detector receives a color or a monochrome image as input image. The output of this algorithm is a picture solely with the detected edges.

2.1.3 Computation of the Strength and Direction of Edges

Upon smoothing the figure**,** the sobel edge operator loops **t**he blurred image obtained. The discrete differential canny edge operator produces a gradient representation of the figure. Horizontal and vertical gradients are evaluated via corresponding Sobel operators.

2.1.4 Calculation of Edge Direction

Edge direction is bounded because the route of the tangent to the contour is 2-dimensional [1: 690]. The arctangent evaluated using equation A=arctan((Gy/Gx) determine the edge direction of each pixel in an edge

direction image during non-maximum suppression stage. The results are rounded off to one of four angles 0°, 45°, 90° or 135° prior to non-maximum suppression figure 2.2 shows the focus of the images.

2.1.5 Non-Maximum Suppression

Non-maximum suppression (NMS) is employed by and large, by marking zero for pixels with less edge strength inside a precise native neighborhood. This native neighborhood will be a precise window with distinct instructions of length five pixels. The linear window thought of is in agreement with the path of the constituent in concern for a chunk in a picture.

2.1.6 Merits of Edge Detection

One among the pre-processing stage, edge detection removes the surplus data from input image, lessens the processing data tremendously and preserves information about the borderline concurrently. The Hough Transform technique extracts basic information like ellipses, lines and circles in edge detection (A. Elhossini et al.,2012). Simulation of pupil detection technique is done by Modelsim and output is viewed through Matlab.

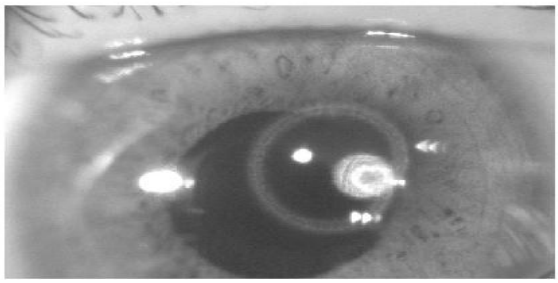

Figure 2.2 a) Input Image in focus

Figure 2.2 b) Pupil Region in focus

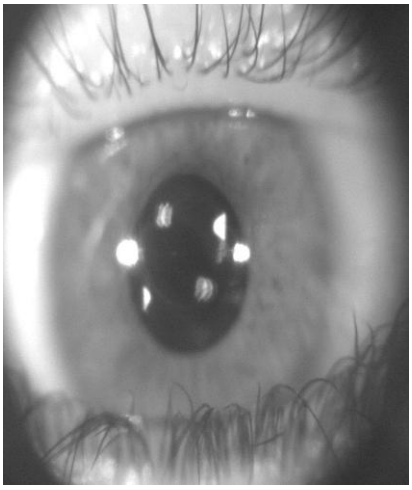

Figure 2.3 a) Input Image in out of focus

Figure 2.3 b) Pupil Region in out of Focus

Iris localization is a significant part in the iris recognition process. In this research, a rapid and a novel technique of iris localization is projected by analyzing gray scale images of eye and its intensity values. Iris is localized by identifying initially the border of pupil followed by canny edge detection. Figure 2.3 shows the image where eyelids are detected after satisfying special criterions and then eyelashes are detached by means of adaptive threshold image.

2.2 SURVEY OF IMAGE ENHANCEMENT USING ADAPTIVE HISTOGRAM EQUALIZATION FOR MEDICAL IMAGE PROCESSING

2.2.1 Introduction

Medical image processing is a demanding and a blooming field of research. The standard of the captured medical pictures estimates the potential of medical image processing since the captured images might not be typical

constantly. Major factors like illumination conditions, age of capturing experience of medical staff govern the medical images. So, distinction sweetening strategies are used for the distinction of medical pictures before being processing. Contrast enhancement algorithms (J. Alex Stark 2000) elucidate the details of a concealed in grey/colour levels. The low contrast images are stabilized via image enhancement algorithms. The widely accepted Histogram Equalization (HE) algorithm, enhances the contrast level by using Adaptive Histogram Equalization (AHE) or Contrast Limited Adaptive Histogram Equalization (CLAHE)(Md. Foisal Hossain et al .,2007).These algorithms are implemented by means of standard programming languages such as Java, Matlab, C or C++. An image with ideal level of contrast is the basic property in medical image processing. Unfortunately, the conditions under which images are taken are not favourable for the research.

Contrast enhancement is unavoidable in case if the photographed object is dim, lacks light or colour thus deteriorating the necessary details for the purpose of image preprocessing. When the contrast level in the image is tremendously low or if the image is too noisy, applying HE also is troublesome because they find difficult to differentiate the real detail and the imperfection that arise while capturing the image. (Wang Yuanji et al.,2003). Consequently, certain alterations are designed to reduce such undesired data. The two key points where the problem arises are exactly before or immediately after the equalization. If the image stabilization treatment is performed prior to the actual equalization, the useful information may be lost along with the noise eliminated and therefore cannot be identified and boosted during the equalization process. On the other side, after the equalization process, the noise removal takes place, it is more hard to get rid because the improvement makes this more apparent and meaningful.

2.2.2 Histogram Equalization

Adaptive Histogram Equalization (AHE) (S. M. Pizer et al .,1987) and Contrast Limited Histogram Equalization (CLAHE) are more complex, hence improved versions of the standard histogram equalization. The conventional histogram equalization algorithm has the issue that the improvement of the contrast is dependent on the whole image statistics. That's why some levels will be used to portray components of the low-interest. Adaptive histogram equalization attempts to reduce this trouble by using a distinct histogram for each pixel in the picture, computed using a screen with the brightness values encircling that pixel called contextual region. This generates an picture that concurrently visualizes items with distinct intensity values in distinct intensity micro-ranges. However, it should be observed that it does not assure that this relationship will be conserved after the equalization in case pixel a value is greater than pixel b value. In addition, in practical terms, it is not feasible to compute a histogram for each pixel due to its computing cost. As a matter of fact, this approach is abolished in most cases and as such the image is separated into a finite number of tiles and a histogram is computed for every one of them. To avoid the appearance of tile limits when applying the conversion to the various pixels, bilinear interpolation is used to create the transitions smoother in the final image. By restricting its improvement, CLAHE is helpful in restricting the looks of certain noise content in low gray level fluctuation areas. However, in some areas of this option, the decreased contrast improvement could conceal the presence of some important information in the picture.

AHE is distinct from the normal HE method because HE only produces one histogram, however AHE technique generates several histograms equivalent to varying picture region and disburses the image's intensity values. In the suggested technique, after using median filtering for picture sharpening, AHE technique is applied for contrast enhancement on modified and then minimize the distinction between input and processed picture average brightness.

Figure 2.4 a) original image

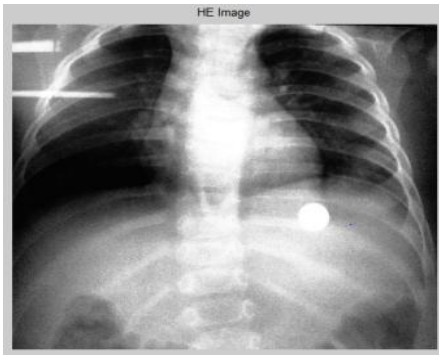

Figure 2.4 b) Enhanced Contrast Image

For adjusting the contrast in a grayscale image, "adapthisteq" is used in this suggested technique. The initial picture has a small difference, with the majority values in the center of the spectrum of intensity. “Adapthisteq” produces output image having values equally dispersed throughout the. Figure 2.4 shows noise produced picture in which high frequency additive noise, such as Gaussian noise exists picture.

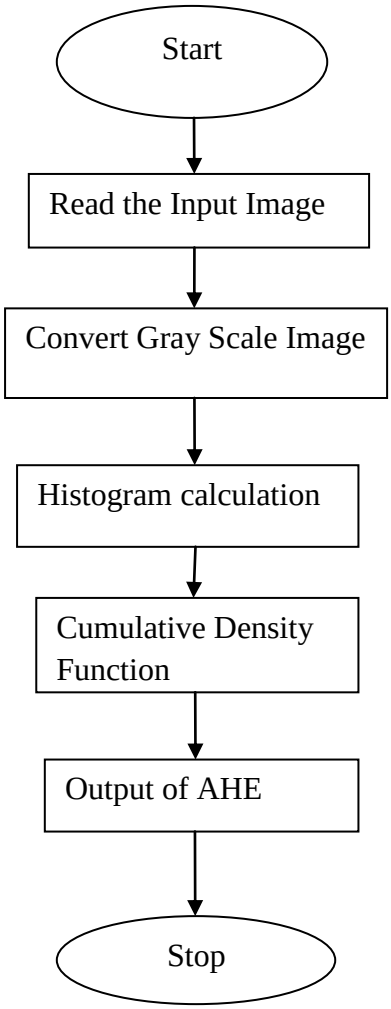

Figure 2.5 Steps Involved in the AHE

AHE provides sole histogram, but AHE produces quite a few histograms that correspond to distinct picture region and disburses the image's intensity values. As shown in Figure 2.5, in the suggested technique, after using median filtering for picture sharpening, AHE technique is used to improve contrast on modified image.

Steps Involved in Implementation phase of the Proposed Algorithm

• Step 1: Comprehend the image as input

• Step 2: Convert input into grey picture if the picture is colored

• Step 3: Calculate Intensity values of each pixel

• Step 4: Calculate Histogram Equalization.

• Step 5: Determine Cumulative Density function.

• Step 6: Calculate the altered AHE function output.

• Step 7: Output picture

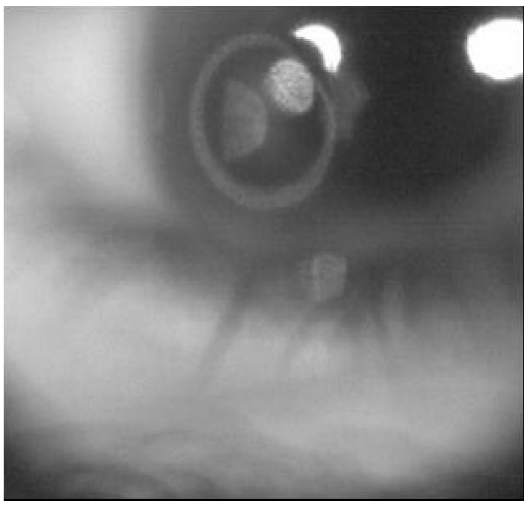

Figure 2.6 a) Noisy Human Eye Image

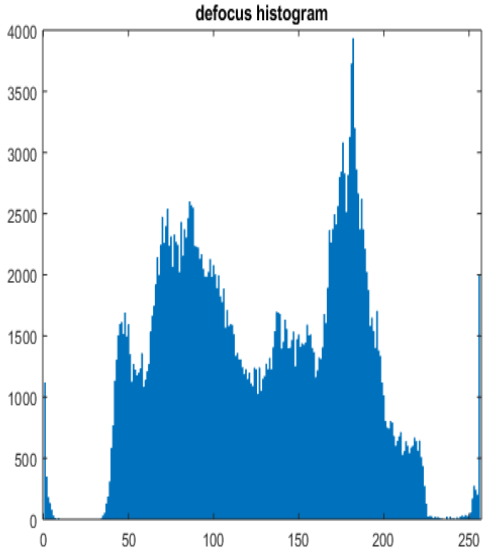

Figure 2.6 b) Histogram of Noisy Image

Simulation of proposed algorithm is done by Modelsim and output is viewed through Matlab. As shown in Figure 2.6, The image / video blending can be enhanced without the introduction of visual artifacts that reduce the

visual quality of a degree associated with the image under study. Figure 2.7 and figure 2.8 shows input and output image for AHE.

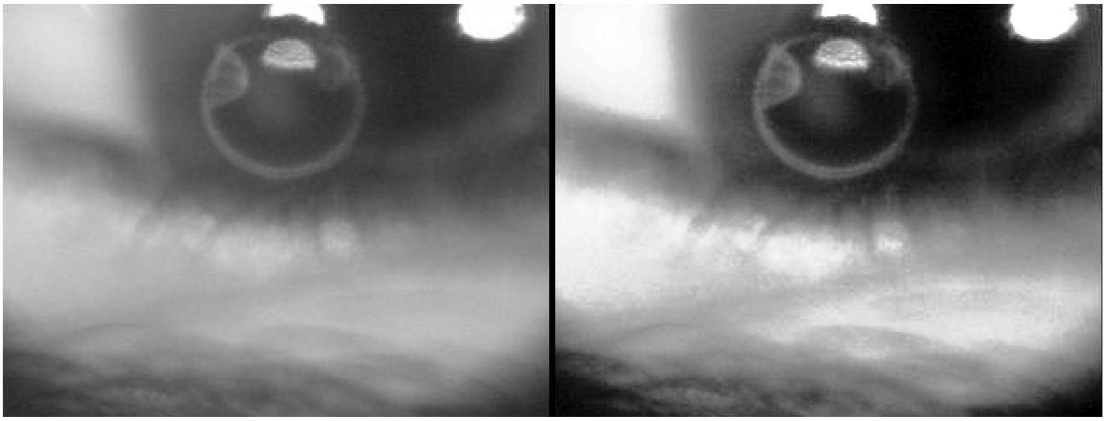

Figure 2.7 a) Input Eye Image **Figure 2.7 b) AHE output Image**

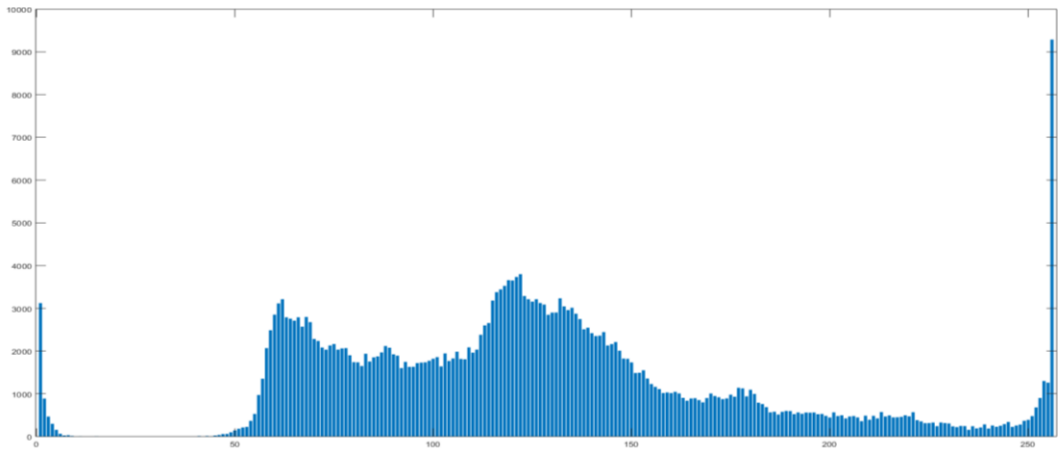

Figure 2.8 Histogram for AHE output Image

Using Adaptive histogram modification algorithm, a novel concept to image enhancement system employs carefully crafted penalty conditions to regulate the multiple elements of contrast improvement. The Histogram of AHE output image is shown in figure 2.8. The investigational results show the efficacy of the algorithmic rule as compared to traditional distinction

sweetening algorithms. The pictures obtained are visually agreeable photos free of artifacts and natural look. A broad range of pictures and video sequences are covered by this techniqueIt also provides a sense of control and robustness through which it is possible to achieve distinct levels of contrast improvement from histogram equalization to no contrast improvement.

2.3 SURVEY OF FPGA IMPLEMENTATION OF NOISE REMOVAL AND SMOOTHENING OF IMAGE USING MEDIAN FILTER

Image process could be a important field inside manufacturing plant automation, and more concretely, in the automated visual inspection. The main challenge unremarkably is that the demand of period of time results. On the contrary, the presence of impulsive noise in the obtained pictures is one of the most common concerns in many of these apps.. Median filter could be a strong technique to get rid of the impulsive noise from a picture. It is a computationally intensive operation; therefore it's exhausting to execute it in real time. This article presents a brand new design and development with FPGAs to be deployed. The realistic results show the usefulness of our enhancements permitting real-time operation and a minimum use of resources

2.3.1 Gaussian Noise

In mathematician sound, price the worth of every pel gets change by a tiny low quantity from its value. A histogram is a graphical depiction of the distribution of information. It reflects the wavelengths exhibited rectangles, having a region equivalent to the observation frequency. The complete histogram region is proportionate to the amount of comments. The histogram displays a normal division of noise. Owing to the central limit theorem that

says that the sum of all the distinct noises depicts Gaussian distribution, the Gaussian model is a pretty model.

2.3.2 Salt and Pepper Noise

The salt and pepper noise could be a sort of impulse noise which is noticeable principally in pictures. It holds black pixels on white background and vice-versa. A significant characteristic of this noise is that the noisy pixel's weight or value has no link or relationship with neighboring pixel color. This sort of noise typically impacts an image pixel touch variety. Looks like white and black dots when you see this kind of pixel. The point of supply of this sort of noise are camera filth and components that are overheated or faulty.

2.3.3 Median Filter

In a image, the median filter is usually used to cut back noise, like the mean filter. Median filter, however, is greater than mean filter, as it conserves the image's essential information like edges. The median filter also functions like a medium filter. It takes into account all pixels of the picture and confirms whether that specific pixel is the fair representation of its neighboring or not replacing the pixel value with the mean of its neighboring pel values.

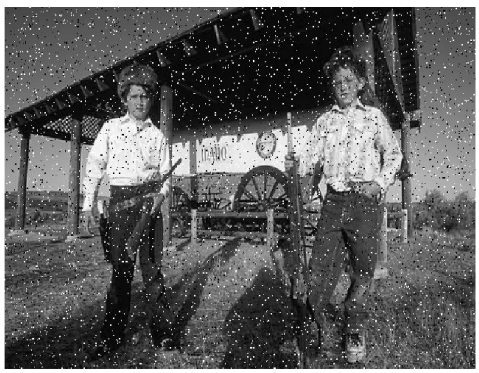

Figure 2.9 a) Noisy Image

Figure 2.9 b) Median Filtered Image

Figure 2.9: a) Noisy image converted as hex file from Matlab. This Hex file is given to Modelsim and applied median filter. Filtered outputs write into another hex file and read as a image in figure 2.9: b) from Matlab.

2.4 SURVEY OF VARIOUS LITERATURE WORKS

A) Fast and precise isolation of pupils based on active contour and morphology

The efficiency of iris recognition schemes, particularly in non-ideal iris pictures, is greatly affected by the segmentation precision. Using a mixture of morphological activities and snake active contour, this quick and precise technique segments the pupil regardless of form. Morphological operations are usually used to check a rough border of the pupil region while the active contour is used to search for accurate boundaries.

The detection of pupils is intended to correctly locate the pupil border. More exclusively, the module comprises of the following steps: (A) elimination of reflection, (B) generation of binary image by threshold, (C) removal of eyelids, (D) assessment of the border of the pupil and (E) precise segmentation of the active contour pupil.

Below is a comprehensive portrayal of the processes for signal processing engaged in every step. For purposes of illustration, Fig. 2.10 displays the main processing procedures engaged and the findings

achieved.

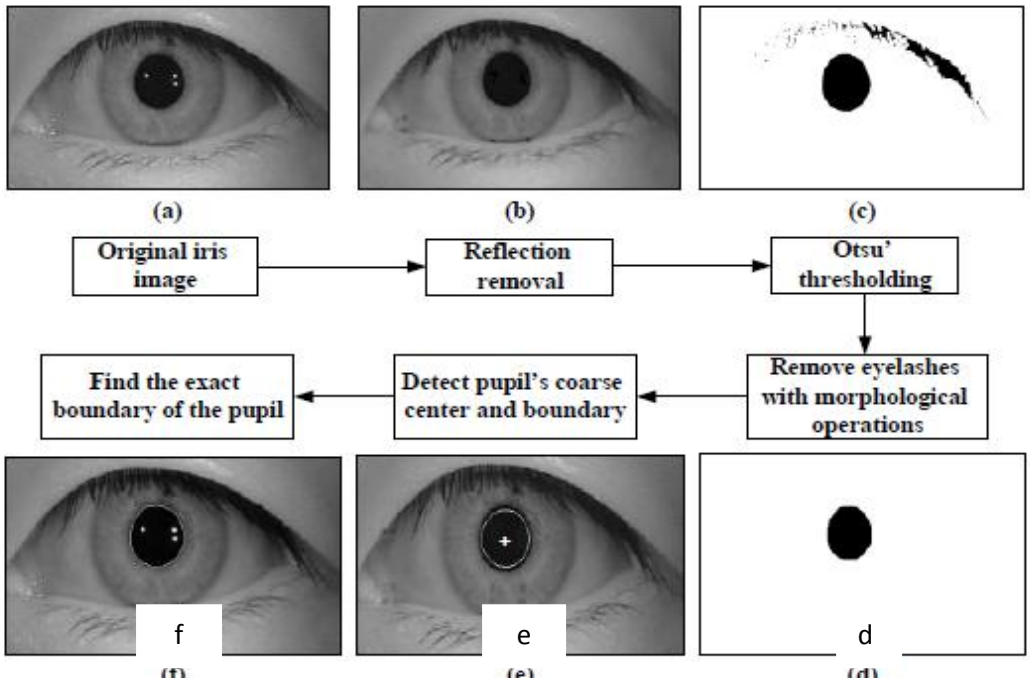

Figure 2.10 Steps involved in the pupillary detection algorithm

Major analysis procedures, i.e. (a) initial picture, (b) removal of reflection, (c) binarization of picture, (d) removal of eyelids, (e) coarse center and border estimation of pupils, and (f) active contour isolation of pupils.

Despite the shape of the pupil, the pupil detection algorithm is an economical and accurate approach to pupil border detection. This study design segments the actual shape of the internal iris border that will add to a more trustworthy and robust iris recognition scheme.

Otsu's Histogram thresholding and morphological operations were utilized to predict the rough pupil border in order to discover the pupil limit. Then, the specific border is observed by a snake active contour. The benefit of

the active contour is that it is possible to achieve circular exploitation and elliptic approximation by generating an extra right contour of the pupil border.

B) Parallelizing Iris Recognition [Rakvic et al., 2009]

This study [Rakvic et al., 2009] shows that three main parts of the Ridge Energy Detection (RED) iris identification algorithm are parallelised: (1) segmentation of iris with local kurtosis ; (2) filtering template development ; (3) hamming range matching template. In specific, the writers [Rakvic et al., 2009] parallelized such parts and showed speeds of 9.6, 324 and 19 times respectively in contrast to a state-of - the-art Processor-based version.

The writers carried out the FPGA experiment on a DE2 board developed by Altera Corporation. The DE2 board comprises of a Cyclone-II EP2C35 FPGA chip and the programming interface needed for FPGA. The Cyclone-II family is intended for apps with superior performance and little power. It includes more than 30000 logic elements and 480000 built-in memory bits. The clock signal from the DE2 board containing a 50 MHz clock was taken.

The parallel algorithm of the writers on FPGA far surpasses their calculated finest Intel CPU design theoretically. The writers wrap up that a complete execution on a top-of - the-art FPGA of a very rapid iris recognition algorithm is more than viable, offering a smaller form-factor solution.

C) Hardware–Software Co-Design of an Iris Recognition Algorithm [Loìpez et al., 2011]

This research[Lopez et al., 2011] has demonstrated one among the finest instances of iris recognition algorithm integrated system design. The

primary objective of this job was to use a reduced-cost FPGA to deploy an iris recognition algorithm. The optional approach used to implement the iris detection algorithm was relied on a co-design of hardware software. Reported investigational findings in this job were achieved using a 40 MHz clocked Spartan-3 FPGA. The system architecture comprises of a microprocessor (Xilinx Microblaze) with 32-bit soft-core and a few specialized hardware units.

All phases of the iris identification algorithm have been introduced, such as preprocessing of images, segmenting iris, normalizing, extracting the features and matching of templates. The less computational exhaustive jobs and those relating to floating-point operations are performed in software through the microprocessor, while the tasks with high computing costs are accelerated by coprocessors, the hardware accelerators. The task of preprocessing the picture to remove reflections and the phase of iris location (pupillary and limbic border detection) were discovered appropriate for hardware application as they took 71 percent of the complete execution moment (all phases) in software. Furthermore, the elimination of reflections and the location of the iris require whole arithmetic activities with an acceleration ratio of more than 11 in contrast to their software implementation.

All other iris identification phases apart from iris location, like eyelid identification and normalizing iris, extracting features and template matching, were performed on microprocessor since they primarily consist floating point activities and symbolize a tiny proportion of complete software implementation time (each < 5 percent). Moreover, their theoretical percentage of acceleration was small. For the detection of pupillary and limbic boundaries, the active contours utility was used. In hardware, this feature has been partly implemented.

The authors [Lopez et al., 2011] acheived their design on a low-cost Spartan 3 FPGA and the findings show that the complete iris recognition algorithm's execution time was 522.6 ms for a picture of 640 x480 pixels with a 40 MHz clock frequency. The finest iris recognition algorithm software solution introduced on a Pentium 133 MHz microprocessor executed in 1112 ms, which is almost 2.12 times faster than the clock frequency 3.3 times reduced system operated by Lopez et al.

D) Hardware Architecture Optimized for Iris Recognition [Grabowski and Napieralski, 2011]

The work [Grabowski and Napieralski, 2011] discusses the application on a multicore integrated scheme of the full iris recognition scheme (1:N). The architecture of this scheme consists primarily of digital signal processors (DSPs) and FPGAs. The iris identification algorithms utilized in this design were created and used by the writers earlier on a PC platform [Sankowski et al., 2010]. The research demonstrates that segmentation of iris to be most time-consuming when performed on Computer-based systems, where it requires much a smaller amount time to calculate when performed using the integrated multicore scheme outlined in [Grabowski and Napieralski, 2011]. Using DSPs, the extraction of feature and the corresponding iris identification phases of the model were also introduced. However, in the future, the writers intend to introduce the template matching phase on specialized hardware via FPGA, as they observed this phase in their embedded system to be the most time consuming phase.

The writers [Grabowski and Napieralski, 2011] introduced their architecture to the BioServer platform biometric implementation consisting of two distinct physical boards: (1) an embedded system consisting of two

PowerPC 440 microprocessors with Virtex-5 FXT Xilinx ML510 as BioSys; (2) biometric computation unit (BioCU) that includes four DSPs and Xilinx Spartan 3AN FPGA. On BioSys ' ML510 platform, the BioCU board is placed into a 32-bit slot.

The writers contrasted the efficiency of their multicore integrated iris recognition scheme with the implementation of three distinct PC-based systems: (1) PC1 based on Intel Core2 6600 2.4 GHz ; (2) Intel Pentium4 3.4 GHz based PC2 ; (3) Intel Core2 Duo T7100 1.79 GHz based PC3. The size of the picture was 640 480 pixels to test the output, the size of the model was 2048 bits and the size of the database was N=10000 templates. Comparison with these applications reveals the best speed of their embedded system.

E) Iris Biometrics for Embedded Systems [Liu-Jimenez et al., 2011]

This work [Liu-Jimenez et al., 2011] presented two Iris biometrics implementation on two different stages used in the development of embedded systems: (1) a microprocessor-based architecture ; and (2) a specific hardware architecture. Such implementations, indeed, do not embrace iris segmentation phase of iris recognition and only include removal of features and matching of templates. The initial application utilizes a 16/32-bit RISC CPU ARM7TDMI microprocessor as well as commonly utilized in many business apps owing to its elevated computational energy and decreased cost. The second application, which is a committed hardware, utilizes Xilinx's Virtex4sx35 FPGA, which has been exclusively intended for digital signal processing. In the first execution running @ 50 MHz, the execution time of microprocessor is 10 times more than the CPU@2.6 GHz computer platform, but in absolute terms, the microprocessor provides a scalable solution because it is clocked 50 times lower than the computer platform. The dedicated hardware in second

application provides the highest processing time, showing 200 times pace than microprocessor-based alternatives and 20 times pace than computer-based solution. The microprocessor and FPGA-based executions have strengths of data protection, size of the system, and price in contrast to regular computer systems. Choosing either of the above mentioned platforms relies upon the system and authorization requisites.

In [Lopez et al., 2011], when the iris recognition algorithm is run on two different microprocessors, Intel Centrino 1.7GHz and 32-bit ARM922 T 160MHz, the iris location feature requires 71 percent and 89 percent of the general algorithm's complete execution duration respectively. The literature analysis submitted in the earlier sections demonstrates that localization of iris is the most tedious phase in the entire iris identification algorithm either operating on a PC platform or on a microprocessor-based integrated scheme [Lopez et al., 2011], [Basit and Javed, 2007] [Grabowski and Napieralski, 2011] with restricted database size or where 1:1 comparison is needed. Consequently, localization of iris is the preeminent option while designing integrated iris recognition systems for dedicated hardware application. The localization of iris was introduced on FPGA in[Lopez et al., 2011] which took 159 ms of implementation time, but neither the iris localization's hardware structure design nor its precision assessment was disclosed. In addition, execution time also appears to be unoptimized and there is scope for improvement with regard to the appropriate algorithm choice to attain greater precision and consistency. In [Lopez et al., 2011], the IDO based algorithm was used for FPGA implementation, but we found the IDO less suitable compared to CHT for FPGA-based parallel implementation. To pass parallelism in IDO-based algorithm, ‘n’ copies of input image must be stored in the memory equivalent to ‘n’ radii regarding the circle detection, since the IDO necessitates

considering the pixel intensity in the image, while an edge map image is required in CHT for parallel execution equivalent to ‘n’ radii, as the CHT doesn’t consider image’s pixel intensity values. The literature appraisal also indicates that single or multicore processors with FPGA-based platforms with (CPUs) and one-chip configurable logic are ideally suited for the implementation of integrated iris identification devices. Implementation of data-intensive tasks, such as iris location on FPGA as a specialized hardware, can therefore unload the CPU by failing to perform computation-intensive functions on it, which could boost the dealing time of the entire scenario. Due to the complexity of this phase, the[Liu-Jimenez et al., 2011] writers introduced specialized hardware for iris recognition, extracting feature and matching phases, but not for iris localization phase. The literature appraisal on the recognition of iris and its integrated systems demonstrate gap in the design of rapid and efficient integrated iris recognition systems.

The efficiency of iris location is atmost essential for the reason that it is the first ever phase in an iris detection algorithm and if the iris location goes incorrect, all the phases after this phase will suffer. Sometimes, when developing a dedicated algorithm hardware, the exactness has to be compromised to decrease the algorithm's intricacy. Hence, the choice of the algorithm is also very crucial before the specialized hardware is designed for an implementation.

Table 2.1 Comparison of Eye Tracking Methods

c) Method	**d) Detection Accuracy (%)**	**e) CPU time (ms)**
f) Khairosfaizal and Nor'aini	g) 86%	h) 45.23ms
i) Yang	j) 92%	k) 43.55ms
l) Zhu and Ji	m) 95%	n) 36.34ms
o) Li and wee	p) 98.1%	q) 49.75ms
r) Lui and Lui	s) 94.1%	t) 12.75ms

The Table 2.1 depicts a Comparison of Eye tracking techniques. It is a method used in science of perception, iris recognition (H. Mehrotra et al.,2013), human-computer Interaction (N. Wang et al.,2014), publicity, medical research, and other such fields. A easy technique (Flores et al.,2011)is an eye-focused camera that captivates their motions as the viewer gaze at some type of stimulus and then the image processing software processes these motion picturesMost contemporary devices (Swirski et al.,2012, Sigut, J., & Sidha 2011) use infrared beams to produce corneal reflection through which the angle of measurement is evaluated. Many use at least 30Hz frequency to detain the information of the very fast eye movements.

In (Zhu and Q. Ji, 2005) different eye detection technique like template, appearance, and feature based methods. The eyes were exactly detecting in these methods and also it is expensive in computational part. In (K. Lin et al.,2008) author given details about a rapid eye detection idea for use in video streams. In(B. Jun et al.,2007), author developed an algorithm for face detection using MCT and Ada Boost. In (B. Jun et al.,2007) ,author developed

a method for eye detection using AdaBoost training with MCT-based eye features. Morphological techniques a tiny low template known as structuring part. This structuring portion is applied to any or all of the input picture places and creates a steady size output. In this method, comparable pixels of input picture with neighbors were endorsed by the output picture pel values region unit. This procedure generates a brand new binary image that will have non-zero pixel price at that place within the input picture if check is no-hitit. There are countless structuring components such as diamonds, square shapes, cross shapes, etc. In medical apps, IMAGE contrast improvement is essential as visual assessment of medical pictures is important within the identification of the many diseases. In functions such as chest x-ray and mammography (A. Laine et al., 1995),(W. Qian et al., 1995), the image contrast is intrinsically low due to the small differences in the coefficients of X-ray attenuation. Two commonly used techniques for worldwide visual enrichment are linear contrast stretching and histogram equalization (A. N. Netravali et al., 1988)– (] R. C. Gonzalez and R. E. Woods, 1995). Local information may be more essential than worldwide comparison in diagnostic medical images. Adaptive histogram equalization (AHE)(] J. D. Fahnestock et al., 1983) and adaptive contrast enhancement (ACE) (R. H. Sherrir et al., 1987) are two eminent techniques of local enhancement. AHE algorithms map the gray pixel values of the relationships acquired from the indigenous histograms. While this enhances image contrast, extensive computations are required (S. M. Pizer et al., 1984). To decrease the computational burden, the bilinear interpolation technique was developed. It first splits pictures into blocks, then calculates those blocks ' mapping features.

2.5 DIFFERENT ALGORITHMS FOR IDENTIFYING IRIS

2.5.1 Daugman's IDO

Daugman suggested the foremost effective technique of localizing iris in [Daugman, 1993], using the IDO shown in Equation (2.1). Used to locate iris, the IDO considers the inner and outer boundaries of iris as two circles. He introduced the IDO to the domain of the picture to look for the exterior limit of iris first then to search for pupil within the exterior limit of the iris. The images were launched by Daugman where the gray difference of iris and sclera in contrast to iris and pupil appears to be more. This applies to pictures captured in VW light. The IDO can be used first to determine the exterior border of the iris due to a preprocessed picture I(x, y). Daugman's IDO is expressed in the mathematical form as.

$$\max(r,xo,yo)|G\sigma(r)*\partial\partial r\oint I(x,y)2\pi r\, r,xo,yods| \quad (2.1)$$

The operator explores for utmost in the hazy partial derivative on the image (x, y) regarding escalating radius 'r' with respect to normalized contour integral of put in image along a 'ds' circular arc of 'r' radius with center coordinates (x_o, y_o). The symbol '*' indicates the procedure of intricacy, and Gσ(r), smoothing function like a Gaussian derivation. It is split by 2πr in order to normalize the circular integral with regard to its perimeter. To brief with, the IDO proceeds as blurred circular edge detector with σ scale, that recursively hunts through the set parameter { x_o, y_o, r } over picture room. First search is the exterior border of iris with a greater value of σ. As soon as the outer iris boundary is located, finer-value search process for inner boundary of the iris is performed within predetermined region. Estimation time connected with iris's

exterior border search method could be decreased by offering a variety of approximation for parameter ‘r’ near to the real border radius.

2.5.2 Wildes’ Method

Wildes suggested the subsequent renowned segmentation method in [Wildes, 1997], on the basis of HT technique. He made HT to spot a picture's circles. The edges contained in the picture are first resolute using an edge detector due to a preprocessed picture I(x, y). Assume the set of edge-points acquired from the algorithm for edge detection (x_i, y_i), where i= 1, 2,…n. Because the edge points could be a constant or curvy contour, a voting method is used to fix a circle in the border. HT, a conventional algorithm for fitting contour, is used for this purpose. The voting operation in the HT method is performed in a space parameter where object candidates are acquired as local maxima in an algorithm-built accumulator room. Wildes has proved the use of HT in the area of iris recognition to conclude the iris limits. For a pair of edge-points, x_i, y_i, where i = 1, 2,. n, HT can be used to match the center circle (x_c, y_c) with radius ‘r’ as the following :

$$H(x_c,y_c,r)=\Sigma h(x_i ,y_i,x_c,y_c,r)ni=1 \quad (2.2)$$

$$h(x_i ,y_i,x_c,y_c,r)=\{ 1 \text{ if } g(x_i ,y_i,x_c,y_c,r)=0 \; 0 \text{ otherwise} \quad (2.3)$$

$$g(x_i ,y_i,x_c,y_c,r)=(x_i -x_c)2+(y_i -y_c)2-r2 \quad (2.4)$$

For every edge-point in the set (x_i, y_i),g(x_i, y_i, x_c, y_c, r) is considered to be 0, if the triplet parameter (x_c, y_c, r) represents a circle through that point. H(x_c, y_c, r) shown in Equation (2.2) is an array that increases its values (indexed by values for x_c, y_c and r) by equation (2.3) and equation (2.4). The

ternion restriction corresponding to the biggest value in the array is regarded to be appropriate parameter set for the circle that suits the contour provided.

2.5.3 Other Methods

Several techniques of segmentation of the iris are accessible in appropriate literature. Table 2.1 provides some of the futuristic methods for iris segmentation and their appropriate primary techniques. Several of the techniques in the table are built entirely on the techniques of HT (or CHT) and IDO. Nevertheless, other processing steps are also used in conjunction with HT and IDO, like those of removal of reflection, edge-mapping of eye picture using different methods, thresholding, morphological operations, filtering operations in a picture, enrichment of image quality and active contours to polish up iris borders, etc. The above mentioned methods of image processing become leading when non-ideal picture information has heterogeneous picture features, improper lighting, low contrast, unfocused and hazy pictures, etc. For specific picture information like NIR images, deviated iris pictures, colored VW pictures and inadequate information for non-cooperative iris, the various techniques mentioned in the table have been created for non-cooperative iris recognition etc. On the other hand, many of the methods developed for NIR images can be useful to VW images and conversely with mild adjustments. The recent techniques demonstrate the enhancement in computational time or precision results or both over the past techniques for the same sort of picture information.

In localizing the iris of the NIR pictures, the pupil is usually located before the exterior limit of the iris as it is the dark compact area in the picture, the border of the pupil is stronger than the exterior border of the iris, and the pupil is noticeable in almost all the pictures as a complete circle. A sub-image

in the region of the pupil is processed to identify the exterior border of the iris after locating the pupil in the picture[Jan et al., 2014],[Wang et al., 2014]. Unlike NIR pictures, the external border of iris is identified in VW pictures before the pupil, as its border contrasts more than the pupil [Chen et al., 2010], [Radman, 2013]. Some techniques for blurred VW pictures first identify the sclera portion in the pictures as it's a prominent white region in the pictures of the eyes [Proenca, 2010].

The literature evaluation shows that the present localization algorithms of iris spot the pupil by means of either intensity thresholding [Zuo and Schmid, 2010] [Khalighi et al., 2015], or edge detection based segmentation techniques [Marciniak et al., 2014]], [Hasan and Amin, 2014], [Jan et al., 2012, , while the external boundary of iris is spotted by either edge detection based technique or IDO based methods.

The image preprocessing is very important in IDO-based methods to guesstimate the rough pupil and iris centers as the IDO could be applied to the chosen pixels in the image or a sub-image consisting iris area can be pulled out. Such preprocessing methods enhance the swift and perfectness of iris localization. For instance, [Radman, 2013] writer, apply circular Gabor filter to detect pupils and iris centers roughly, tagged along by IDO to detect centers perfectly. The removal of shadow is a prevalent move in almost all techniques of localizing iris as IDO is more susceptible to mirroring and it may mislead the detection of circles in CHT-based techniques [Jan et al., 2013].

First ideal edge maps of the iris picture are produced in the HT-based algorithms with minimal false edges to identify the iris circles perfectly and effectively as shown in [Hasan and Amin, 2014]and [Jan et al., 2012]. The generation of optimal edge-maps are demanding, if the imagery chosen (like

CITHV4 database images) are noisy. The noises such as lighting reflections, non-uniform illumination and low contrast noisy images are first removed in preprocessing stage as described in [Jan et al., 2012, 2013, 2014], [Wang et al., 2014], to pull through the accurateness and execution time of the iris localization. The picture in painting methods is used to remove the iris picture image reflection spots and the histogram equalization is used to compensate for inconsistent lighting and low demarcation. For the iris localization in turbulent NIR images from CITHV4 database, [Wang et al., 2014] authors projected a painting approach relied on Navier-Stokes equations to eradicate the mirror image spots and Probable boundary (Pb) edge detection operator to answer inconsistent illumination.

2.6 IRIS - BIOMETRIC FEATURE

The properties of the iris that augment its appropriateness for usage in high confidence identification systems are conversed in this section [Daugman, 1993], [Daugman, 2004]. The merits and demerits of using iris as a biometric identifier are addressed below.

Merits:

1. Iris could be an eye's inner, highly protected organ. It is inherently separated from the outside setting and shielded from it. It is difficult to alter it surgically without the danger of vision being unacceptable.

2. Iris is unwavering all the way through the individual’s life. The human iris commence to create throughput the 3rd month of conception. The formation is wholesome by the 8th month of conception. Moreover the pigmentation, remains in the first year following birth.

3. There is a elevated level of arbitrariness in iris structure, to make the iris exclusive for each individual and therefore a trusted biometric identifier.

4. A hot iris detection examination can be done easily to prevent hoax in the scheme using an iris photo or motion picture because the iris reacts to light and pupil's evolving size demonstrates natural physiology.

5. Iris pictures are ample for personal recognition with high certainty. Pictures could be watched over from distances of up to 3 feet.

6. Without physical contact, picture is caught at certain distance from a focus, making the identification method minimally intrusive.

7. There is no pattern of iris genetic determination. The look alike twins have distinct patterns of iris as well as the same person's left and right eye irises are distinct as well.

Demerits:

1. Iris is a tiny destination for remote capture (>1m).

2. Iris is a motion object in the recognition of uncooperative iris that is hard to obtain.

3. Iris hindered by eyelashes, eyelids, and lightings complicate the automatic iris recognition algorithms.

4. The iris should be captured by NIR illumination ; lighting should not be apparent.

2.7 IRIS IMAGE ACQUISITIONS

The iris is preferred to be captured by NIR illumination; illumination should not be apparent or bright. Image acquisition environment will determine the iris picture data quality. Different camera sensor, lens, lighting and distance capture choices will lead in variable quality information[Wildes, 1997]. Near infrared (NIR) lighting sources and NIR cameras are used by almost all commercial iris recognition technologies. This is because in stipulations of capturing textural data in iris, NIR cameras are efficient. Visually dark brown (almost black) irises show little variety in color and therefore contain almost no supportive data for iris recognition. The iris identification systems often require cheap and low-quality sensors and optics due to the necessity to be low cost. This significantly limits the distances captured and the quality of the information collected. Protection of eye from overheating and injury, it is necessary to be within the predetermined threshold for the strength of the NIR illumination [Matey et al., 2006]. As cited earlier, the NIR iris images are traditional inputs into the iris recognition system, but in recent past, biometricians have focused on visible wavelength (VW) iris images obtained in the visible electromagnetic spectrum band. [Proenca et al., 2010]. A range of variables support this trend: (1) visible optical cameras are inexpensive and have a very high resolution ; (2) these cameras can capture long-distance facial or iris pictures and can also be used to validate a suspect or violent person; (3) no extra NIR camera would be needed for today's smartphones to run the iris recognition application; (4) the wavelength of the NIR may be detrimental as the eye doesn’t react impulsively with its usual processes (blinking, pupil contraction, and aversion) [Proenca, 2010].

CHAPTER 3

IMAGE ENHANCEMENT USING FILTERING TECHNIQUES

The Pupil detector receives the image from the different data standard iris database and detects pupil on the image. Proposed architecture used 640*480 resolutions for pupil detection. After received the clear image, image processing algorithm is to be applied. Median filter decreases the noise of salt and pepper meanwhile Gaussian filter smoothens the image. Then proper threshold is applied to convert black and white image. So that easily can detect black region in an image. Find out exact pupil region by applying morphological dilation operators. Sobel edge detection is applied after the morphological dilation to separate background and pupil region.

This chapter describes the initial process of smoothen the image using Gaussian filter and remove noises using median filter and its hardware architecture with results.

3.1. INTRODUCTION

Image filtering is the process that enables us to do some modifications or apply filters on pictures. Typically the filtering or filter is a thing via which a thing is passed to oust the unwanted particles contained in it. Here the image filtering is done when I obtain the picture from camera or other device I suppose to do some effects or modifications on it through image filtering techniques for mitigating the blur or unwanted substances like noise on the image to develop the visual excellence of the image (K. Bahrami et al., 2015).

The image filtering is also known as image smoothing which is one of the most eminent process and widely employed for the image processing ones. The scope of smoothening is to lessen blur and enhance the visual clarity of the particular image by employing diverse filtering techniques (C. G. Boncelet et al., 1991). The most typically used algorithms for filtering images are linear algorithm and non linear filtering algorithms (Z. M. Ryu et al., 1986). The non linear filter is quite distinct characteristics while compared to linear filter because the response of the given input will not adhere the principles specified earlier. Filtering becomes a substantial method of signal processing system. It includes the degradation of signal and its performance. Most filtering-based techniques have been based on linear processing methods in latest years. This survey compares the different picture filtering methods for the image processing scheme in this study. The methods for filtering images are Adaptive filters, Median filters, Spatial filters, Gaussian filters, Average filters, Fuzzy filters, etc.. These filters are categorized as Linear and Non Linear Filters.

In recent years there is a vast amount of compact or portable devices coming in image processing and multimedia applications which are smart phones, camera, tablets, wearable's, gadgets, etc. These smart devices typically have restrained computing, power consumption, and storage services which are demanding high latency sensitive applications. So that the techniques of energy efficient methods are becoming the vital one for mitigating the power consumption of resource constrained devices. There are several methods to attain energy efficient methods in the architecture. The most of the image processing or filtering applications gives output for the human assumption that shows restrained view and the minor deviation in the output image could not be identified. This application which typically called as fault tolerant application that is minor deviations in the output is reasonable. Filtering is often called

smoothing which eradicates the unwanted noise and vague impressions in the particular image and surge the high decree of the image by applying appropriate filters such as Gaussian Filter, Fuzzy Filter(F. Russo and G. Ramponi,1995), Adaptive Filter, Median Filter, and FIR Filter, etc.

3.2 IMAGE FILTERING TECHNIQUES

The image filtering algorithm also called software image filtering that process the image or snap to bypass a specific set of frequency components. When maps to audio, reflection, and communication the word frequency is measured is cycle per second. To understand the patterns as component frequency in images the image filtering is often used to filter the images to obtain the high definition content without noise, blur, and unwanted things. The filtering is also used to improve the patterns of spatial determined by the intensity of light instead of light frequency.

The image consists of collection of component frequencies. To determine how filtering process happens it can prototype the imaging functions such as pass adaptive, median, and various other frequencies. The scope of image filtering is to identify the needed data in certain levels of frequency spectrum to expel the unwanted frequencies. In many apps, object sensing, mapping, and categorization are relevant in picture filtering algorithm smoothing filters. These are applied for the preprocessing the redundant details and noise. There are two filters are used in this work,

a) Gaussian Filter.

b) Median Filter

3.2.1 Gaussian Filter

The Gaussian filter is one of the commonly used methods for filtering images and also it is denoted as weighted non linear filter which is employing for ousting the blur and noise of the image. The Gaussian Filter (Garg et al.,2016) is typically utilizing for the preprocessing method in the particular image before going to the edge detection to oust the redundant particles or entities caused by noise. In order to efficiently utilize or implement GF (Gaussian Filter) the equation of Gaussian is resolved by the operating system kernel of variant sizes. The better size of OS Kernel is good in the Gaussian expression or equation which renders high definition quality for viewing the image visually in the lower cost computational complexity. To attain the filtered image the convolution operation is performed with the Gaussian Kernel along with sub matrix image which exhibits constant multiplier floating point since it consumes high energy.

3.2.1.1 Gaussian mask

Figure 3.1 demonstrates Gauussian mask also known as Gauussian filter, one of the prominent and extensively used filtering algorithms in filtering techniques. The Gaussian Filter (G) is defined as G(x,y) = ½ (pi)(e^(x+y)). Where G is the Gaussian Filter, x and y are the coordinates. The Gaussian Mask that uses a Gaussian Function(Cabello et al., 2015) for expressing the normal distribution in the formula and also for reckoning the alteration to employ to every pixel in the picture identified if not the procedure recurs again to extract the matched eyes from the millions of records stored in the database. The rationale is to construe what type of response I get from the given input value to attain a specific process or what could be the complex problems allied in a given process. The forms of image operations can be explored in digital

images to translate a key in image to an output image. It is categorized in to three operations based on their characterization. The method of picture filtering is used as a pre-processing to remove redundant stuff, noise, and picture blur. Filtering is the process that the data that is originated from smart devices such as tablets, phones, etc.

Figure 3.1 Gaussian Mask

Being a prominent and extensively used filtering algorithm in image processing or filtering methods, Gaussian filter. The rationale is to construe what type of response I get from the given input value to attain a specific process or what could be the complex problems related in a particular operation.

3.2.1.2 Convolution operation

The Convolution operation is a imaging process that process a multiple shift integration operation. During the run time the pixel of each image is integrated or centralized over other pixels in an old image. The earlier values of pixel under the Operating system kernel is multiplied by the associated processing pixels for example all are same as 1. The outcomes of all

multiplications are integrated in to one image and the outcome values are reported in the output image. The kernel processing is for calculating the simple mathematical methods for many typical image processing operations. In the image filtering context it renders a way to separate the two arrays of numbers in the equal dimensions which can be utilized in image filtering techniques. The pixel values yielded are basic nonlinear and linear associations of some keyed in pixel values.

Generally smoothening can be designed by complying the novel image of taken picture of the size x and y includes Gaussian mask. It is acquired through calculating the sum total of products of the keyed in and output image with the 3*3 matrix using the convolution operation. In convolution linear filtering can be applied using a method called discrete convolution. Ceaseless convolution is typical in image and signal processing systems but the snaps or images are not discrete. Here I employ only discrete convolution.

a) Specifies the weight of pixel as an image, represents as K.

b) K the image representation commonly called kernel in convolution.

c) Here the kernel operation is associative.

The earlier values of pixel under the Operating system kernel is multiplied by the associated processing pixels for example all are same as 1. The outcomes of all multiplications are integrated in to one image and the outcome values are reported in the output image. The kernel processing is for calculating the simple mathematical methods for several typical image processing operations. The range of picture filtering is to define the information required for expelling unwanted frequencies at certain frequency

concentrations. In many apps, object sensing, mapping, and categorization are relevant in picture filtering algorithm smoothing filters.

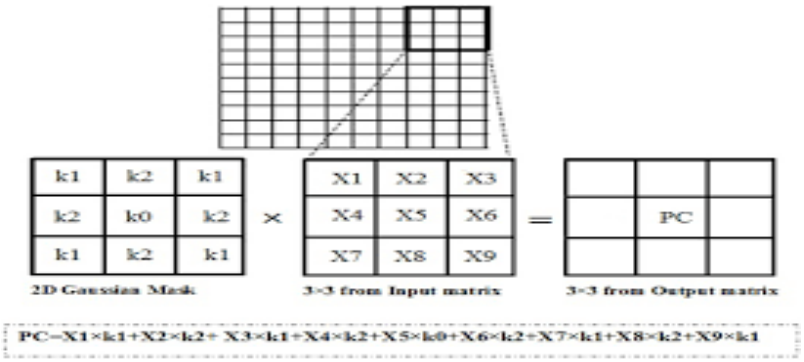

Figure 3.2. Convolution Operation

The Convolution operation is an imaging process that processes a multiple shift integration operation. During the run time the pixel of each image is integrated or centralized over other pixels in an old image shown in Figure 3.2.

3.2.2 Hardware Architecture of Gaussian Filter

The GF is the non-linear weighted filter used to smudge and de-noise the picture. The pre-processing filter is most frequently used to take out the undesirable edges due to noise. The Gaussian equation is approximated by a kernel of distinct dimensions to effectively execute the GF. The larger kernel size is the approximation of mathematician expression with greater quality at the value giant complexity of the operation. Convolution of the Gaussian kernel with the image sub-matrix is performed to achieve filtered image. Because the right kernel shows the steady multiplier factor of floating purpose, it consumes great energy.

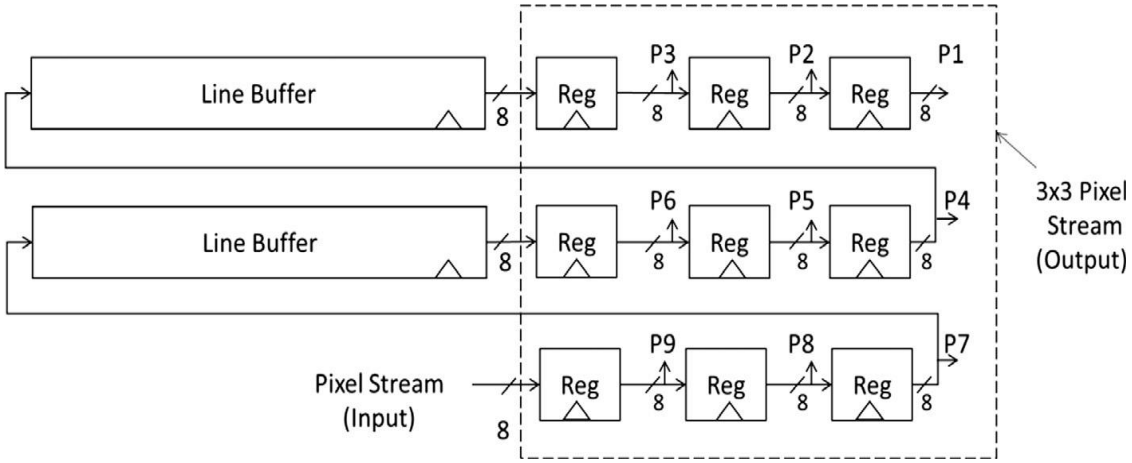

Figure 3.3 3x3 sliding window architecture

The impact of the 3x3 sliding window is done via the architecture shown in Fig. 3.3, the architecture of the sliding window. This architecture takes a pixel stream of the image as input (one pixel per clock cycle) and provides a 3x3 pixel stream (3x3 pixels per clock cycle) as output after an initial delay approximately equal to the time needed to fill the line buffers. The output, 3x3 pixel (P1, P2,P3. . .P9) stream is used in computation with the 3x3 filter mask (kernel) of a particular filtering operation.

Most of the current GF filter design shows approximation of kernel coefficients (Davies, 2012), change of window size, architectural modification and use of approximate arithmetic in precise design. The coefficients of the floating point kernel are estimated to a fixed point and a two-form sum of power to reduce the complexity of implementation. In addition, distinct kernel window sizes are regarded for quality energy trade-off. In addition, some methods change the architectures to obtain energy-scalable Gaussian filtration. Lastly, by embedding approximate adder, some of the energy-efficient

architectures are acquired. These architectures provide a high-quality trade in energy.

The smoothing of the initial picture eliminates the random noise and irregular intensities that can lead to redundant false edges in the edge detected picture. It conjointly aids within the image binarization (image thresholding) step by decreasing the false black pixels within the binary image. The Gaussian filter architecture is shown in Fig.3.4 The actual image is smoothened via Gaussian filter.

$$k = \frac{1}{16}\begin{bmatrix} 1 & 2 & 1 \\ 2 & 4 & 2 \\ 1 & 2 & 1 \end{bmatrix}$$

$$I_G = k * I$$

$$\mathrm{P5}' = (\mathrm{P1} + 2 * \mathrm{P2} + \mathrm{P3} + 2 * \mathrm{P4} + 4 * \mathrm{P5} + 2 * \mathrm{P6} + \mathrm{P7} + 2 * \mathrm{P8} + \mathrm{P9})/16 \quad (3.1)$$

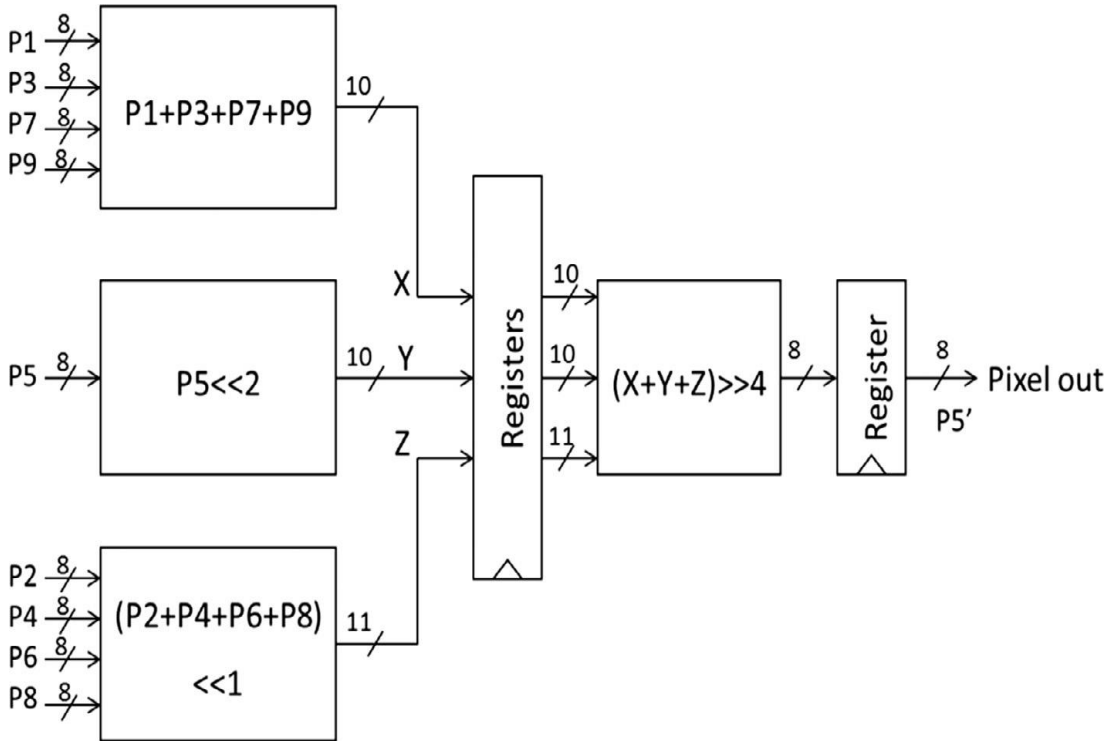

Figure 3.4 Gaussian Filter architecture

The Gaussian filter design indicates in Equation the 3x3 filter mask or kernel (k) for Gaussian picture processing. The Eq 3.1 shown above convolves k with the input picture (I), giving a smooth picture (IG). Multiply k components with respective picture window pixels to get the weighted amount as per Eq 3.1. Gaussian filter module's hardware architecture uses the Eq 3.1. as illustrated in Figure 3.5. In addition to the adders, the architecture uses the shifters to perform operations of multiplication and division, and in a single clock cycle, shifting is obtained by more than one bit. To get 1 output picture element turnout per clock cycle within the design, the pipeline register area unit

has been introduced. The pixel input values (P1, P2, P3 .. P9) alter each cycle of the clock.

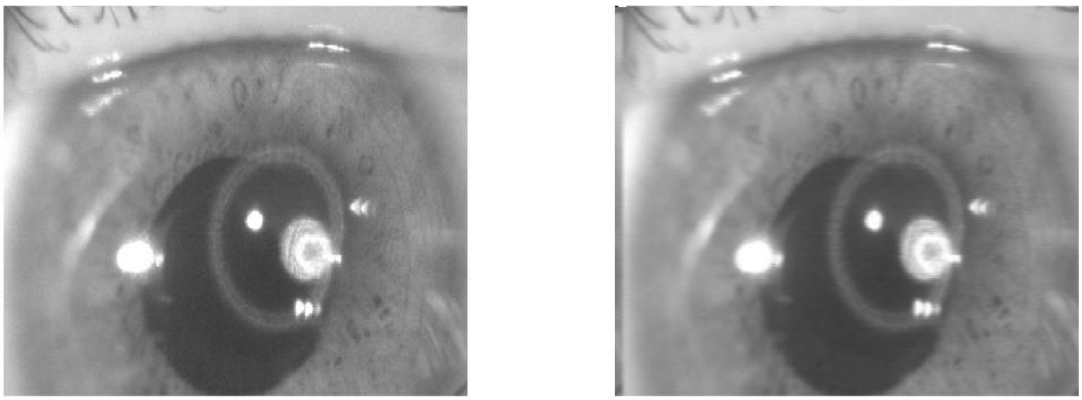

Human Eye original image Gaussian filtered Image

Figure 3.5 Gaussian filtered output image

3.3 MEDIAN FILTER

Median filter is one of the second techniques of image filtering. A median filter is a non-linear digital image filtering method (C. Chen et al.,2013). The median filter technique is mostly used for expelling noise or blur from the signal or image. This reduction of blur or noise is a common filtering or preprocessing steps to enhance the outcomes of subsequent processing. The detection of edge in an image can be denoted as an example. Median filtering is widely used in the processing of digital images since under some laws or conditions the median filtering preserves edges on the particular image when mitigating the noise and also possesses applications in digital or signal processing. The boundary issues in median filtering are,

a) Dodge the boundaries processing with or without adding the signal and image boundary conditions.

b) Fetching the attributes related to images in the signal. The images in example entries from the boundaries of horizontal or vertical elements could be selected.

c) Shrinking the boundaries near the window such that every window is complete.

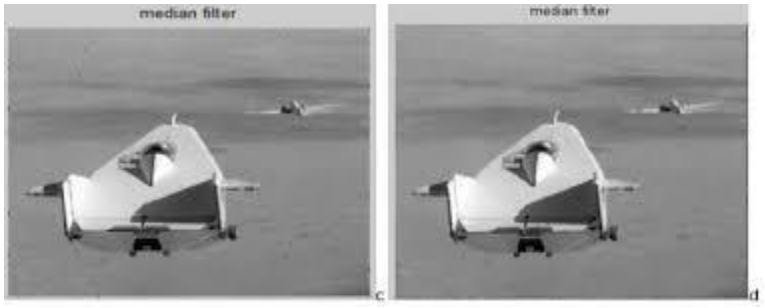

Figure 3.6 Median Filter

The Median Filter shown in Figure 3.6 is comes under the non linear digital image filtering technique or method. The median filter technique is mostly used for expelling noise or blur from the signal or image. This reduction of blur or noise is a common filtering or preprocessing steps to enhance the outcomes of subsequent processing.

3.3.1 Objective of Median Filtering

The objective of median filtering technique is mostly used for expelling noise or blur from the signal or image. This reduction of blur or noise is a common filtering or preprocessing steps to enhance the outcomes of subsequent processing. The objectives are as follows,

a) To exclude signal weakening which includes counters of objects and edges blurred.

b) Make sure better pixels of the image are intact regardless of the volume and noise density of the image.

c) Abstain from the situation of replacing the acknowledged pixel of noise with some other pixel of noise.

d) Mitigate the algorithm’s time complexity.

e) Facilitate the median filtering to sense and preserve details of redundant noise in images.

3.3.2 Hardware Implementation of the Median filter

The median filter is normally accustomed scale back noise in a picture, just like the mean filter. Median filter, however, is more better than medium filter because it maintains significant picture information like edges (Dongkyun Kim et al.,2012). The median filter also operates like a medium filter. It examines each pixel of the picture and whether or not that specific pixel is the representative of its neighbors. Rather than replacing the constituent's value with the average of its neighboring unit values.

It substitutes for the neighboring constituent values median. The median is measured by first cataloging into numerical order all the constituent values from the surrounding neighborhood, then replacing the constituent being thought-about with the constituent value of the center. If the middle constituent square neighbors measure in even variety then the mean of the square measure of the 2 middle constituent values used. Neighbor values-115,119,120,123,124,125,126,127,150

115	119	120
123	124	125
126	127	150

Figure 3.7 Sample 3x3 image window

The above shown Figure 3.7 calculates the middle value of a pixel neighborhood. The center constituent value of one hundred and fifty is very atypical of the surrounding pixels and is substituted by the average value: 124.

The improved median filtering algorithm alike the adaptive median filter and the standard median filter, while implemented lessened the noise in the image. While the chosen signaling window, the simple strategy is to look at the sample values and change the clatter and indistinct or blurred pixels with the median / efficient average. A on-the move fastened 3 × 3 window with constituent neighborhood is employed for this strata. The operation of the enhanced algorithm is implemented for each motion. The usage of 3x3 fixed window reduce the complexity and the time needed to sort the ascending pixel

values. The algorithm suggested pull off very decent outcomes whilst the impulse noise in the picture is either 50% or less than it.

Sorting of window pixels to extract average is accomplished by 2 methods: commonplace and multilayer. In a commonplace methodology, a 3×3 median window that holds 9 pixels is sorted together via 8 bit comparator elements (or pixel comparators). Fig. 3.8 reveals the structure of Interior comparator elements. These components evaluate 2 pixels, and propel higher worth constituent into the output, H and lower constituent into the output, L.

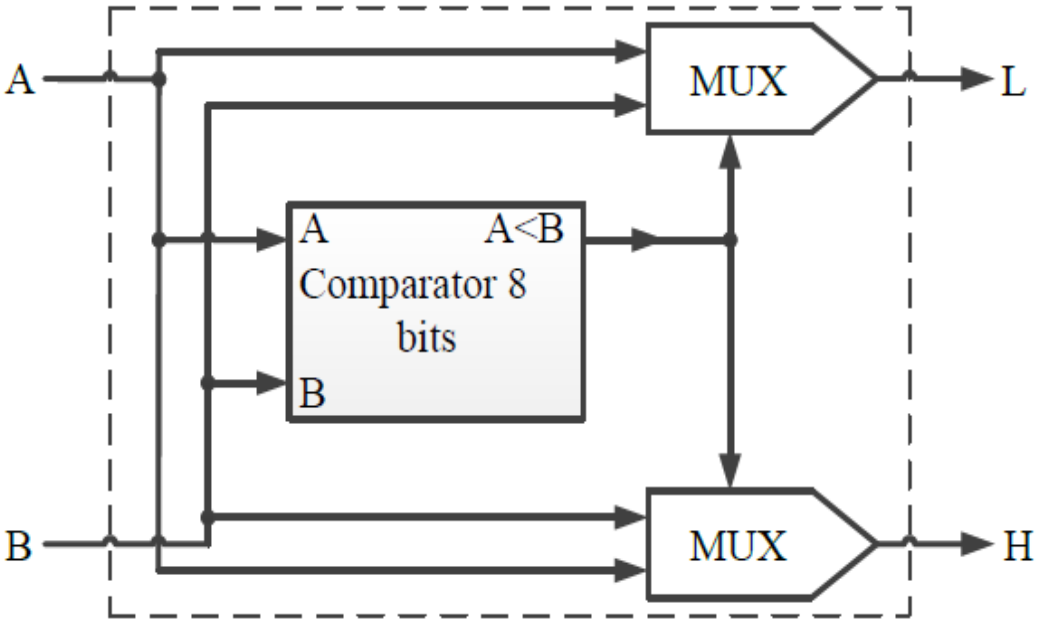

Figure 3.8 Internal structure of comparators

Figure 3.8 shows some changes might be created within the customary algorithmic program to scale back needed hardware components to apply the median filter. As a replacement of sorting all 9 pixels collectively for this

purpose, each column of the median window is categorized in 3 sorting blocks separately. These sorting blocks categorize in ascending order the 3 input pixels. The outputs of these are subsequently divided into 3 fresh sorting blocks and categorized in layer 2 again. The average value in the production of layer 3 could be obtained by continuing this operation. This technique is a media filter multilayer application. The structure of the multilayer sorting algorithm for 9 pixels of a three-way window is shown in Figure 3.9 (D. Richards,1990). As in Figure 3.8, the 3 comparators shown helped in the construction of each of the sorting block in Figure 3.9

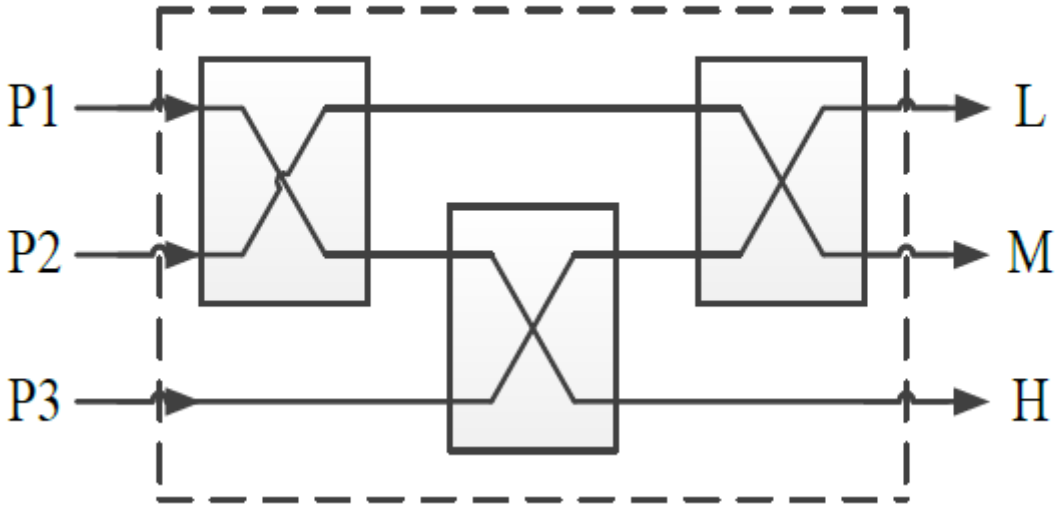

Figure 3.9 Arrangement of a 3 pixels sorting block

Method for multilayer application was suggested based on the removal of non-median pixels. In reality, the average value could not be any pixel that is greater or smaller than 5 of the other pixels in the median window. This technique proved that the output of the filter is the median pixel as shown in Figure 3.10. using only 7×3=21 comparator elements (M. Karaman.,1990).

Pipeline structure is introduced for this method (S. A. Fahmy et al.,2005). The displayed structure reduced number of comparator to 15. In this framework, instead of sorting median window columns into distinct 3 pixel sorting blocks, single block is used to categorize all columns in the filter layer one.

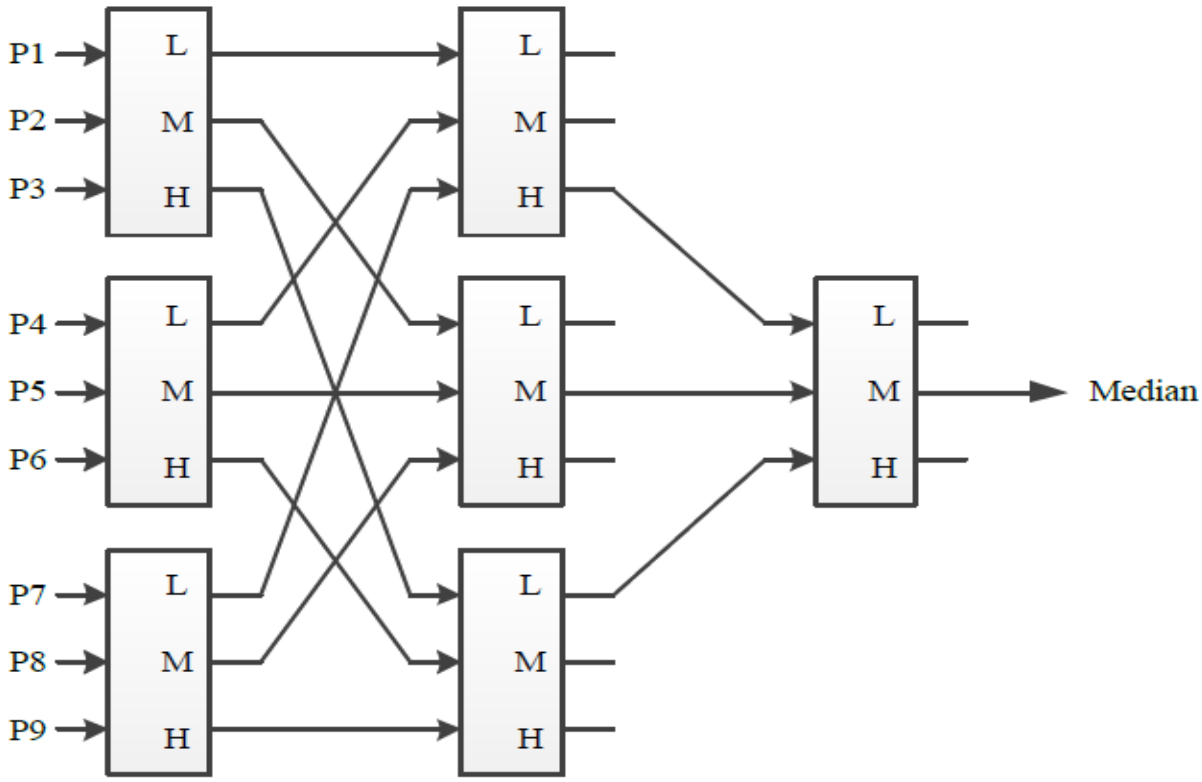

Figure 3.10 Multilayer sorting of pixels.

The figure multilayer sorting of pixels recommend for a 3-level pipelined filter with pipelined median multilayer architecture as depicted in Figure 3.10. In the projected structure, the 3 levels of filter used are pipelined. This construct recognizes as input 9 pixels and returns as output the median pixel.

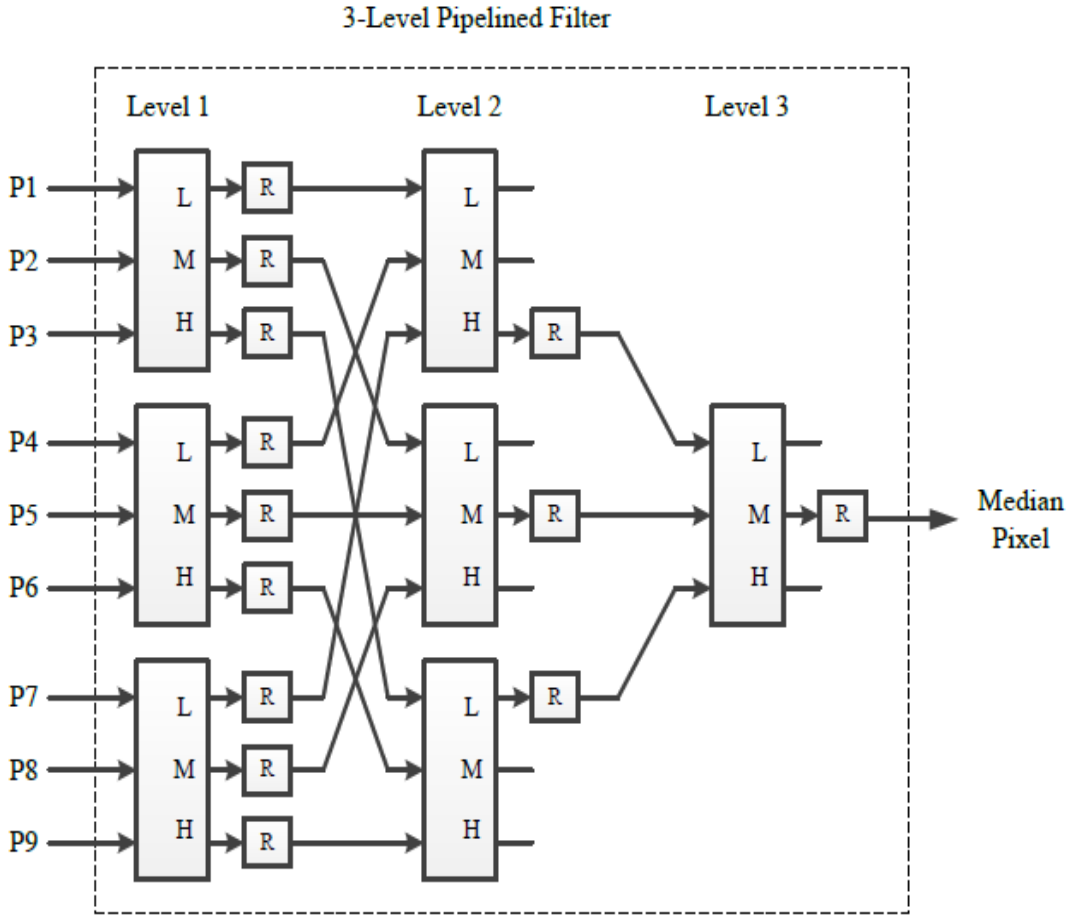

Figure 3.11 Architecture of multilayer median filter

The Figure 3.11 shows the association between the pixels in a 3 × 3 window is primary. They encompass a huge impact on one another, and the distortion that happens is very insignificant if any of them are substituted by the other. When the window size grows, the association between the pixel at the far end of the window and the middle pixel value has a secondary relationship in a 5 × 5 window furthermore a tertiary relationship with the 7×7 window. Consequently, the pixel value at the sloping end of a larger window is not directly related to the center value and can therefore lead to a major

distortion. The enhanced median filter adheres the method of overlapping windows from the normal median filter and the adaptive median filter.

3.3.3 MATLAB Results of Median Filter

MATLAB is a computing language of high efficiency. It incorporates computing, visualization and programming in an easy-to-use setting where well-known mathematical notation expresses issues and solutions. Typical uses comprise:

- Mathematical computations
- Developing algorithm
- Modelling, simulation, and prototyping
- Data examination, exploring, plus visualizing
- Technical and engineering graphics
- Developing Application using graphical user interface

MATLAB is a mutual system whose fundamental part is an array that doesn't necessitate orienting. This enables to unbind several technological computing issues, particularly those with matrix and vector formulations, during a blink of the eye you may want to write a program in a non-interactive scalar language such as C or FORTRAN.

Matrix laboratory referred as MATLAB enables quick access to matrix computer code promoted by the LINPACK and EISPACK projects. At present, the code developed by the LAPACK and ARPACK used by MATLAB, which is the high-tech in matrix computation software.

MATLAB has developed as a vital tool in various fields over a number of years by many users. It is a commonly accepted instructional tool for introductory and sophisticated university mathematics, engineering and science research. In enterprises, MATLAB is the preferred instrument for studies, growth and to assess productivity.

MATLAB provides application-specific alternatives otherwise referred as toolboxes.

MATLAB enables specific technology to be taught and used by toolboxes. Toolboxes are large collections of MATLAB features (M-files) that extend MATLAB's boundaries to meet particular contentious regions. Tool boxes are offered in region like signal processing, managing systems, wavelets, neural networks, symbolic logic, and simulation.

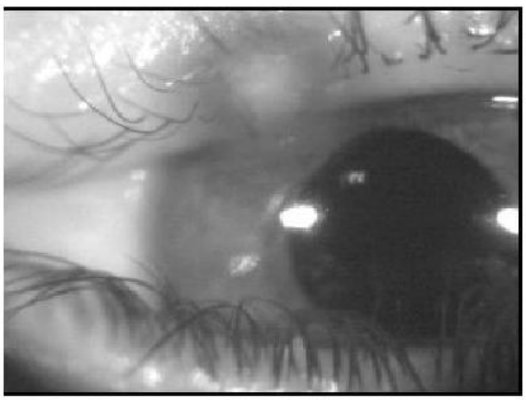

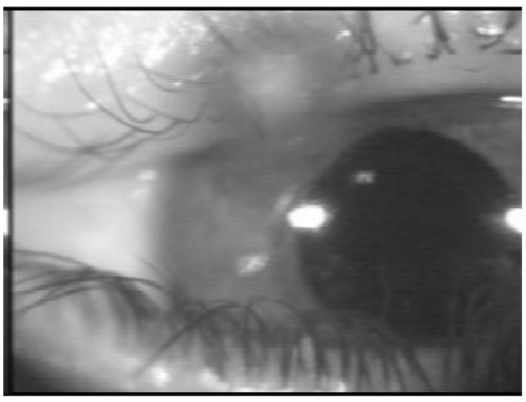

Figure 3.12a) Noisy Image **b) Median Filtered Image**

Figure 3.12 Median filtered output image

Figure 3.12 a. Noisy image converted as hex file from Matlab. This Hex file is given to Modelsim and applied median filter. Filtered output write into another hex file and read as a image in Figure 3.12 b. from Matlab.

3.4 EDA TOOLS SPECIFICATION

Pupil Detection Hardware architecture design is done by Verilog HDL. Both Gaussian and Median filters are written in Verilog HDL and its importance explained in below. Simulation waveform is obtained through Modelsim EDA tool. Synthesis and FPGA implementation carried out in ALTERA Quartus II tool.

3.4.1 Popularity of Verilog HDL

Verilog HDL, a typical hardware description language offers several helpful options for hardware style. Verilog HDL could be a common hardware description language is simple and ready to use as shown in Figure 3.13. It is alike in syntax to the C artificial language. Experts in C programming can recognize Verilog HDL.

Verilog HDL allows the mixing of distinct design levels within the similar model. Thus, a programmer will outline a hardware model behavioural code. By understanding one language for input and hierarchical design a programmer can work with ease. Verilog HDL, a language of choice for programmers is compatible in many of the logic synthesis tools .

Verilog HDL libraries are offered by manufacturing suppliers for simulation of post logic synthesis. Verilog HDL therefore allows the widest vendor option. The Artificial Language Interface (PLI) may be a strong characteristic that permits user to write custom C code to travel with Verilog's

internal knowledge structures. With the PLI, designers will tailor a Verilog HDL machine .

3.4.2 VHDL

VHSIC (Very high Speed Integrated Circuit) Hardware Description Language, an associate of VHDL is a hardware description language to portray the structure and/or behavior of hardware designs moreover to sculpt digital systems confining from the algorithmic to gate level. The VHDL design is capable to be simulated and/or synthesized, making it possible to rapidly create complex hardware models.

```
ENTITY entity_name IS
        generics
        port declarations
END entity_name;

ARCHITECTURE arch_name OF entity_name IS
        enumerated data types
        internal signal declarations
        component declarations
BEGIN
        signal assignment statements
        process statements
        component instantiations
END arch_name;
```

Figure 3.13 Basic Modeling structure for VHDL.

3.4.3 Modelsim SE 10.1a

This chapter discusses ModelSim's fundamental simulation procedure.

3.4.3.1 Basic steps for simulation

Step 1 – Collecting and Mapping Libraries Files required to run on ModelSim:

Step 2 - Designing files (VHDL and/or Verilog), as well as stimulus for the design libraries, together working and resource modelsim.ini file (routinely created by the library mapping command) .

Step 3 - Providing Stimulus to the Design.

Stimulus to a design can be provided in numerous ways:

- Based on language
- Interactive ModelSim command force based on Tcl
- Developing a VCD File and use Extended VCD as Stimulus
- Third-party generation tools.

3.4.4 Simulation Environment

A specified environment is required to conduct a simulation in the Unix file system. The simulation environment defined in the file 'modelsim.ini' is mandatory in the current directory from which Modelsim is initiated. The simulation environment is in the library structure that includes standard libraries (e.g. 'IEEE') as well as customized, design centric libraries.

Three user defined libraries used during the lab are – 'DESIGN', 'TB'and 'SYNTH' i.e the working library, the test bench library, and a library for simulations respectively. A library in the file system is represented by a folder. It is not necessary to create the necessary directories ' DESIGN, ' ' TB ' and ' SYNTH ' with the command mkdir because Modelsim would not render them out as libraries. The standard libraries are available in the system and are hidden for the user. It is created automatically by a script at the outset of the laboratory. If there is no structure, kindly contact the supervisor.

3.4.4.1 Simulation flow

The VHDL descriptions code is compiled into a binary machine friendly format. VHDL compiler is inbuilt with Modelsim. The Compiler also verifies the syntax and searches for the used libraries. The binary knowledge for simulation is held in the library after compilation. The simulator initiates only following the identification of the signals to be traced and shown. The simulation results are stored either in a wave form file or otherwise the file ’vsim.wlf’ is created or revoked in the current directory. This file represents the basis for analysis of simulation results and is read by the graphical user interface of the Modelsim automatically once a simulation has completed. Figure 3.14 illustrates the simulation flow.

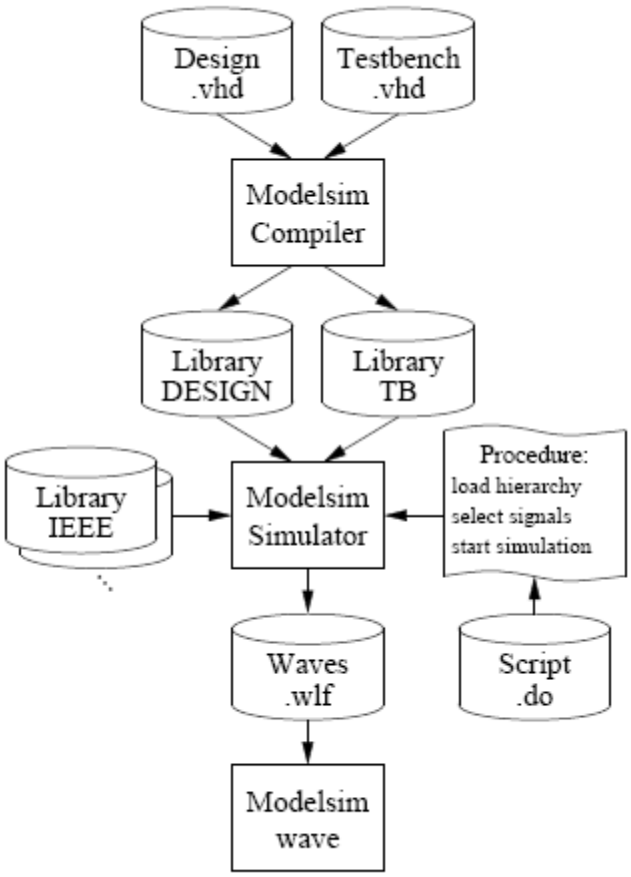

Figure 3.14 Simulation Flow

3.4.4.2 Graphical User Interface (GUI)

A feasible method to simulating VHDL code is implemented in this chapter. Modelsim offers several simulation options and supportive commands.

3.4.4.3 Compiling

Figure 3.15 shows the window once the item ' Compile ... ' from the ' Compile ' menu is chosen to compile a VHDL code. The design is collected into

the target library in the upper portion of the window in the pull down field. Select one or more VHDL files using the navigation, window. VHDL files are accumulated into the denoted library. The Command Window points out the errors in the VHDL code, warnings and messages of the compiler. The Selected Source Code is edited by ‘Edit Source’ if required. The switch ’Check for: Synthesis’ inside’default Options...’ if enabled allows synthesis during compilation. The compile window remains open, till ‘Done’ is clicked. This allows multiple processes to be started successively, as well as in separate librariesIt is vital to begin with the smallest level and follow the hierarchy to the top in order to compile a hierarchical circuit description. Once the complete hierarchy has been compiled , recompiling only the modified files is adequate in several cases.

For selecting one or more VHDL files, the navigation window is used. The selected VHDL files are compiled into the denoted library by clicking on' Compile.' VHDL code errors and warnings and emails from the compiler are displayed in the command window. You can edit the chosen source code with' Edit Source'.

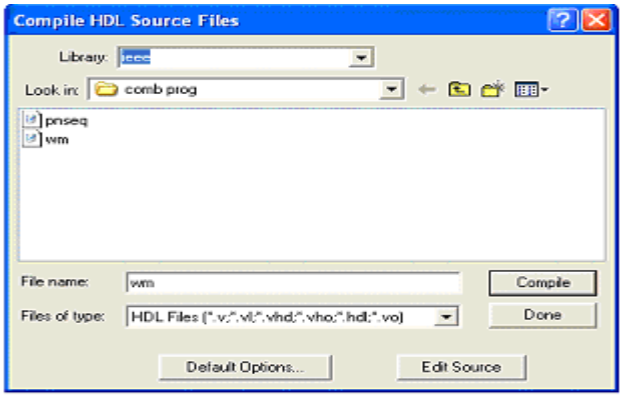

Figure 3.15 Compiler Window

The design is collected into the target library in the upper portion of the window in the pull down sector. For selecting one or more VHDL files, the navigation window is used.

3.5 MODEL SIM SIMULATION

ModelSim could be a authentication and simulation tool for Verilog VHDL, System Verilog and mixed language designs. This lesson offers a fast abstract impression of the environments of the ModelSim simulation. It is split into four subjects that you will learn more about in the classes that follow are shown in Figure 3.16.

- Fundamental flow of simulation
- Flow of the Project
- Flow of the Multiple library
- Tools for debugging

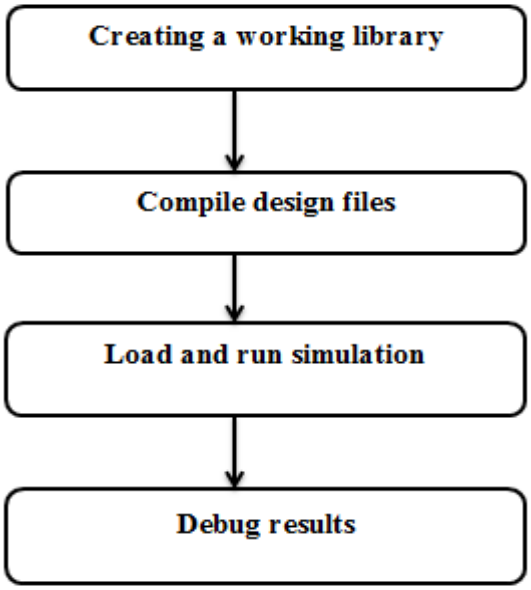

Figure 3.16 Model SIM Simulation Flow.

3.6 MEDIAN FILTER SIMULATION OUTPUT

Simulation results showed the performance of improved median filter. Simulation is done by Altera- Modelsim 10.1d and design is in Verilog language.

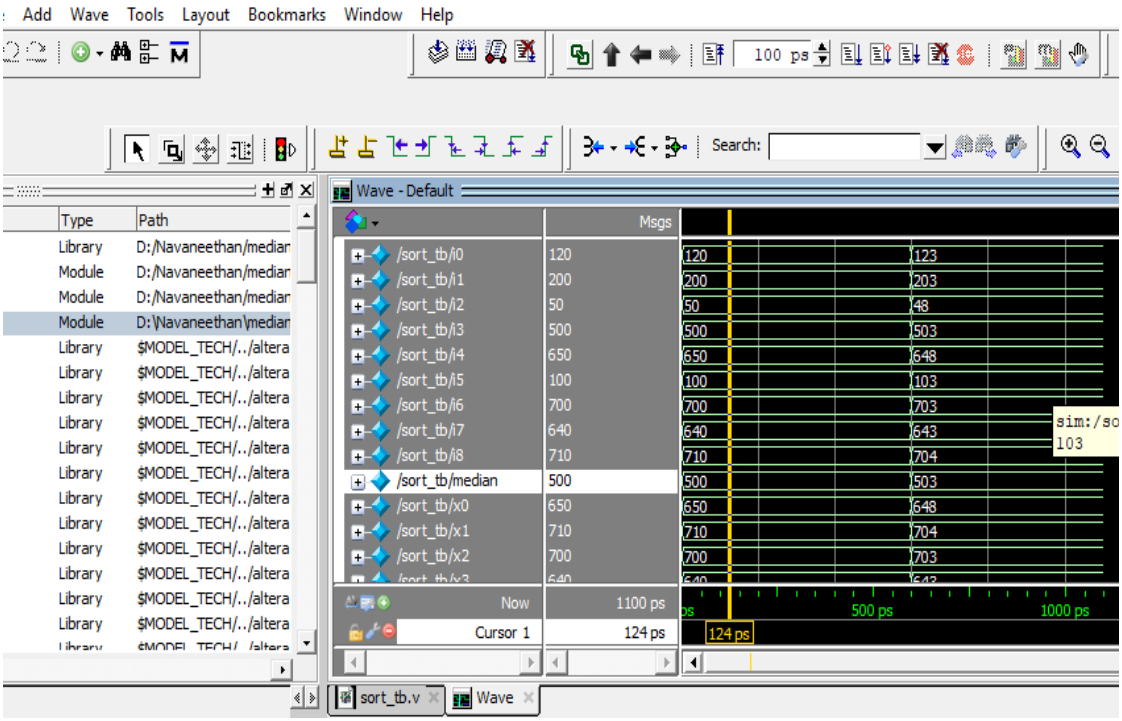

Figure 3.17 Improved Median Filter output waveform

In Figure 3.17, input pixel data's are given to median filter 120,200,50,500,650,100,700,640,710. After sorting 50,100,120,200, 500,640,650,700,710. The median value 500 is shown in the output waveform.

3.7 SYNTHESIS RESULTS OF MEDIAN FILTER

Synthesis and FPGA implementation carried out in ALTERA Quartus II tool.

3.7.1 Quartus II Design Planning

The first step in style to come up with is to select your application's easiest device. The device selection impacts the rest of your style cycle, as well as board specification and design. The majority of this planning is carried out outside the software of Quartus II, but this chapter offers some suggestions to

help with the scheduling process. Choosing the family of devices that best fits your design specifications is essential. Dissimilar families offer different trade-offs, including cost, performance, logic and memory density, I/O density, power utilization, and packaging. Different groups give various trade-offs, inclusive of price, efficiency, density of logic and memory, density of I / O, use of energy, and packaging. Feature specifications such as support for I / O norms, speedy transceivers, global / regional clock networks, as well as the amount of phase-locked loops (PLLs) accessible in the computer should also be considered. Within the Selector Guides available on the Altera website, you can review the required alternatives of each device family.

A difficult aspect of the design planning process can be the determination of the necessary device density. Devices with lots of logical resources and improved I / O counts will introduce bigger and possibly more complicated designs, but may cost more. Choose a machine to meets your design criterion with certain safety margin, if you want to insert more logic to the style cycle later or set aside on-chip debugging logic and memory believe about the needs for particular types of dedicated logic blocks, like memory blocks of varying dimensions, or digital signal process (DSP) blocks to execute certain arithmetic functions. You can use their source usage as an estimate for fresh design if you have previous designs that target Altera equipment. With the device selection set to Auto, you can compile existing designs in the Quartus II software to review the use of resources and discover which device density fits the design.

Altera proposes to solely use the latest version of third-party synthesis instruments since tool suppliers often add fresh characteristics, solve tool problems, plus improve Altera device efficiency. The Quartus II Software

Release Notes lists the version of each synthesis tool officially supported by the Quartus II software version. To use the correct Library Mapping File (.lmf) for your synthesis netlist, state your synthesis tool in the New Project Wizard or the EDA Tools Settings page of the Settings dialog box. Synthesis tools can provide the ability to create a Quartus II project and pass restrictions such as the setting of the EDA tool, the choice of devices and the timing requirements specified in your synthesis project. This capacity can be used to save loads of time once your Quartus II project has been set up for positioning and routing. You should partition your style for synthesis and create various output net list files if you want to take benefit of an incremental compilation methodology.

3.7.2 Device summary of Median filter Synthesis Result

Figure 3.18, Altera cyclone II FPGA consumes 3101 logic elements, 1466 combinational functions and 2352 dedicated logic registers. This resource utilization showed 9% in the total logic elements.

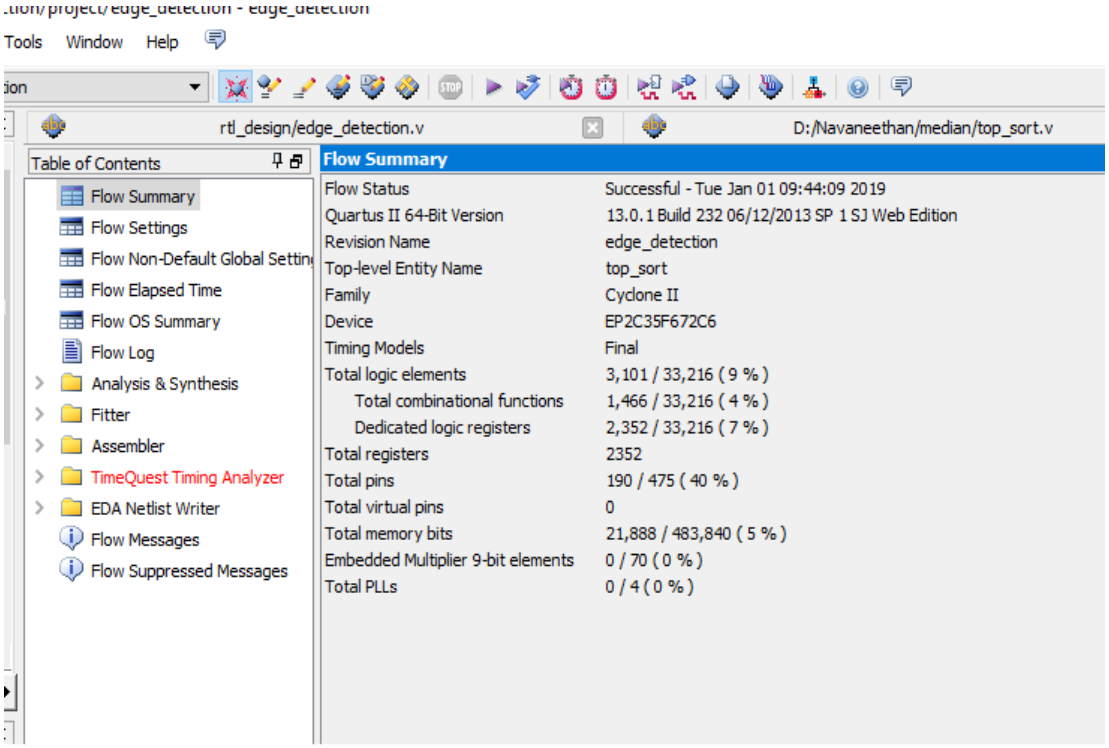

Figure 3.18 Synthesis result of Improved Median filter in Cyclone II EP2C35 FPGA

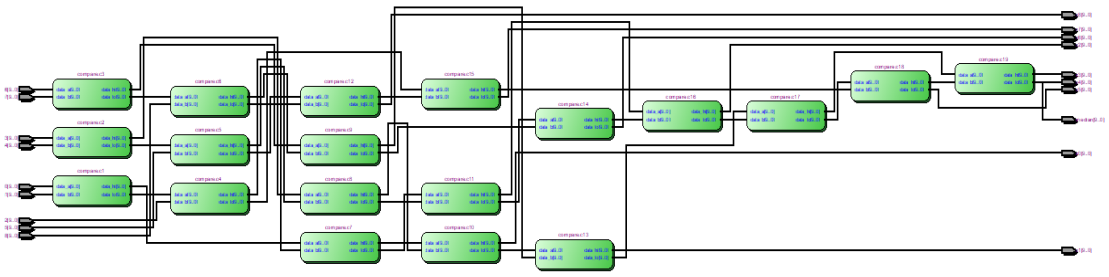

Figure 3.19 RTL view of Median filter

Figure 3.19 represents complete RTL schematic of the improved median filter design.

3.8 SYNTHESIS RESULTS OF GAUSSIAN FILTER

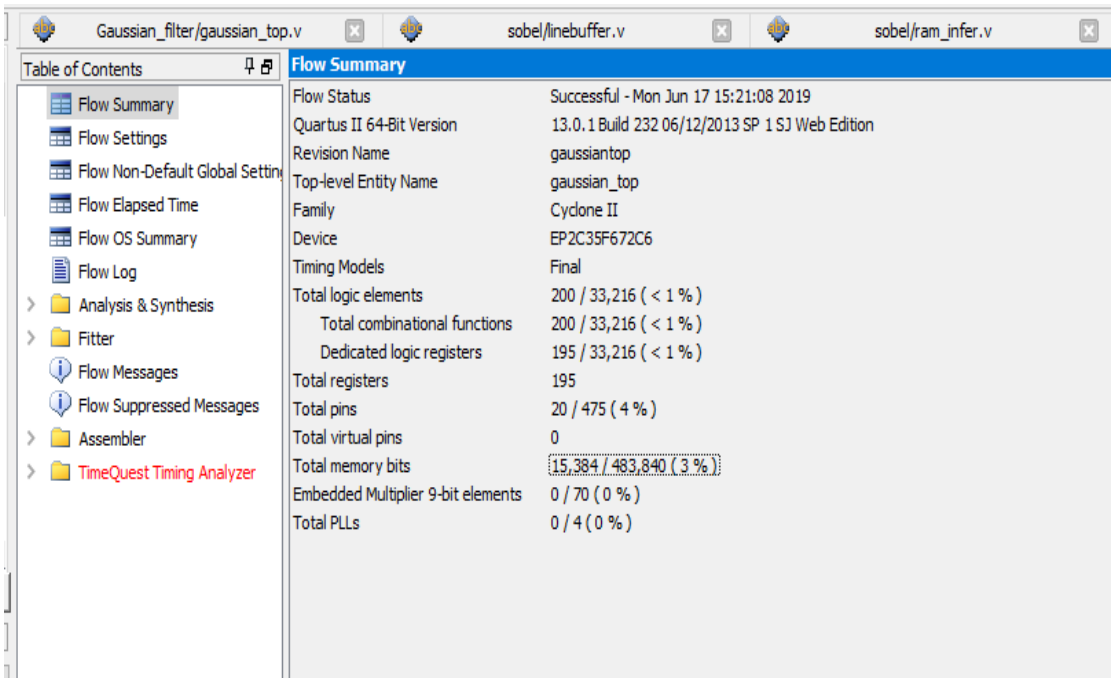

Figure 3.20 Logic element utilization of Gaussian filter in Cyclone II EP2C35 FPGA

Figure 3.20, Altera cyclone II FPGA consumes for Gaussian filter are 200 logic elements, 200 combinational functions and 195 dedicated logic registers and 15384 memory bits. Figure 3.21 shows RTL Schematic outlook of Gaussian filter **.**

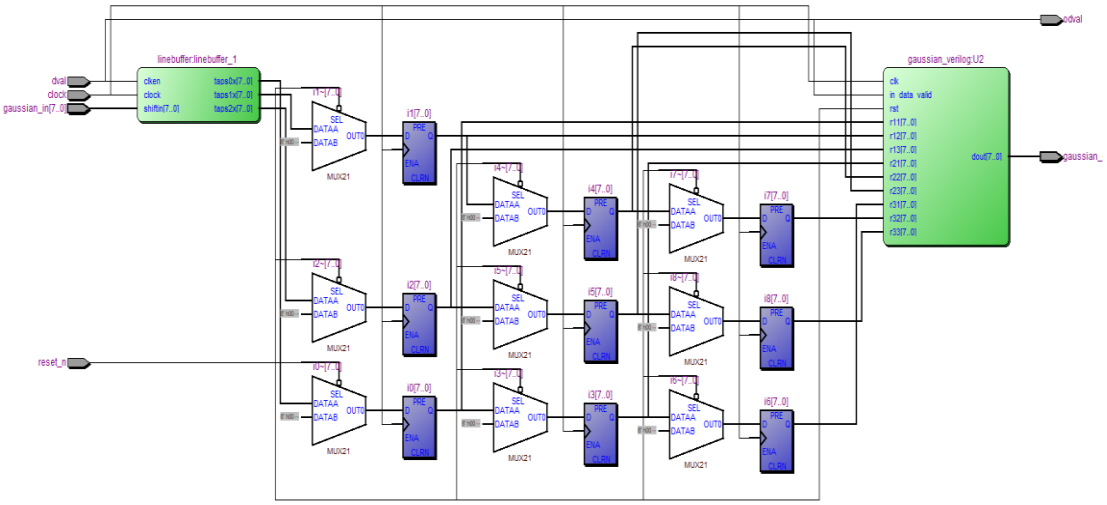

Figure 3.21 RTL Schematic view of Gaussian filter

To create a suitable power budget and design the supplies for power, voltage regulators, heat sink, and cooling system, device energy consumption must be correctly estimated. The estimation and analysis of power has come up with 2 important requirements:

- Thermal planning means that the cooling solution is adequate to disperse the heat produced by the machine. In specific, the temperature of the worked out junction is required to fall within the requirements of the ordinary device.
- Power provider planning— Power supplier should provide sufficient current to sustain the operation of the device.

Power consumption in FPGA systems relies on the design, making the specification and layout of the board a challenge. The Altera Power Play Early Power Estimator spreadsheet permits estimating power consumption prior completion of the design by processing information on the device resources used in the design, plus the operating frequency, toggle rates and environmental considerations.

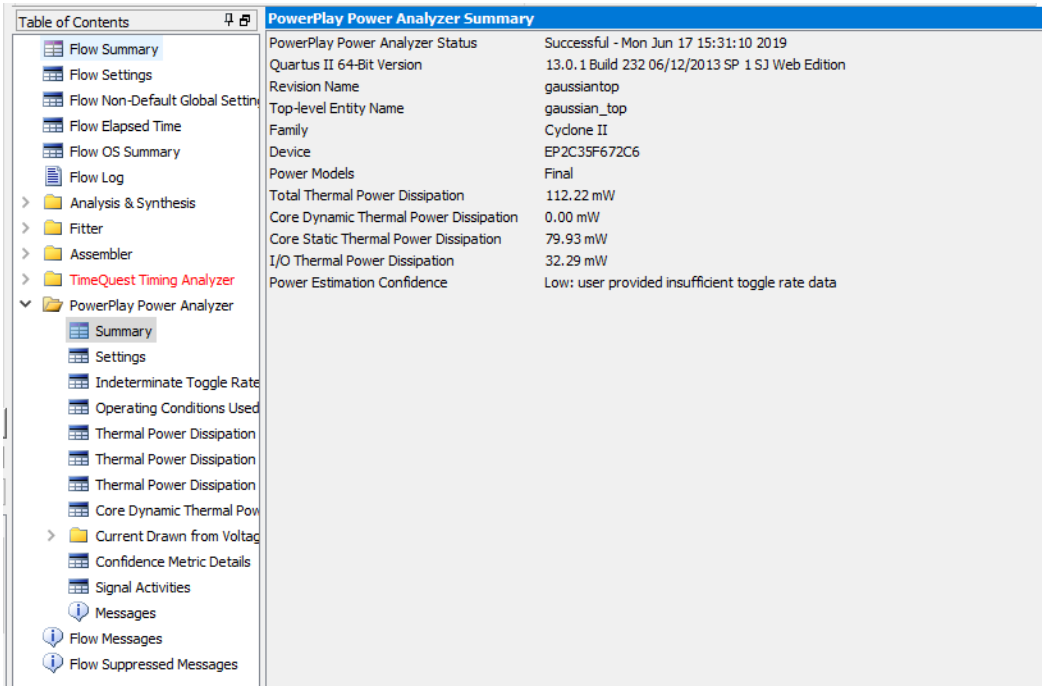

Figure 3.22 Power dissipation of Gaussian filter

Figure 3.22 shows the total power dissipation of 112.22mw, and other power dissipation of Gaussian filter.

3.9 CONCLUSION

This chapter concludes the image enhancement for human eye using Gaussian and Median filter techniques with Matlab output and also Model sim waveform output. Synthesis is done by Altera quartus II tool for device utilization and RTL schematic view.

CHAPTER 4

MORPHOLOGICAL OPERATIONS WITH EDGE DETECTOR

This chapter discusses the threshold applied to separate the human eye pupil region followed with morphological operation and sobel edge detection technique.

4.1 GLOBAL THRESHOLD

Thresholding aims to segment a picture by locating to one intensity level wherein all pixels whose intensity exceeds a certain threshold value, while setting to intensity level the pixels whose intensity is lower than that threshold. Various threshold images shown in figure 4.1.Typically thresholding ultimately binarizes an image by altering every pixel to ‘0’ or ‘1’, ‘0’ being black and ‘1’ being white. This alteration reduces the size of the figure moreover is advantageous in relevance with fax machines and copy machines.

Standard thresholding for the whole picture utilizes a universal threshold value. The pixel value of interest is compared with the global threshold, to set the new pixel value as black if lesser or white if it is greater. For a test image which can be pre-determined to be 8-bit grayscale, an instance of this method can be seen below wherein the specified global threshold is 30.

Binary image is a simple generating thresholded image. To realize binary image, it is designed to generate functionalities import to the threshold of image module. Dramatically, It is essential to coordinate binary images with

generation of calculation and processing intensity values in binary format. Here manual threshold value is applied to separate human eye pupil region from the eye image. The constant threshold value here is 30.

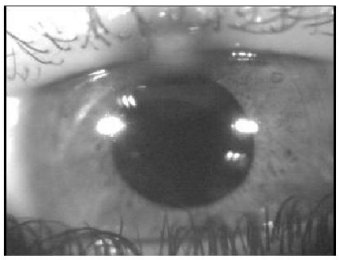

Original Image

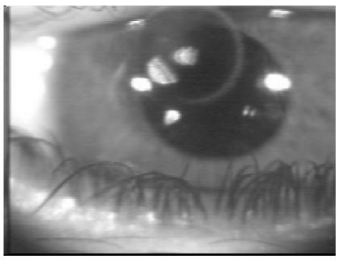

Gaussian filter image

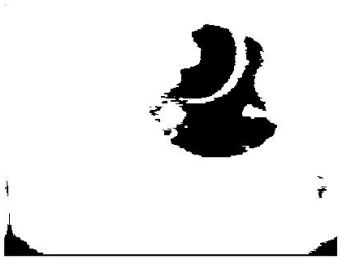

Threshold image

Figure 4.1 Thresolded image

4.1.1 Synthesis Result of Global Threshold

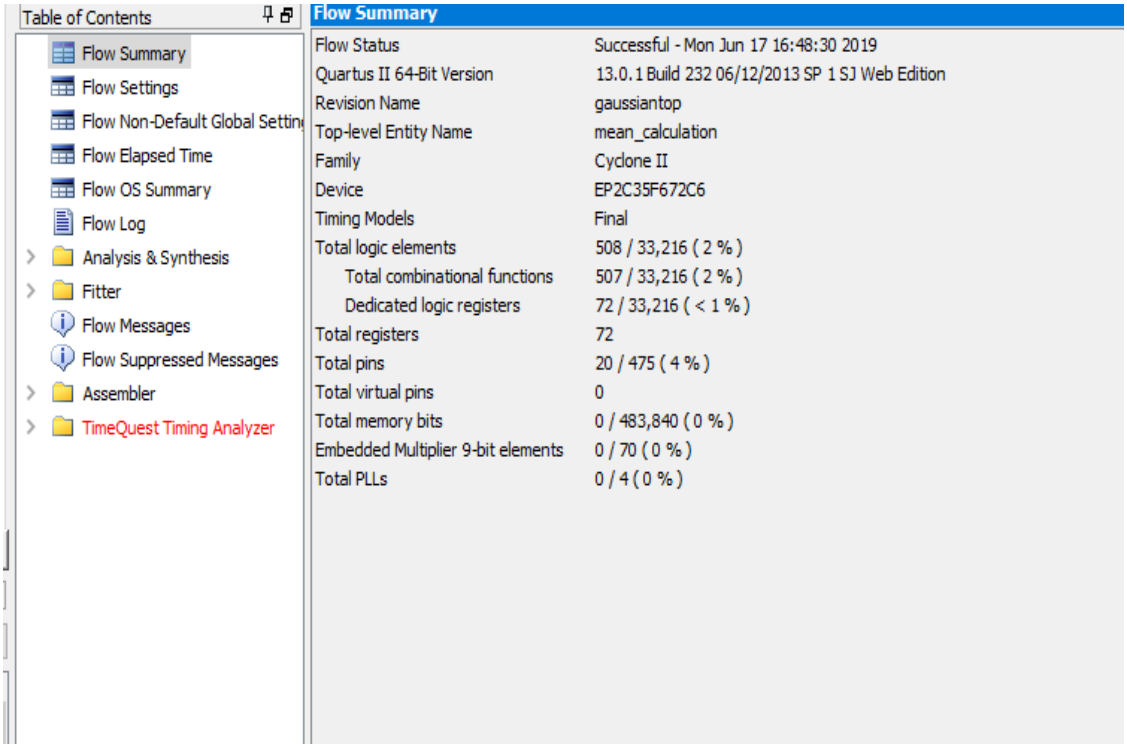

Figure 4.2 Logic element utilization of Global Threshold

Figure 4.2 shows the Altera cyclone II FPGA consumes for Global threshold are 508 logic elements, 507 combinational functions and 72 dedicated logic registers. Figure 4.3 depicts RTL Schematic view of Global Threshold.

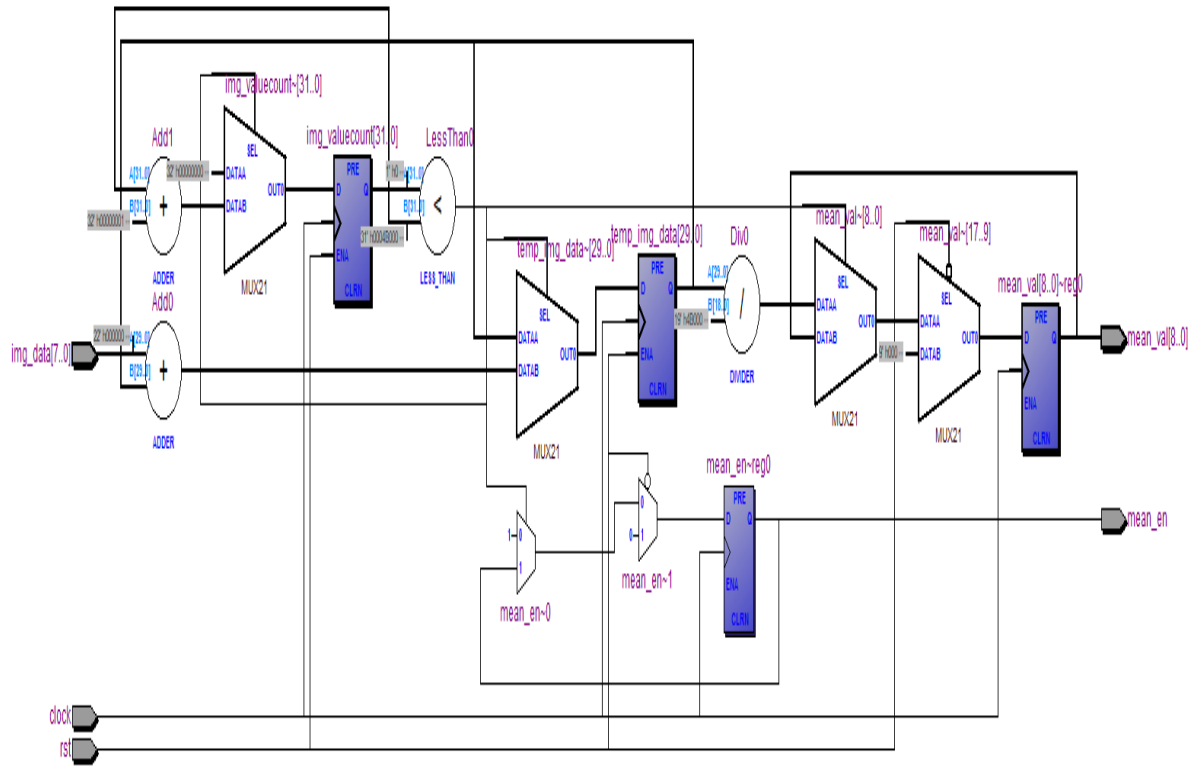

Figure 4.3 RTL Schematic view of Global Threshold

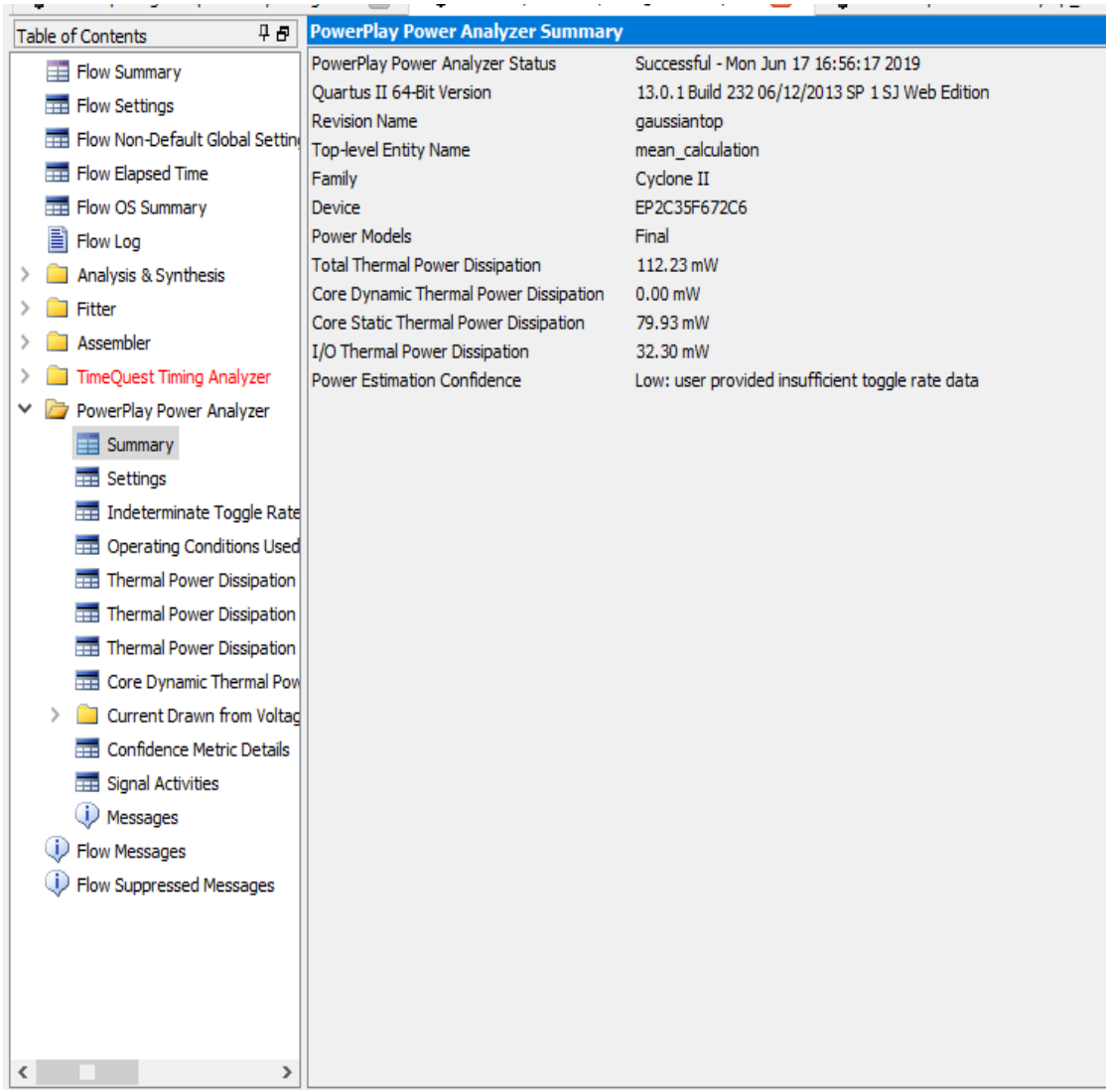

Figure 4.4 Power dissipation of Global Threshold

Figure 4.4 shows the total power dissipation of 112.23mw and other thermal power dissipation.

4.2 MATHEMATICAL MORPHOLOGY

The basic operators of Mathematical Morphology include: Binary Dilation and Erosion, Binary Opening and Closing.

Mathematical morphology is powerful method which is essential for shape information to image geometrical structures, depending on clinical practice, topology, random functions and lattice theory. Its miles maximum generally implemented to impact of images, although it can be documented in solids, spatial systems, areas ranging graphs, and surface meshes. Regularly instances, human beings might follow dilation, erosion, opening, closing and edge detection when they decide to apply mathematical morphology to address pictures. In picture forensics, detecting forgeries in digital papers is becoming a main problem. The chance of using scanning, editing and printing to readily manipulate and reproduce paper files enables some of the malpractices and is also viewed as an accent activity in countless crook behavior. Atypical abuses are the generation of false documents and the manipulation of current ones in order to give statutory form to deceptive data, to whip signature and identity, to reproduce copyrighted material, to alter delicate written data viz correspondences, certifications, etc.

Typically, image analysis begins with a pre-processing phase that involves activities such as noise reduction. Segmentation should be performed before it for the specific identification phase to extract only the portion that has helpful data. Segmentation of images could be a main and challenging component of the evaluation of images. The quality of a photo analysis' ultimate outcomes may depend on the segmentation phase. On the other side, segmentation, particularly automatic image segmentation, is one among the most challenging part in image processing. The segmentation method's

objective is to outline fields within the picture that have certain characteristics that homogenize them. The definition of these characteristics should fulfill the general condition that the union of adjacent areas should not be homogenized if I tend to bring an equal set of characteristics into consideration. Usually I can establish after segmentation that the discontinuities in the picture match the limits between areas. In broad-spectrum, morphological operators rework the first figure into another figure during the interaction with the opposite figure of a particular form and size, referred as the structuring element. Spatial options of the photographs that area unit alike in form and dimension to the structuring component area unit conserved, whilst other features are suppressed. Morphological operations will therefore alter the data of the picture, sustaining the features of its form and eradicating irrelevances. Morphological operations can be used for many reasons in perspective of apps, including edge detection, segmentation, and image enhancement.

A number of significant factors concerning the morphological method are:

1. Morphological operations deal with the structural alteration process to determine a picture's dimensional content material with its inner structure formation retaining the steadiness of significant geometric features.

2. Based on properly advanced morphological algebra which can be used to illustrate and optimize.

3. In terms of a very tiny elegance of fundamental morphological operations, explicit digital algorithms are feasible.

4. There are strict theorems of depictions by which morphological filters are expressed in the regulations of the primal morphological operations.

In broad-spectrum, morphological operators convert a detailed substantial of the original image into any other image with the combined identification of definite shape and size, referred as the structuring element. Spatial features of the imagery are incorporated with shape and dimension to the structuring element instead other features are suppressed.

Therefore, morphological operations can be used for homogenized image, specific factor characteristics which are robust in prevalence data of intensity variation. Digital image processing addresses with systems that enhance image by noise removal and obtaining only the desired information. Image segmentation is a main footstep in the digital image process, dividing an image into its constituent region or object sharing homogeneous characteristics. The primary aim of the segmentation technique is to impulse a image that helps to annotate the object scene a lot of information within the region of concern. An edge is defined as borderline of objects or abrupt modification of an image which is random that assist to spot and recognize the objects in a given image (D. Chudasama et al.,2014). Region-based segmentation methods split a image into region with analogous characteristics such as colour, texture, etc.

Region Growing formula conducts an image segmentation by investigating the nearby pixels of a set of points, known as seed points, and deciding whether or not the pixels can be categorized into the seed point cluster. (Maini et al.,2009). In Split-merge technique (Er. Komal Sharma et al., 2013) whole Image that is taken into consideration as a cacophonic seed area out into quadrant till the undiversified sub-portion is acquired after the

cacophonic Merging method merges 2 neighboring areas in step with comparable characteristics.

In the latest past, a great deal of attempt has been made to blindly detect non-linear gray-level imaging filtering (Yuan et al., 2011), particularly in the median filter. Many of these techniques focus on binary images with suitable alteration, but are not specifically concentrated on the features of binary images. At the same time, though morphological filtering is generally utilized in binary image processing, it has not been used in development of forensics detection effectively to exhibit their application. This made the researchers move towards using morphology as a tool for efficient forensic detectors to manipulate images. Splicing detector was used in mathematical morphology method. In image compression, morphological operators were introduced to determine the block size. Nevertheless, no step has yet been taken to embrace a forensic technique to sense the use of morphological filters in a digital image.

4.3 MORPHOLOGICAL OPERATIONS BASED SEGMENTATION

There may be numerous flaws in binary images. Binary areas built by easy thresholding are distorted by noise and textures in certain conditions. Morphology is a wide range of image processing activities which modify pictures on the basis of their dimensions. One of the info process tactics is believed to be useful in the picture process. It has multiple applications viz eliminating noise, scrutiny of texture, extracting the boundaries via image enhancement etc . Morphological image processing pursues the objective of removing these flaws to maintain image configuration. Morphological operation area unit ensures only the accompanying ordering of image element values, instead of their numerical values, so that they have a lot of binary

images in the area unit. When applied to monochrome images, however, their lightweight transfer features exists in unfamiliar region unit and therefore their complete component values do not seem to be taken into consideration. Morphological methods check the picture with a small instance called the structuring component. This component is used to any or all doable input pictures places and produces an output of the equivalent size. In this technique, comparable pixels of input image with neighbors were endorsed by the output image picture element values region unit. This operation generates a replacement binary figure within which it'll have non-zero picture element price at that site within the input picture. Numerous structuring components such as diamond shaped, square shaped, cross shaped etc. are associated there.

4.3.1 Structuring Elements

An important aspect of the dilation and erosion process is that the structuring element usually tests the input picture. Flat structuring components consist of a 0's and 1's matrix, typically much lower than the picture being processed. The origin component in the structuring element recognizes the value of interest. The pixel in structuring unit comprising 1's, outline the structuring element’s neighborhood. These pixels are also considered in the phase of dilation or erosion. Non-flat, structuring elements apply 0's and 1's to describe the level of the x and y plane structuring element as well as adjoin height values to label the 3^{rd} dimension.

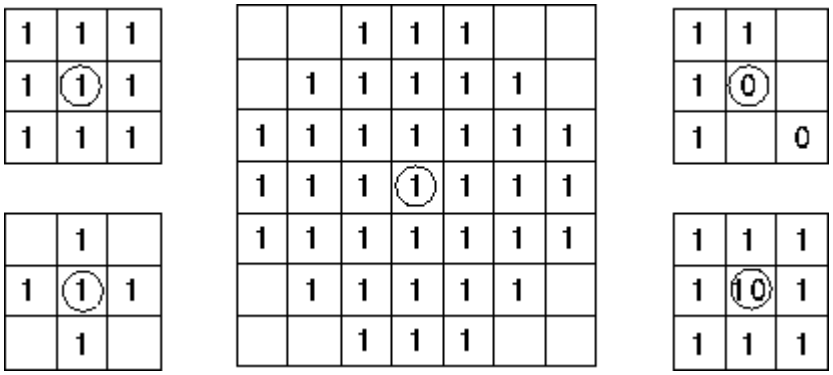

Figure 4.5 Example structuring elements.

The structuring of Figure 4.5 shows that all these morphological operators take 2 knowledge items as input. One being the input image, which for many operators can be either binary or grayscale. The other is the element of structuring. This determines the exact information of the operator's effect on the picture. Sometimes the structuring element is called the kernel, but for the similar objects used in convolutions I reserve that word.

The structuring component holds a pattern since the coordinate of variety of distinct points related to some focal point.

Normally Cartesian coordinate's area unit used then a suitable method on behalf of the component is as little figure on an oblong grid. Figure 4.6 demonstrates multiple structuring components of varying dimensions. In every case the beginning is manifested by a hoop around that time. The source need not be in the middle of the structuring element, but generally so. As prompted in the figure, the most frequently seen form is structuring components that fit into a 3 range grid with its origin in the middle.

Note that every purpose within the structuring component could have a worth. The components have only one value, conveniently represented as one, in the easiest structuring components exercised with binary images for activities like erosion. Other values may have more challenging components, such as those used for cutting or monochrome morphological operations.

Deployment of an oblong grid to symbolize a structuring component does not mean that each point in an oblong grid symbolize the structuring element. Therefore the weather one contains a few blanks. In several books, these blanks are presented as 0's, whereas this is perplexing consequently it is avoided here.

While a morphological operation is administered, source of a structuring component is habitually transformed to every element position within the figure sequentially. So points between the translated area unit of the structuring component compared to the underlying values of the image image element. The facts of this evaluation and its impact in the result rely on the morphological operator is getting used.

The structuring component could be a tiny binary image, denoted as a matrix with the values of '0' or '1':

- The size of the matrix indicate the dimensions of the structuring part.
- The pattern of '0' or '1' indicates the form of the structuring part.
- Associate source of the structuring part is typically '1' in all its pixels, even if the source is outside the structuring element.

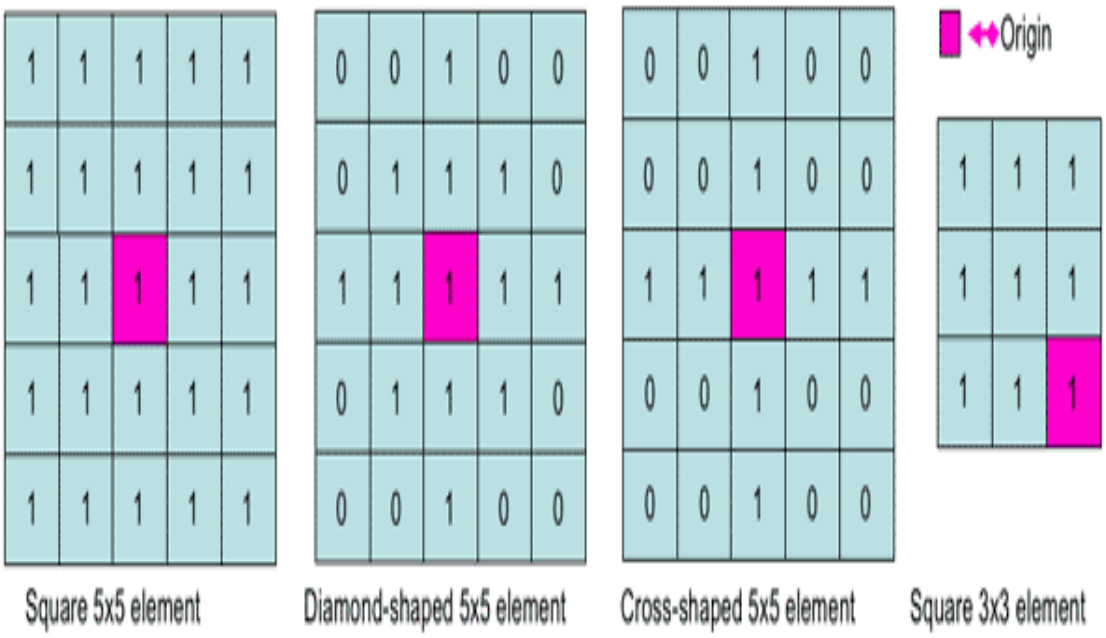

Figure 4.6 Different structuring elements.

A common apply is to own odd dimensions of the structuring matrix and therefore the source outlined because the centre of the matrix. The role of Structuring parts in morphological image process is similar to convolution kernels in linear image filtering. The structuring element is supposed to match the picture if and only if the respective picture pixel is also 1 for each of its pixels set to one. A structuring element is therefore claimed to strike or satisfy an picture if the respective image pixel is also 1 for at least one of its pixels set to

1.

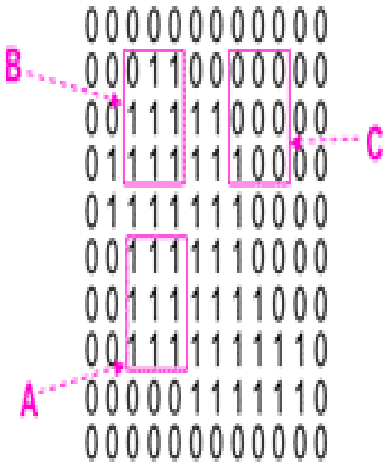

$$s_1 = \begin{pmatrix} 1 & 1 & 1 \\ 1 & 1 & 1 \\ 1 & 1 & 1 \end{pmatrix} \qquad s_2 = \begin{pmatrix} 0 & 1 & 0 \\ 1 & 1 & 1 \\ 0 & 1 & 0 \end{pmatrix}$$

		A	B	C
fit	s_1	yes	no	no
	s_2	yes	yes	no
hit	s_1	yes	yes	yes
	s_2	yes	yes	no

Figure 4.7 Fit and hit of a binary image with structuring elements s_1 and s_2

The Figure 4.7 fit and hit of binary image narrates pixels with zero of the structuring component area unit neglected, i.e. specify points wherever the equivalent image price is unsuitable. The basis for the morphological procedure is opening, closing in logical AND, OR notation dilation, erosion and defined by set assessment. Amongst them 2 operations area unit used dilation and erosion during the study. Dilation inserts pixels while erosion detaches the pixels at margins of the objects. This insertion or deletion of pixels relies on the structuring component used for image processing.

4.3.2 Binary Dilation

Dilation is discovered by placing the center of the instance over each of the original image's foreground pixels so that all the subsequent copies of the structuring element are united using the translation. First, it considers binary images. In many applications governed by a set of pixels, the binary image is

used to transform artifacts in the binary image background. For instance, the set containing components can represent a 3 X 3 binary object in an picture whose origin is located at the top left corner:

S = {(O, 0), (0,1), (0, 2), (1, 0), (1, 1), (1, 2), (2, 0), (2, 1), (2, 2)}.

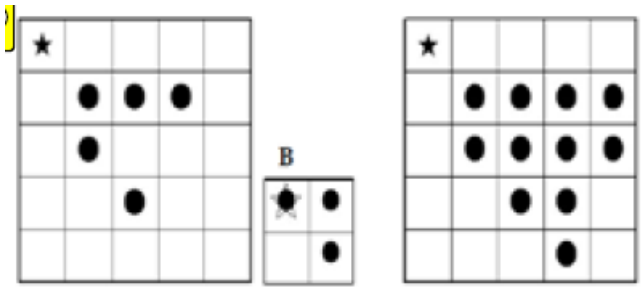

Figure 4.8 Binary Image Dilation

Dilation is computationally segregated by template spaces over each of the initial image's foreground pixels along with the use of the translation to sample an image. From Fig.4.8, apparently shows the developed images have expanded for dilation element shapes of the structuring element in the original set of images when eroded.

The A by B dilation is outlined as:

$$A \oplus B = \{z \in E | (B^s)_z \cap A \neq \varnothing\}, \quad A \oplus B = \bigcup_{b \in B} A_b$$

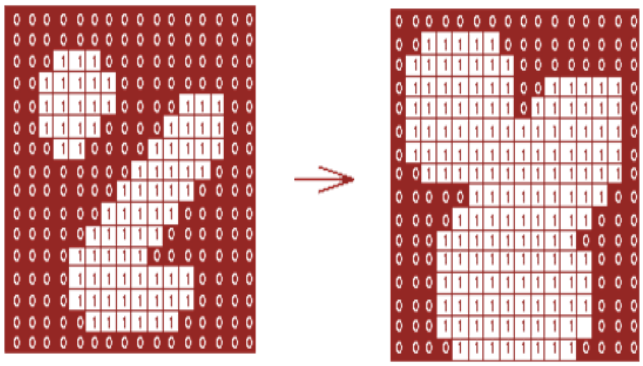

Figure 4.9 Dilation effect on Binary Images

The dilation of a binary image f by a structuring element s (referred to as $f \oplus s$) in Figure 4.9 generates a fresh binary image g = $f \oplus s$ with those at all places (x, y) of the origin of a structuring part that hits the input picture f.

Figure 4.10 and 4.11 shows the output of dilation with structuring element. g(x,y) = 1 if s hits f or 0 otherwise, replicating for every pixel coordinates (x_i, y_j). Dilation process has alternative brunt to erosion process, that is casts a pixel layer to each of outer and inner boundary regions.

Binary image **Dilation: a 2×2 square structuring element**

Figure 4.10 Dilation effect with structuring element

The fissure enveloped by one region and breach among different regions decreases, furthermore the incursions in boundary area are filled.

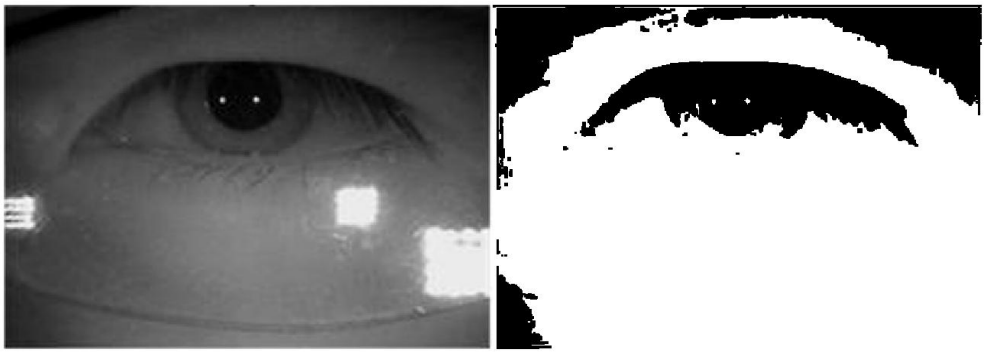

Figure 4.11 a) Original Image b) Dilation output

Dilation is discovered by placing the center of the instance over each of the original image's foreground pixels so that all the subsequent copies of the structuring element are united and generated using the translation.

4.3.3 Erosion

Erosion, scrapes the margins of regions of foreground pixels (black pixel in this study). Thus regions of foreground pixels contracts in terms of size, and holes inside that portion become bigger. Erosion, it is useful for the representation of image components to the boundaries of object like experiment, black pixels. Thus it can perform when dilation related to image components in generalization of description process. Basics of erosion effect on binary images shown in figure 4.12.

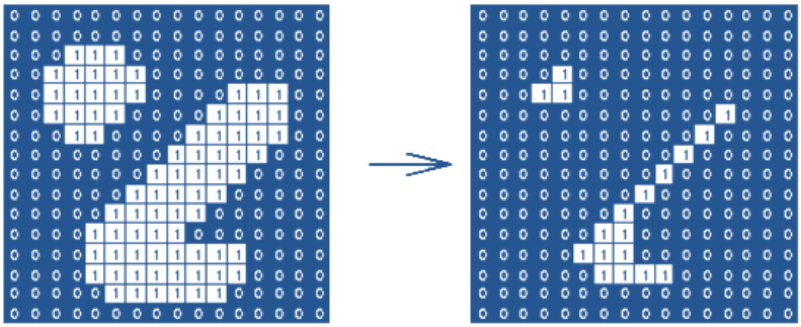

Figure 4.12 Erosion effect on Binary Images

Greyscale image | **Binary image by thresholding** | **Erosion: a 2×2 square structuring element**

Figure 4.13 Erosion effect on Greyscale image

Erosion eliminates diminutive details from a binary image in addition to contraction of ROI, too. By deducting the eroded figure from the actual figure, margins of each region can be found: $b = f - (f \ominus s)$ where f is an image, s is a 2×2 structuring component, and b is a figure of the region boundaries Figure 4.13 and Figure 4.14 depicts the erosion output of 2 different pictures

Figure 4.14 a) Original Image b) Erosion output

Erosion, it is useful for the representation of image components to the boundaries of object like experiment, black pixels. Thus it can perform when dilation related to image components in generalization of description process.

4.3.4 Opening and Closing

Mathematical morphology has two major vital operators such as Opening and Closing. It is mainly applied over the binary images. However, the fundamental effect opening approach is alike erosion. Here, removal of few foreground pixels is done from the edge regions of foreground pixels. This method is little destructive compared to erosion. Whereas, closing is same like dilation that is enlarges the boundaries the foreground image and shrinks the background color holes. It remains less destructive than original boundary shape. During opening, dilation process is carried out after the erosion technique. In case of closing, reverse operation of opening is carried out i.e dilation process is followed by erosion utilizing same structure element in both closing and dilation. In general, opening disconnects the smaller links of different image parts, while closing fills the space among different image parts. These gap filled with letters are shown in figure 4.15.

Opening processes contains erosion process followed by dilation and is used to eradicate all pixels in areas that are excessively small to integrate the element of structuring. At this juncture the structuring component is commonly referred to as a question, as it looks for miniature objects to strain out of the figure. Closing fills in holes plus small gaps and it comprises of dilation and erosion respectively.

The opening process of an image represented by f using a structuring component s (represented by $f \circ s$) is an erosion process and then a dilation process:

$$f \circ s = (f \ominus s) \oplus s$$

Binary image **Opening of an image using a 2×2 Structuring Component**

Figure 4.15 Opening effect on Binary image

The fundamental effect opening approach is alike erosion. Here, removal of few foreground pixels is done from the edge regions of foreground pixels. This method is little destructive compared to erosion.

Binary image **Closing: a 2×2 square structuring element**

Figure 4.16 Closing effect on Binary image

Opening is associate unchanged operation: once a picture is opened, succeeding openings with the same structuring component will not have supplementary effect on that image:

$(f \circ s) \circ s) = f \circ s$.

Closing fills holes within the area whereas retaining the same initial area sizes. The closing of an image f by a structuring element s (denoted by $f \bullet s$) is a mixture of dilation and erosion respectively as shown in figure 4.16.

$f \bullet s = (f \oplus s_{rot}) \ominus s_{rot}$

Figure 4.17 a) Opening output b) Closing output

Closing is same like dilation that is enlarges the boundaries the foreground image and shrinks the background color holes. It remains less destructive than original boundary shape. In opening, the erosion approach accompanied by dilation takes place. In case of closing, reverse operation of opening is carried out i.e dilation process is followed by erosion utilizing same structure element in both closing and dilation. These differences are verified with Figure 4.17.

4.3.5 Synthesis Result of Morphology Opening and Closing

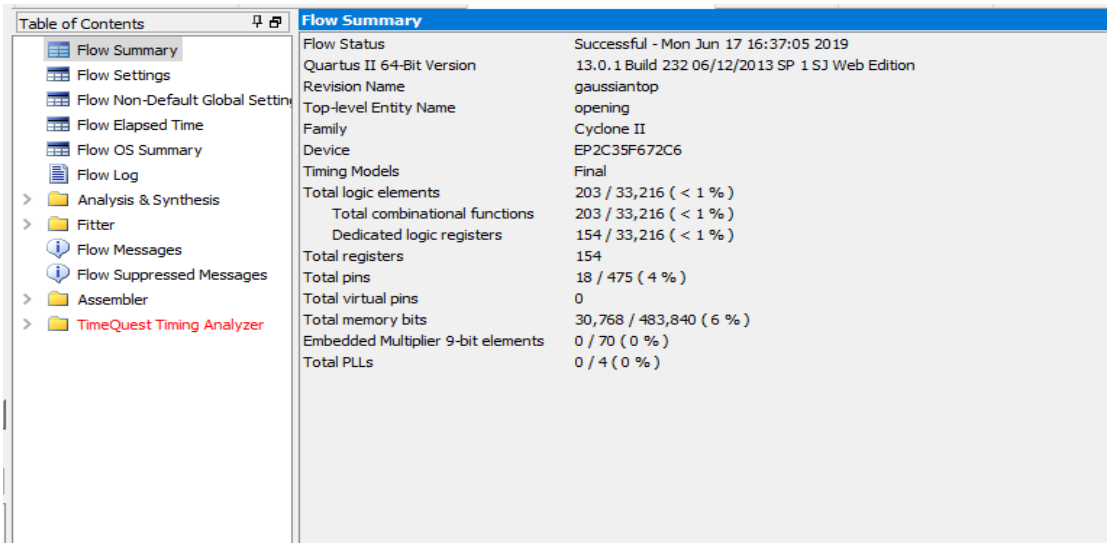

Figure 4.18 Logic element utilization of Morphology Opening

Figure 4.18, Altera cyclone II FPGA consumes for Morphology Opening are 203 logic elements, 203 combinational functions and 154 dedicated logic registers .

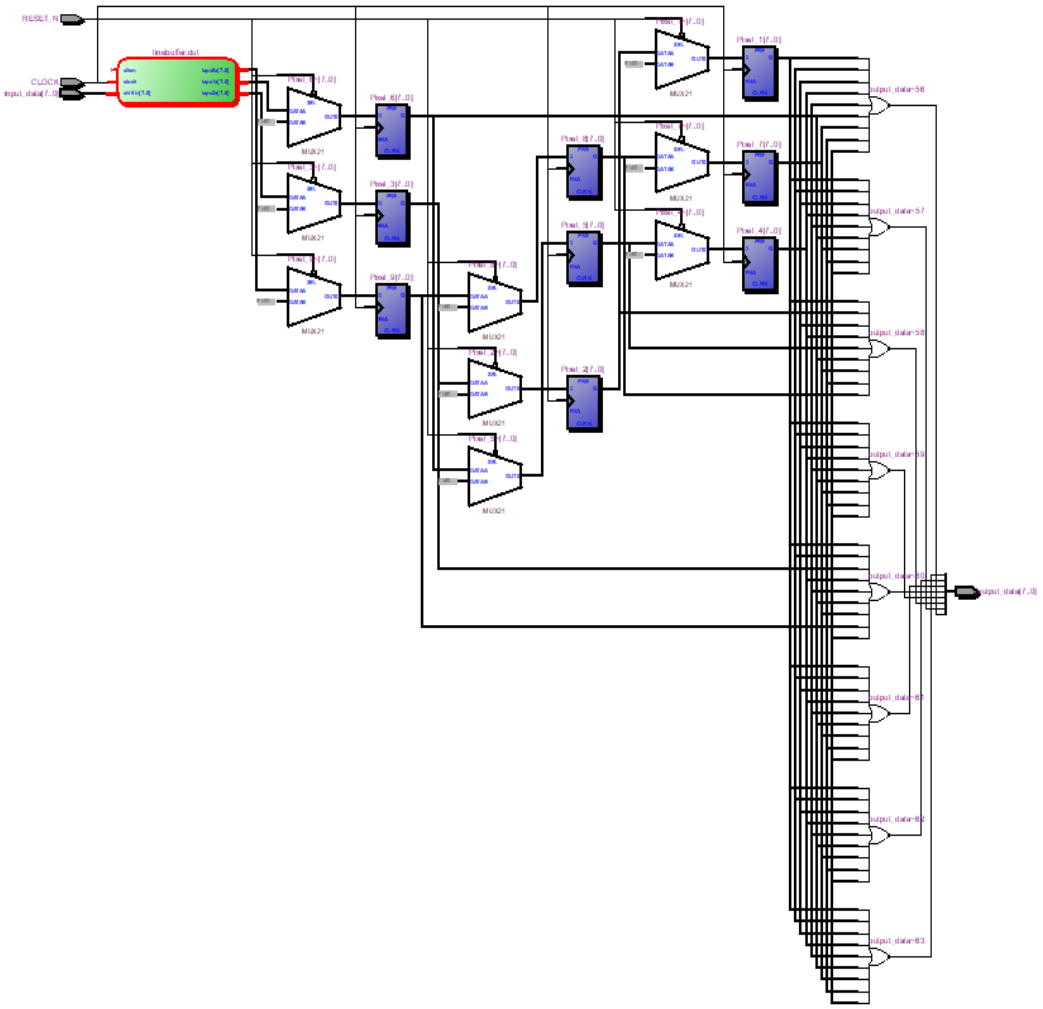

Figure 4.19 RTL Schematic view of Morphology Opening

In opening, and closing the same structure element is utilized. The FPGA based opening shown in Figure 4.19.

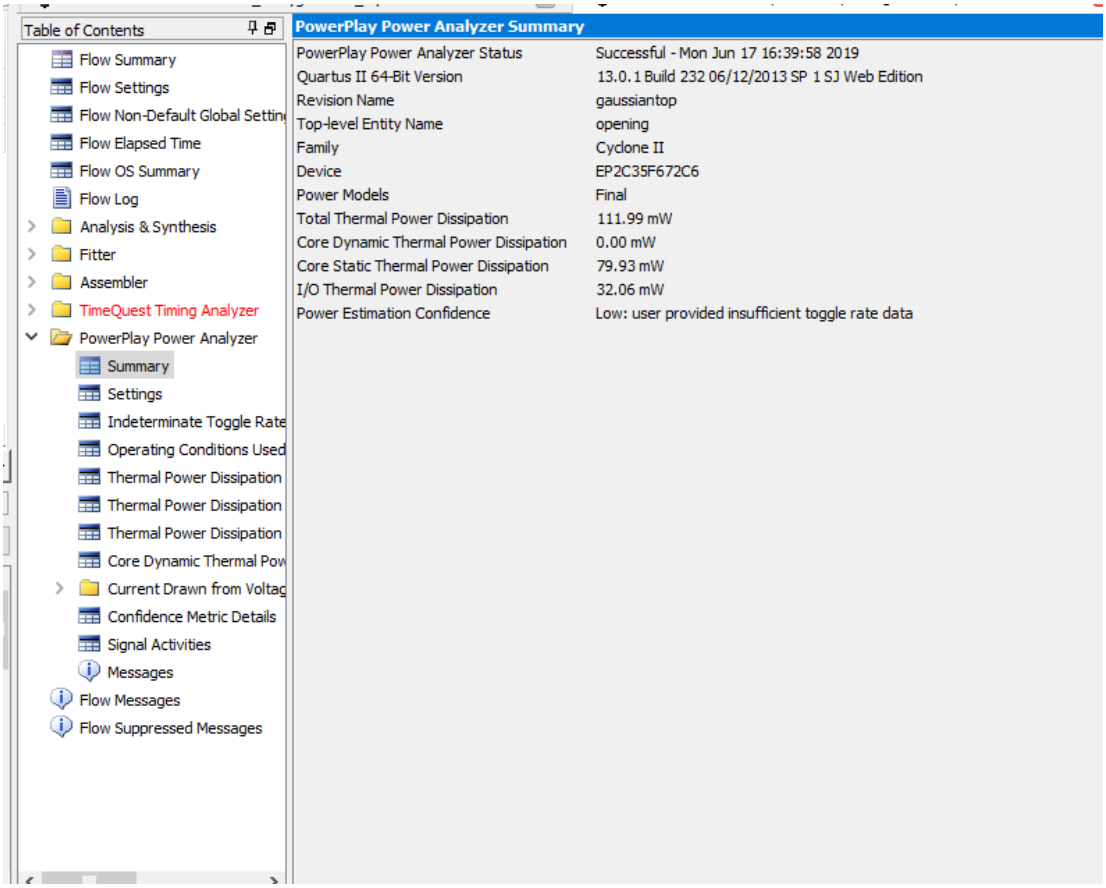

Figure 4.20 Power dissipation of Morphology Opening

Figure 4.20 shows the total power dissipation of 111.99mw. Synthesis Result of Morphology closing is also same as Morphology opening.

4.4 FUNDAMENTALS OF EDGE DETECTION

Edge detection can be a elementary method of low-level picture and sensitive edges are needed for processes of greater level. The majority of different aspects, however, could also be categorized into 2 classifications:

Gradient: The gradient method identify the perimeters by searching for the utmost and least within the computation of the image shown in figure 4.21

Laplacian: In the second by-product of the picture, the Laplacian methodology searches for zero crossings to find corners.

A border has the 1-dimensional shape of a ramp and its position will be highlighted by the picture by-product. Edge detection relates to the distinctive maneuver and the location of sharp discontinuities in each picture.. Classic edge detection methods require converting the picture to a degree operator (a 2-D filter), which is designed to be susceptible to huge gradients in the picture while returning zero values in uniform areas. It is possible to obtain very large quantities of edge detection operators, each designed to be susceptible to bound edge types. Variables related within the choice of a foothold detection operator includes:

- Edge orientation: The operator's pure mathematics decides a distinctive direction where it is most susceptible to edges. For horizontal, vertical or diagonal edges, operators are often optimized to appear.
- Noisy environment: Edge detection is tough in vociferous figures, as frequency content is high in the noise and the edges -. efforts to reduce them end in hazy and unclear boundaries. Operators exercised

on gravelly figures are usually larger in scope, as they can reduce localized noisy pixels by averaging sufficient data. This results in localization of the images to minimum level.

- Edge structure: All edges need not indulge a shift in intensity step. Effects such as diffraction or poor focus may end up in objects with boundaries printed through a gradual intensity modification. In these cases, the operator chosen needs awareness about this gradual change. New wavelet-based strategies always describe the changeover character for each draw close order to differentiate. For instance edges associated with to edges associated with a face

An edge has single dimensional form of a slope and calculative the consequence of the image will show up its location. Suppose I got the subsequent signal, with a foothold shown by the jump in intensity below:

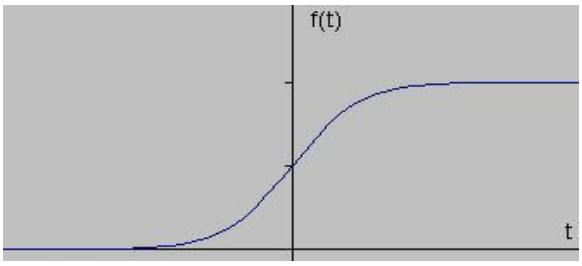

Figure 4.21 Gradient of signal f(t)

If I tend to acquire the gradient of this signal (in single dimension, is the first derivative with respect to t) the following is obtained as shown in Figure 4.22

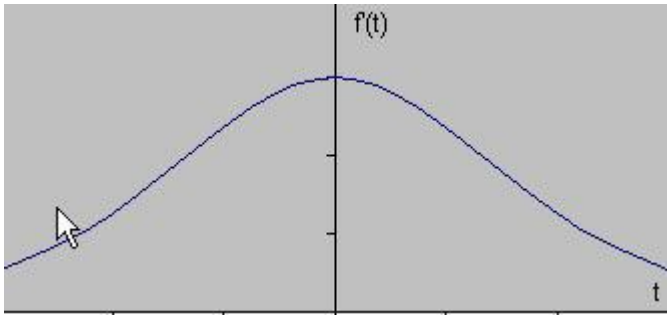

Figure 4.22 First Derivative of Gradient of signal f(t)

Undoubtedly, the by-product is mostly located within the initial signal in the center of the sting. This methodology for finding a footprint is distinctive feature of the edge detection filter "gradient filter" family and involves the Sobel methodology. If the value of the gradient goes beyond some threshold, a pixel location is concluded as a foothold location. As stated previously, edges may have greater values of intensity of elements than those near them. So once a threshold is ready, you will compare the price of the gradient with the price of the brink and see a foothold every time the brink is exceeded. In addition, the second by-product is zero once the primary by-product is at most. As a consequence, finding the zeros within the second by-product is different to discovering the location of a grip. This method is considered because of the Laplacian and as a result the 2nd by-product of the signal is shown :

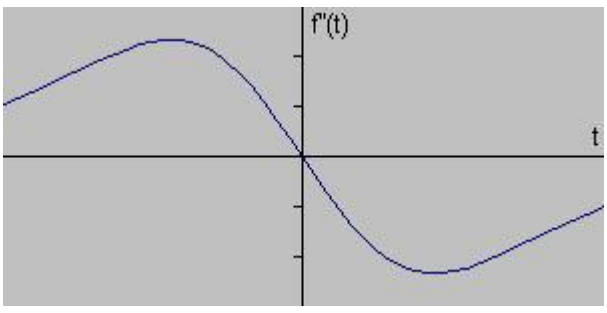

Figure 4.23 Second Gradient Derivative of signal f(t)

The Figure 4.23 indicates to the maneuver of attribute and spotting pointed discontinuities through every image. The discontinuities change abruptly in the intensity of the pel which characterizes the borders of objects in an extremely scene. Classic edge detection methods engage converting the image to a degree operator (a 2-D filter), which is designed to be delicate to enormous gradients in the image while reverting zero values in uniform regions.

4.5 EDGE DETECTION OPERATORS

4.5.1 Sobel Operator

The Sobel operator comprises of a duo of 3×3 convolution kernel as in Figure 4.24. A kernel revolves by 90°.

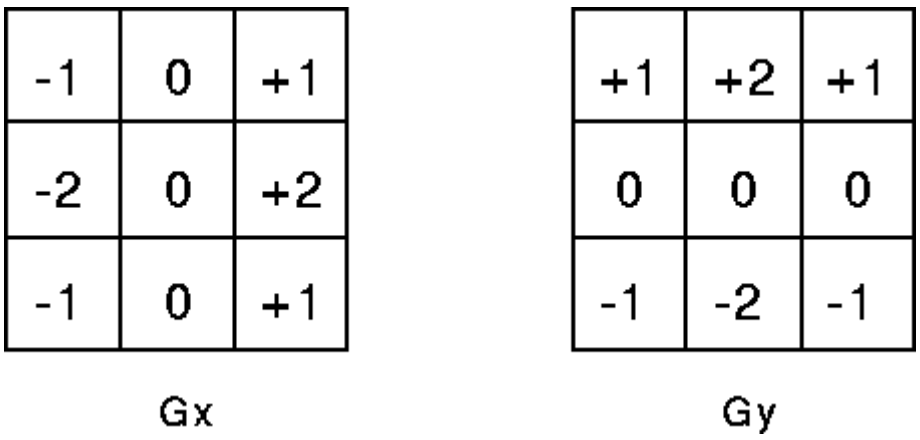

Figure 4.24 Convolution kernel of Sobel Operator

The area unit of the Figure 4.24 convolution kernels was intended to react to edges working parallel and perpendicularly in relation to the part grid, one kernel for every two vertical orientation. The kernels is audited individually to the put in picture, to give separate dimensions of the gradient

part in every direction (call these Gx and Gy). The result will then be pooled alongside to seek out entirely the enormity of the gradient at every purpose and consequently the direction of that gradient. The gradient magnitude is computed by:

$$|G| = \sqrt{Gx^2 + Gy^2} \quad (4.1)$$

Normally, an estimated magnitude or enormity value is computed using:

$$|G| = |Gx| + |Gy| \quad (4.2)$$

which is much more rapid to compute.

The orientation of angle of the sting (comparative to the element grid) gives the spacial gradient as :

$$ø = \arctan\frac{Gy}{Gx} \quad (4.3)$$

4.5.2 Robert's Cross Operator

The Roberts Cross operator carry out a straightforward, speedy to compute, 2-D spatial gradient dimension on an image. Pixel values at every purpose within the output characterize the calculable scale of the spacial gradient of the put in image at that time. The operator comprises of a of 2×2 convolution kernel as in Figure 4.25. An individual kernel turned opposite 90° like the Sobel operator.

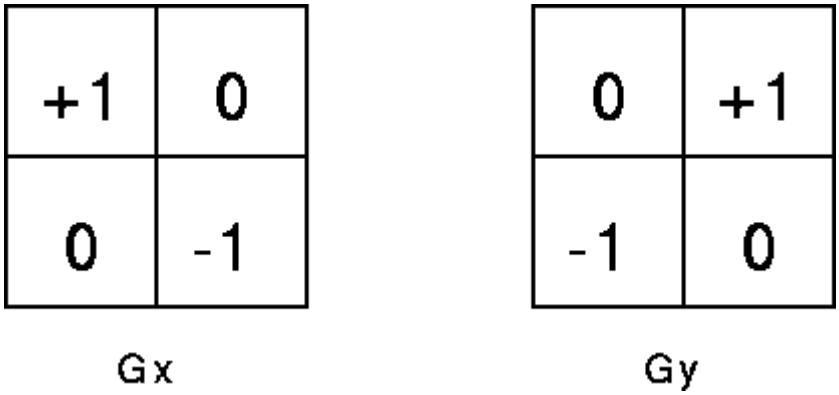

Figure 4.25 Robert's Operators Convolution kernels

These kernel square measurements are intended to respond to the element grid at a maximum of 45°, one kernel for every two perpendicular orientations. The kernel is applied one by one to put in image, to create individual measurements of the gradient element in every orientation (consider as Gx and Gy).

These are combined along to search out absolutely the degree of the gradient at every purpose hence the course of that gradient. The magnitude of the gradient is computed by:

$$|G| = \sqrt{Gx^2 + Gy^2}$$

Normally, an estimated magnitude is evaluated using:

$$|G| = |Gx| + |Gy|$$

which is much quicker to calculate.

The angle of orientation of the sting giving rise to the spacial gradient (relative to the element grid orientation) is given by:

$$ø = \arctan\frac{Gy}{Gx} - \frac{3\pi}{4}$$

4.5.3 Prewitt's Operator

Prewitt is alike the Sobel operator and is applied in images to sleuthe vertical and horizontal edges.

$$H1 = \begin{bmatrix} 1 & 1 & 1 \\ 0 & 0 & 0 \\ -1 & -1 & -1 \end{bmatrix} \qquad H3 = \begin{bmatrix} -1 & 0 & 1 \\ -1 & 0 & 1 \\ -1 & 0 & 1 \end{bmatrix}$$

4.5.4 Laplacian of Gaussian

The Laplacian is an isotropic 2-D measure of a picture's second spatial derivative. A picture's Laplacian highlights areas of dense intensity change and is thus generally applied to detect edges. Usually, the Laplacian is applied to a image that was smoothed initially with one thing approximating a mathematician smoothing filter in order to lessen its noise sensitivity. Generally the operator requires as input one monochrome picture and generates another monochrome picture as output.

An image's Laplacian L(x,y) that holds pixel intensity values I(x,y) is given by:

$$L(x,y) = \frac{\partial^2 I}{\partial x^2} + \frac{\partial^2 I}{\partial y^2} \qquad (4.4)$$

As the key in figure is described as a pixel cluster, a separate intricate kernel which will estimate the second derivatives within the description of the Laplacian is seeked. The 3 regularly used minute kernels are shown in Figure 4.26.

0	1	0
1	−4	1
0	1	0

1	1	1
1	−8	1
1	1	1

−1	2	−1
2	−4	2
−1	2	−1

Figure 4.26 Three separate approximations to the Laplacian filter

Since the approximation of a second by-product measurement on the picture, these kernels are very susceptible to noise. The picture is generally smoothed mathematically before the Laplacian filter is applied. This pre-processing step decreases the noise components of high frequency before the differentiation step. In reality, as the convolution operation is associative, the Laplacian filter is used first to twist the mathematical smoothing filter, and such twisted hybrid filter with the figure accomplish the necessary effect. Doing stuff like this has two benefits:

- As both Gaussian and Laplacian kernels are generally greatly smaller than the image, this tehnique typically needs extremely few mathematical operations.
- The pre calculated LoG (`Laplacian of Gaussian') kernel ends up in execution of convolution merely once during processing time itself on the image.

The LoG in 2D spatial operate focused on ‘0’ and the mathematician variance is computed as:

$$LoG(x,y) = -\frac{1}{\pi\sigma^4}\left[1 - \frac{x^2+y^2}{2\sigma^2}\right]e^{-\frac{x^2+y^2}{2\sigma^2}} \tag{4.5}$$

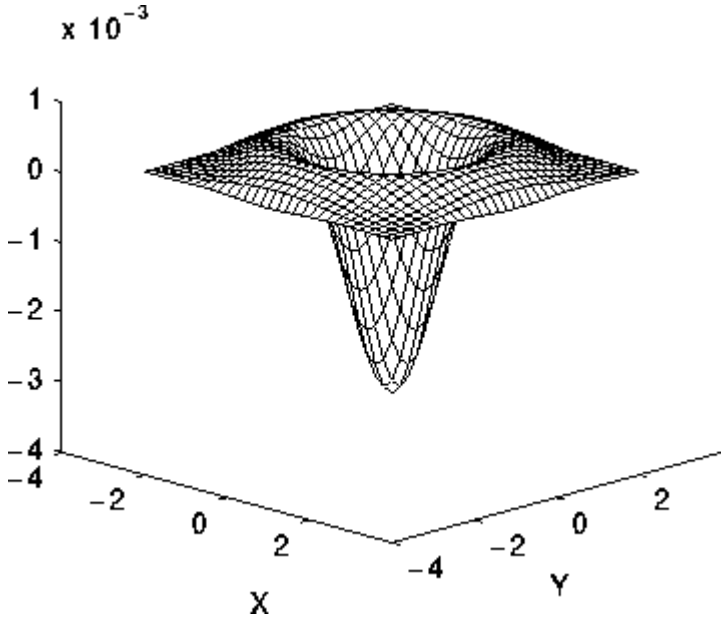

0	1	1	2	2	2	1	1	0
1	2	4	5	5	5	4	2	1
1	4	5	3	0	3	5	4	1
2	5	3	-12	-24	-12	3	5	2
2	5	0	-24	-40	-24	0	5	2
2	5	3	-12	-24	-12	3	5	2
1	4	5	3	0	3	5	4	1
1	2	4	5	5	5	4	2	1
0	1	1	2	2	2	1	1	0

Figure 4.27 Discrete approximation to LoG function with Gaussian σ = 1.4

Observe that the Figure 4.27 the Gaussian is formed more and more slender, the LoG kernel becomes an equivalent because the easy Laplacian kernels depicts in Figure one. This has no impact due to smoothing on a discrete grid with a really small mathematician (< zero.5 pixels). The easy Laplacian can therefore be seen on a separate grid as a restricting situation of the LoG for restricted Gussians.

4.5.5 Canny Edge Detection

Another more complicated technique used is the Canny edge detector, which was designed to locate strong edges and ignore noise. The edges should be very near to the real edges further should not identify more than one edge pixel where only one exists.

The actual image is smoothed through a Gaussian filter to eliminate noise. The Sobel magnitude as well as gradient values are calculated on the smoothed image. Using a technique called non-maximum suppression; weak edges are discarded by comparing edge values along the same gradient direction. Two arbitrary threshold values are chosen, tlow and thigh. Any pixels values below tlow are immediately discarded. Remaining edges are preserved only if any pixels within a 3 pixel x 3 pixel neighboring window have a value above thigh. Depending on the image, different edge detectors will work better or worse. Generally the aforementioned edge detectors provide consistent results, but it is important to choose the optimal detector and threshold values through testing.

4.6 SOBEL EDGE DETECTION

After Morphological operation in human eye pupil detection process, Sobel filter is executed to extract the edges of pupil.

The Sobel operator is utilized in image method, notably at intervals in edge detection algorithm. It is precisely a separate differentiation operator that operates the associated computing approximation of the gradient of the picture intensity.

The effect of the Sobel operator is either the corresponding gradient vector or the standard of this vector for each purpose within the figure. The Sobel operator depends on converting the picture in horizontal and vertical direction with a tiny, discrete, and integer-valued filter and is as a result comparatively cheap in computational terms. Apart from this, the result generated by gradient approximation is comparatively coarse, especially for picture variants of high frequency. The operator calculates the gradient of the image intensity for every purpose in an easy way, offering the way of the highest probable increase from light to dark and the percentage of change in that direction. The outcome however illustrate "abruptly" or "smoothly" the changes in figure during the moment thereby seemingly it's that portion of the image indicates a footing, along with the possible orientation of that edge. In follow, the magnitude (associate edge) calculation is consistent and trouble-free to understand than the direction calculation.

The 3x3 convolution kernel is shown in figure 4.28. The two filters are based on the context of process vertical and horizontal edges (the left and right) which eliminates the need of derivatives. The filters are defined by the classification of image processing with the whole input image. To sample the

robustness in the center of the grid sliding over the linear operator for that pixel, the pixels in the middle are weighted more heavily before sliding the enhancement of the external pixels.

$$h_x = \begin{bmatrix} -1 & 0 & 1 \\ -2 & 0 & 2 \\ -1 & 0 & 1 \end{bmatrix}, \quad h_y = \begin{bmatrix} -1 & -2 & -1 \\ 0 & 0 & 0 \\ 1 & 2 & 1 \end{bmatrix}$$

Figure 4.28 Sobel edge detector mask

The Sobel operator is crucial to compute spatial gradient measurement which is fast and classical method to highlight the gradient method of high-spatial occurrence and measurement in edges. Theoretically, to determine edge points in derivative approximation due to its importance it computes a feature detector image intensity function particularly for computer vision. Perhaps employing Sobel operator, this is the most efficient characteristics to produce detection of grayscale vector and its normal vector shown in Figure 4.28.

4.7 HARDWARE ARCHITECTURE OF SOBEL FILTER

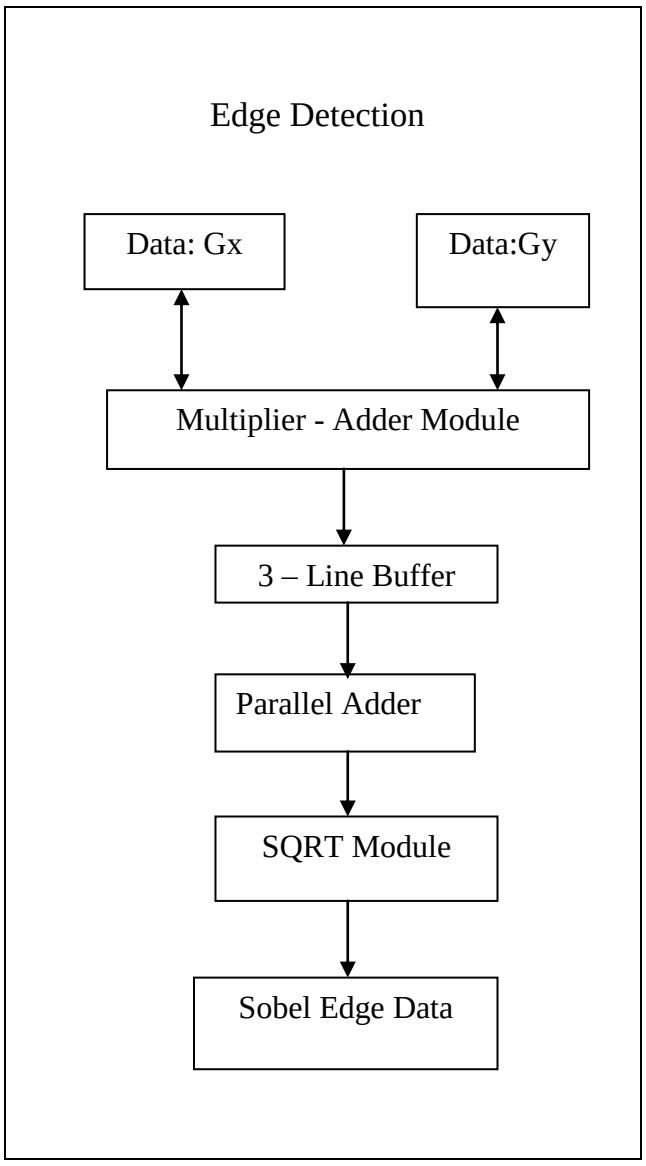

Figure 4.29 Proposed Edge detection operations Block Diagram

-1	0	+1
-2	0	+2
-1	0	+1

Gx

+1	+2	+1
0	0	0
-1	-2	-1

Gy

The calculation is given below in detail

$$\mathbf{G_x} = \begin{bmatrix} -1 & 0 & +1 \\ -2 & 0 & +2 \\ -1 & 0 & +1 \end{bmatrix} * \mathbf{A} \quad \text{and} \quad \mathbf{G_y} = \begin{bmatrix} +1 & +2 & +1 \\ 0 & 0 & 0 \\ -1 & -2 & -1 \end{bmatrix} * \mathbf{A}$$

Gx = [f(x+1,y-1)+2*f(x+1,y)+f(x+1,y+1)]-[f(x-1,y-1)+2*f(x-1,y)+f(x-1,y+1)]

(4.6)

Gy = [f(x-1,y-1) + 2f(x,y-1) + f(x+1,y-1)]-[f(x-1, y+1) +
2*f(x,y+1)+f(x+1,y+1)] (4.7)

G = sqrt(Gx^2+Gy^2) (4.8)

Now and then, so as to enhance potency, the approximation of the above equation: |G| = |Gx| + |Gy| is utilized. Consider this pixel as an edge pixel if G is bigger than a definite limit.

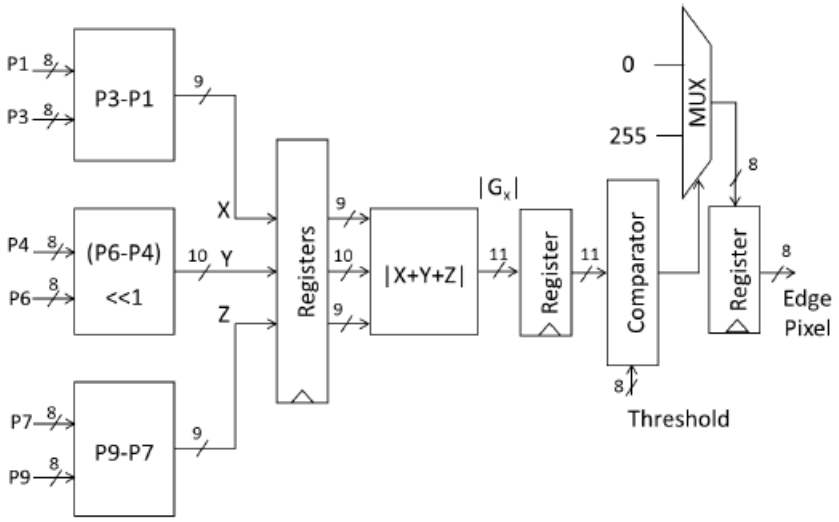

Figure 4.30 Hardware architecture of Sobel edge detector

The relatively inexpensive Sobel edge detector in terms of computations is shown in figure 4.30.

4.7.1 The Three-Line Buffer

The Three-line Buffer which can be easily configured by Mega Wizard Plugin Manager was designed to improve performance in this work. The buffer provides sufficient drive capability in RAM based shift register which does not requires control circuits to improve resource utilization. Every pixel contains 30 bits of data that represents color of RGB, 10 bits for each color has 10 bits. The element is only allowed if the clock edge of the input shift is stored in different slots. The pixel data is a cluster of estimated data for the top-level module and output screen. The pixel output grids are used to examine the detection modules at the end of the edge.

4.7.2 Multiplier-Adder

The Multiplier-Adder uses Mega Wizard Plugin Manager for generation purpose. To perform operation it uses three multipliers and one adder to adapt a chain of fixed point in the module. In the Sobel edge detection algorithm, it generates edges to highlight object location as a sequence of multipliers and additions.

$$Gx = [f(x+1,y-1)+2*f(x+1,y)+f(x+1,y+1)]-[f(x-1,y-1)+2*f(x-1,y)+f(x-1,y+1)]$$

$$Gy = [f(x-1, y-1) + 2f(x, y-1) + f(x+1, y-1)]-[f(x-1, y+1) + 2*f(x,y+1)+f(x+1,y+1)]$$

The multiplier-adder module is associated to the Three-line buffer suitable for their separability, and one of the inputs is from Line0 to Line2 in most cases for a suitable detector. The other inputs elements are arranged in the 3x3 matrix structure. The parts of Gx and Gy were computed using this module.

4.7.3 Parallel Adder & SQRT Module

The Parallel Adder is capable of finding arithmetic sum used in computation of Sobel operator to determine the analysis of logic operationThe lead of Multiplier-Adder, a digital circuit that executes the operation design provided in the Parallel Adder and is then added mutually. The calculations are capable of finding computation which is signed. Then the findings of two outputs produced by Gx and Gy reduce the procedure will lastly be calculated and then provided to the SQRT element.

The SQRT module is normalized by Mega Wizard Plugin Manager before processing. It includes input of 32-bit and output of 16-bit.The edge level G is represented by changes near edges for calculation and designed to implement the number of input bits. If the toggle switches set G above a certain limit, more important bits will be acquired as an edge pixel to the suitable pixel.

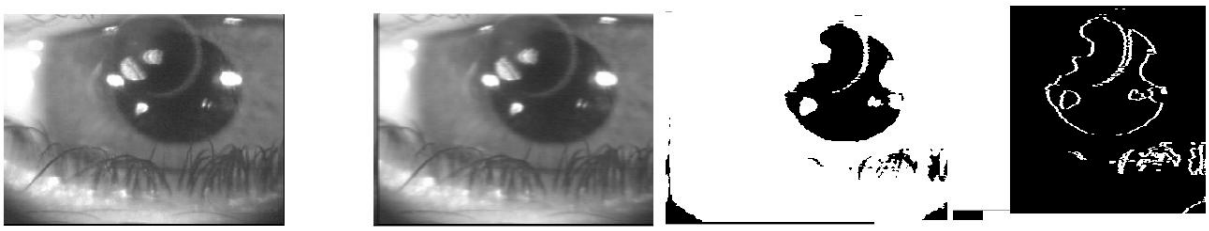

Original image **Gaussian filter image** **Threshold with Morphology image** **Sobel Edge image**

Figure 4.31 Sobel Edge detection Image

The outputs are specified in Figure 4.31.

4.7.4 Synthesis Result of Sobel Edge detector

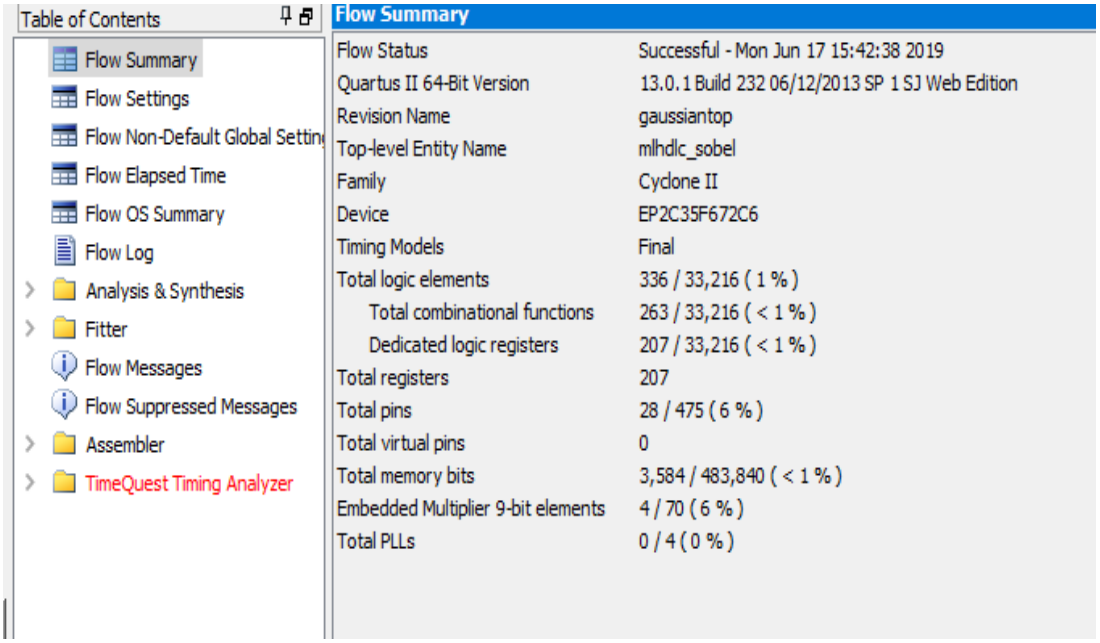

Figure 4.32 Logic element utilization of Sobel Edge detector

Figure 4.32, Altera cyclone II FPGA consumes for Sobel Edge detector are 336 logic elements, 263 combinational functions and 207 dedicated logic registers .

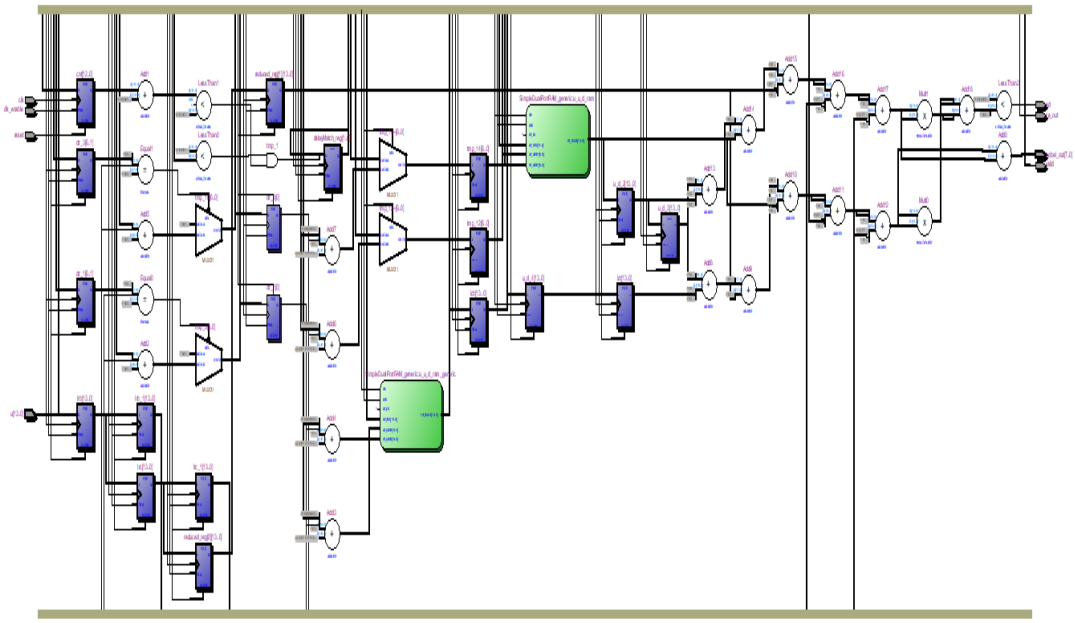

Figure 4.33 RTL Schematic view of Sobel Edge detector

Sobel operator is crucial to compute spatial gradient measurement which is fast and classical method toinsist the gradient method of greater spatial frequency and measurement in edges. Theoretically, to determine edge points in derivative approximation due to its importance it computes a feature detector image intensity function particularly for computer vision. Figure 4.33. shows RTL Schematic view of Sobel Edge detector.

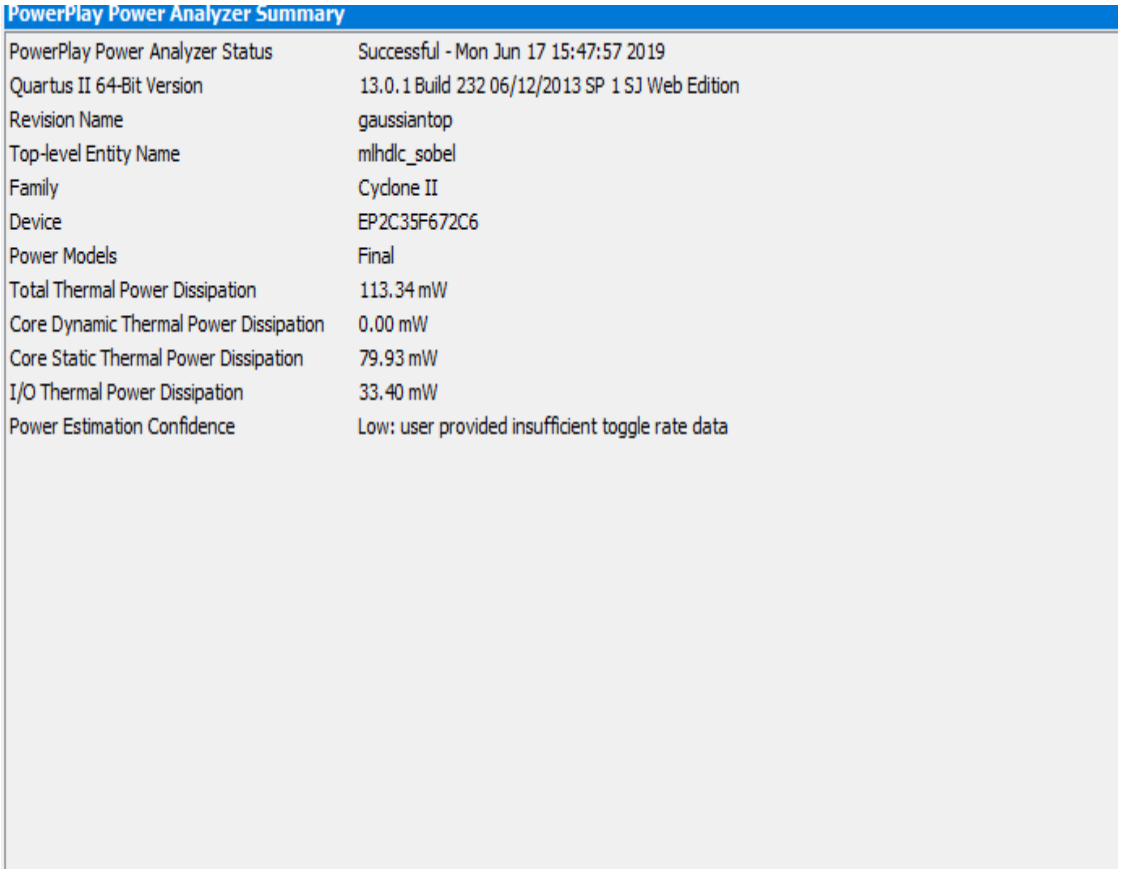

PowerPlay Power Analyzer Summary

PowerPlay Power Analyzer Status	Successful - Mon Jun 17 15:47:57 2019
Quartus II 64-Bit Version	13.0.1 Build 232 06/12/2013 SP 1 SJ Web Edition
Revision Name	gaussiantop
Top-level Entity Name	mlhdlc_sobel
Family	Cyclone II
Device	EP2C35F672C6
Power Models	Final
Total Thermal Power Dissipation	113.34 mW
Core Dynamic Thermal Power Dissipation	0.00 mW
Core Static Thermal Power Dissipation	79.93 mW
I/O Thermal Power Dissipation	33.40 mW
Power Estimation Confidence	Low: user provided insufficient toggle rate data

Figure 4.34 Power dissipation of Sobel Edge detector

Figure 4.34 picturize the total power dissipation of 113.34mw

4.8 CONCLUSION

This chapter concludes the manual threshold applied to segment the pupil region and Morphological dilation carried out then finally sobel filter is exactly identify the edges of pupil region.

CHAPTER 5

RESULTS AND ANALYSIS OF IMPLEMENTATION

Implementation analysis determines system performance relative to specific requirement. The outcome of the implementation of the Pupil Detection Methodologies with Median Filter and Gaussian Filter processes are discussed in this chapter. Logic utilization summary, Chip planner summary and clock summary Synthesis Results for analyzing the Human eye pupil detection are discussed.

5.1 PUPIL DETECTION

Pupil region detecting model based on threshold value (intensity value) pooled with data on the pupil edge gradient reserves the pupil detection's elevated precision. Only the search of the pupil region in the block created by the constraints of the edge points of the pupil and the associated gradient data can also enhance the effectiveness of the pupil center location.

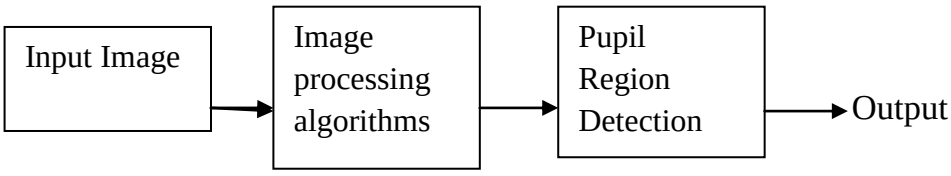

Figure 5.1 Proposed Block Diagram

The projected block diagram shows the exact time period pupil chase is a crucial process in a vivid eye view. Initially, the feature-based algorithmic rule sighted the situation of the face area and is accustomed spot the pupil on

the face. Next, use the pupil to find out where humans are glance where we can improve the efficiency for locating the pupil center.

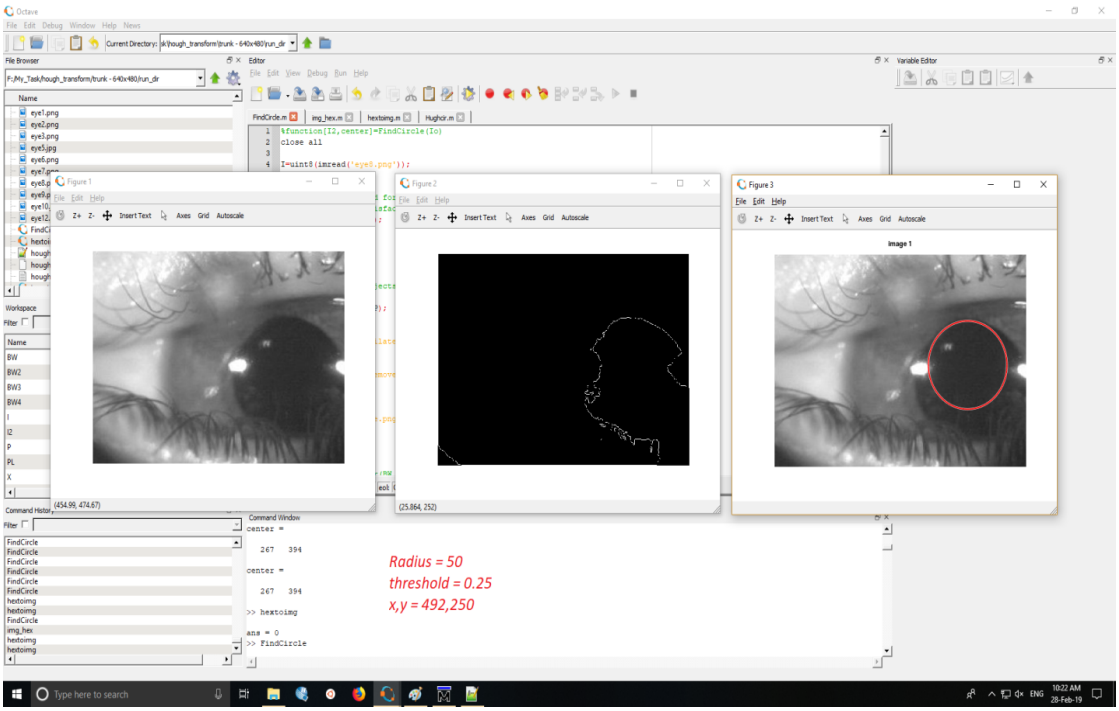

Figure 5.2 Pupil Detection output

Figure 5.1 and figure 5.2 explain the clear pupil detection result pupil detection is vigorous and correct recognition of the pupil position could be a vital building block for head-mounted eye chase and requirement for purpose on prime, like vivid human–computer interaction or attention analysis. Due to essential variation in the gaze at (e.g., reflections, illumination, , occlusions, etc.), individual dissimilarities in eye physiology, the pupil still has difficulty in investigative job in images captured under real-world circumstances, as distinct resource of noise, like contact lenses or make-up.

Upon location of the pupil, the binary image helps to identify the coarse parameters of the pupil. The middle of mass is calculated to calculate

the core of the student. Let (xi yi),i=1 ... N indicate the remaining pixel picture domain coordinates. The center (*xc*, *yc*) of the pupil is evaluated by computing the center of mass of the pixels:

$$(x_c, y_c) = \frac{1}{N} \sum_{i=1}^{N} (x_i, y_i) \tag{5.1}$$

while *N* denotes the total number of black pixels. Undeniably, the pupil will be approximated as a circle to see its coarse radius.

5.1.1 Pupil Detection Image1

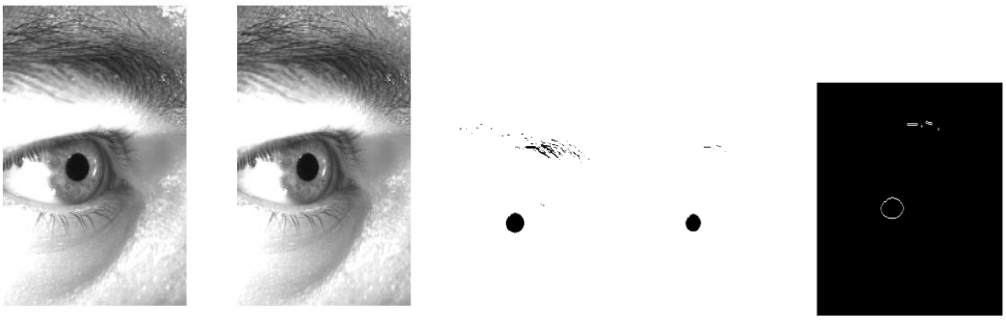

Original image **Median filter** **Threshold** **Morphology** **Sobel filter**

Figure 5.3 Pupil Detection Methodologies with Median Filter

In Figure5.3 explain the flow of pupil detection methodologies. Original image is filtered by median filter to eliminate noises in original image. On the filtered picture, the correct limit is applied to separate the pupil region.

Here I used threshold value is 30. Dilation process is involved to remove extra eyelashes and eyelids. Finally Sobel filter has given clear pupil region.

5.1.2 Pupil Detection image 2

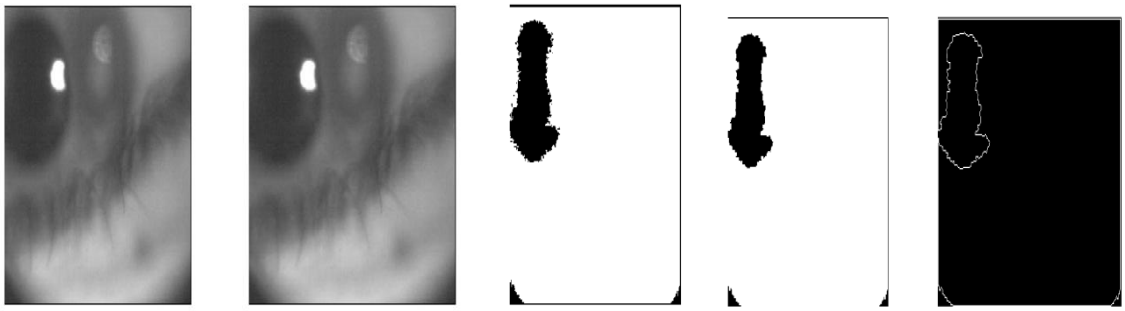

Original Image **Gaussian Filter** **Threshold** **Morphology** **Sobel Filter**

Figure 5.4 Pupil Detection Methodology with Gaussian Filter

In Figure 5.4 explain the flow of pupil detection methodologies with Gaussian filter. Gaussian filters have the characteristics of not over-shooting a step input when minimizing the time of increase and fall. This conduct is strongly linked to the reality that there is the minimum doable cluster delay in the Gaussian filter. The perfect time domain filter is considered, even though the sinc is that the ideal frequency domain filter Original picture is filtered with Gaussian filter to smooth the initial picture. Then Threshold is applied to separate the pupil region. Morphological Dilation and Sobel filter is given exact pupil region.

5.2 ALTERA QUARTUS II SYNTHESIS RESULT

5.2.1 Comparison table

Comparison Table 5.1 gives Xilinx and Altera platforms FPGA's results. From this table logic elements utilization is reduced 3% in pupil Detection system. Total combinational LUT's are also reduced from 64% to 15%.

Table 5.1 Device utilization for Altera Cyclone II FPGA

Logic utilization	**Used /Avail**		**Utilization (%)**	
	Existing work (virtex 5)	Proposed work (cyclone II)	Existing work (virtex 5)	Proposed work (cyclone II)
Total logic elements/Slices	45,716 /207,360	6,151 / 33,216	22%	19 %
Total combinational functions / LUT's	133,916/ 207,360	5,070 / 33,216	64%	15 %
Dedicated logic registers/ slices	39,914 / 51,840	2,899 / 33,216	76%	9 %
Total memory bits	288 /10,368	55,936/ 483,840	2%	12 %

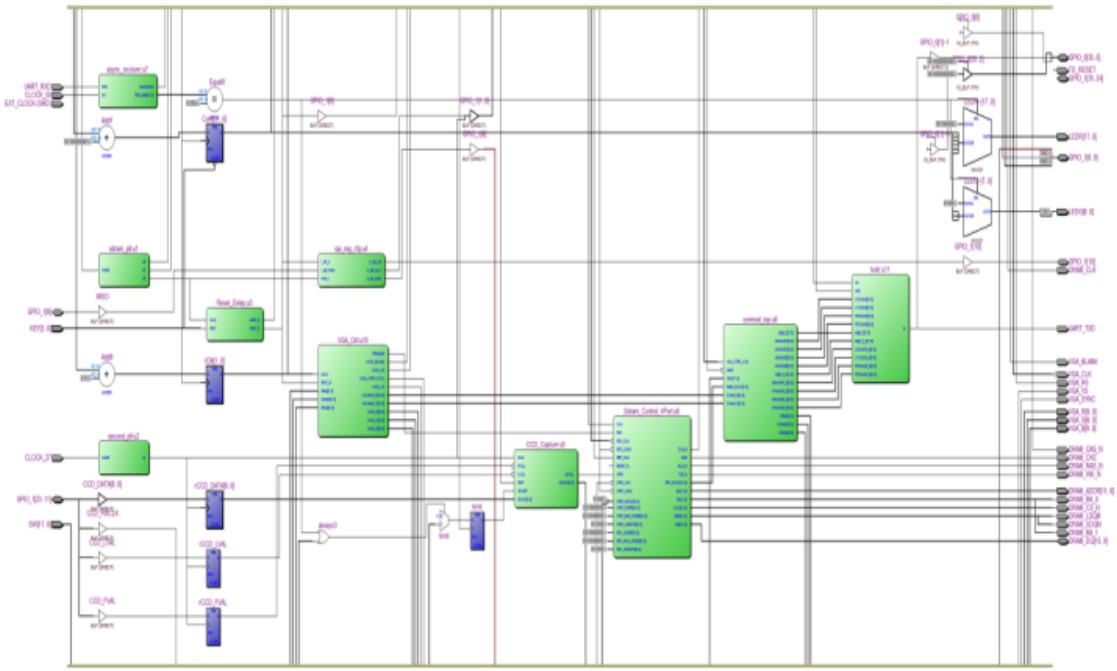

Figure 5.5 Human eye pupil detection system.

Figure 5.5 shows the RTL view of Human eye pupil detection system in Cyclone II FPGA EP2C35F672C6 device. The detection and hunt of pupils is a vital step in the development of an interaction scheme between human and computer. We tend to examine pupil detection and hunt by picture process methods to create the eye-computer interaction scheme of a person. The illumination usually directly affects the image quality in the picture process methods. If illumination influences is no, it is possible to acquire a picture of excellent image quality.

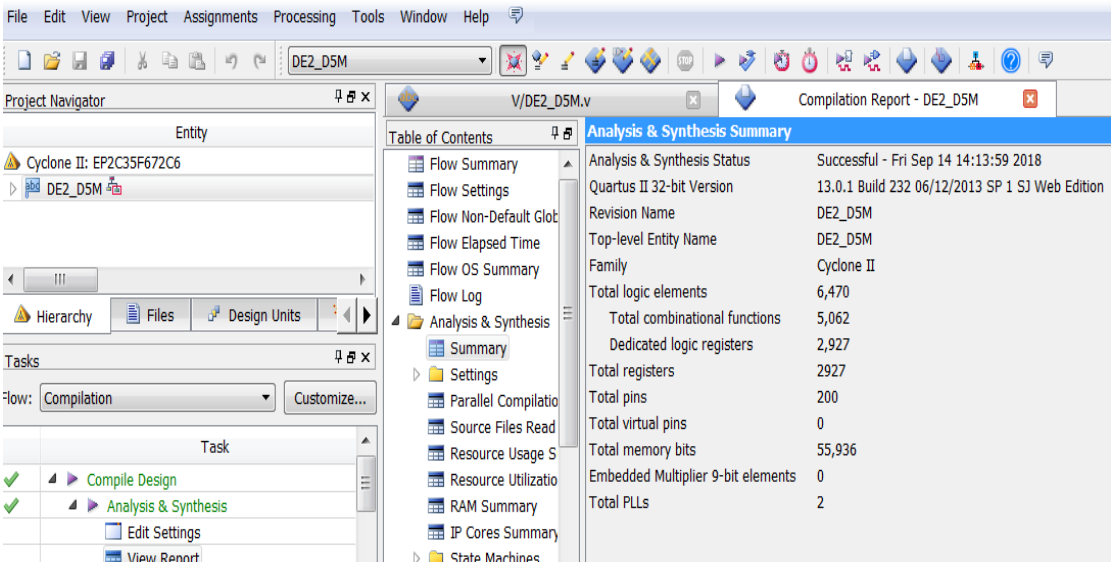

Figure 5.6 Logic utilization summary

Figure 5.6 shows the Logic utilization summary of Cyclone II EP2C35F672C6 device. Among 33,216 logic rudiments, the proposed design has taken 6,470 logical elements (19%). We tend to examine pupil detection and hunt by picture process methods to create the eye-computer interaction scheme of a person. The illumination usually directly affects the image quality in the picture process methods.

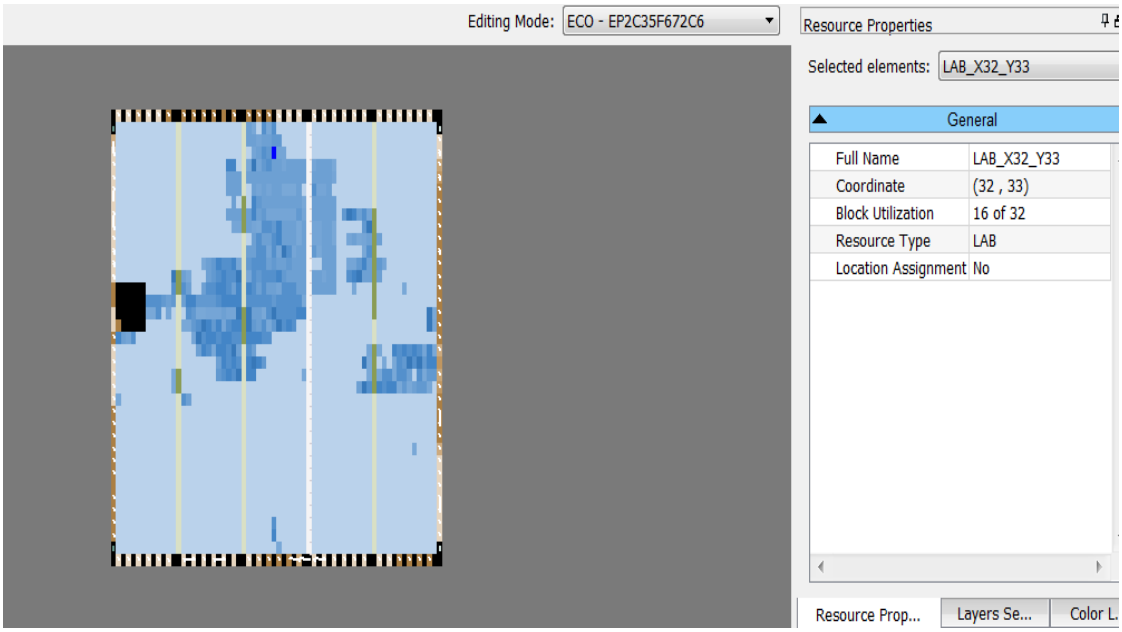

Figure 5.7 Chip planner summary

A noticeable demonstration of chip resources is provided by the Chip Planner. Together with the Resource Property Editor, you can use the Chip Planner to modify the connections between resources and make alterations to the properties of logic cells, I / O elements and PLLs after compilation.

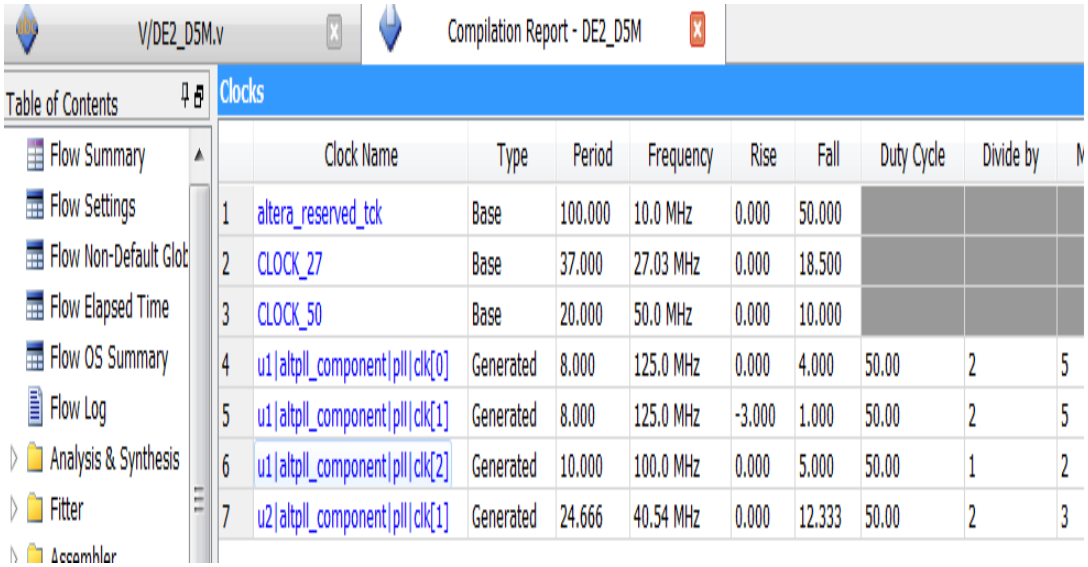

	Clock Name	Type	Period	Frequency	Rise	Fall	Duty Cycle	Divide by	M
1	altera_reserved_tck	Base	100.000	10.0 MHz	0.000	50.000			
2	CLOCK_27	Base	37.000	27.03 MHz	0.000	18.500			
3	CLOCK_50	Base	20.000	50.0 MHz	0.000	10.000			
4	u1|altpll_component|pll|clk[0]	Generated	8.000	125.0 MHz	0.000	4.000	50.00	2	5
5	u1|altpll_component|pll|clk[1]	Generated	8.000	125.0 MHz	-3.000	1.000	50.00	2	5
6	u1|altpll_component|pll|clk[2]	Generated	10.000	100.0 MHz	0.000	5.000	50.00	1	2
7	u2|altpll_component|pll|clk[1]	Generated	24.666	40.54 MHz	0.000	12.333	50.00	2	3

Figure 5.8 Clock summary

Figure 5.7 and 5.8 shows the Chip planner summary and clock summary of Cyclone II device. The clock outline report is AN audit path of all individual entries created victimization the clock. You can report on any date vary and build corrections to existing entries.

CHAPTER 6

CONCLUSIONS

Eye detection is the beginning of the iris recognition system which is very effectively to be applied in medical equipment's like Non-contact tonometer, Fundus Camera, Optical coherence Tomography etc. The proposed threshold-based pupil detection technique detects eyes with distinct dimensions without so much computational job and without using databases of separate dimensions for each picture. Eye tracking and eye movement analysis may be particularly interesting for apps based on user-computer dialog as they represent steps that can provide useful data on human visual and attention dimensions. In this work, here proposed dedicated hardware architecture for eye detection. To detect eyes of distinct dimensions without so much computational job and without using databases of distinct dimensions for each picture, a pupil detection technique based on a limit is feasible. Pupil detection is experimentally tested with 100 human eyes which gives 95% result successfully. Hardware reduction is also improved than existing method.

Limitations and Future Work

The advanced system is semi automatic. Before the detection phase, the user has to make several adjustments. Before detection of the eye, the eye database must be constructed. The user must identify the region eye detection threshold concentrations. These steps make user dependent on our proposal. By performing automatic pupil detection, future work can be a less user-dependent scheme. Instead of the thresholding , adaptive thresholding can use and circular Hough transform may also be implement to detect pupil region in future.

REFERENCES

1. Alex Stark, “Adaptive Image Contrast Enhancement Using Generalizations of Histogram Equalization”, IEEE Transactions on Image Processing, Vol. 9, No. 5, May 2000.

2. Amer Al-RahayfehAndMiadFaezipour, D, 2013. Eye Tracking and Head Movement Detection:A State-of-Art Survey. IEEE Transitional Engineering and Health Medicine, pp. 1536-1284, 2013.

3. Bahrami K, A. Kot, L. Li, and H. Li, “Blurred image splicing localization by exposing blur type inconsistency,” IEEE Trans. on Information Forensics and Security, vol. 10, no. 5, pp. 999–1009, 2015.

4. Basit A and M. Y. Javed, “Localization of iris in gray scale images using intensity gradient,” Opt. Lasers Eng., vol. 45, no. 12, pp. 1107–1114, Dec. 2007.

5. BonceletC. G, Jr., R. Hardie, R. Hakami, and G. R. Arce, • LUM filters for smoothing and sharpening,.in Nonlinear Image Processing II, E. R. Dougherty, G. R. Arce, and C. G. Boncelet, Jr., Editors, Proc. SPIE, vol. 1451, pp. 70-74, 1991.

6. Bowyer K. W, K. Hollingsworth, and P. J. Flynn, “Image understanding for iris biometrics: A survey,” Comput. Vis. Image Underst., vol. 110, no. 2, pp. 281–307, May 2008.

7. Bowyer K.W, K. Hollingsworth, P.J. Flynn, Image understanding for iris biometrics: a survey, Computer Vision Image Understanding. 110 (2) 281–307, (May 2008).

8. Braunagel C, E. Kasneci, W. Stolzmann, and W. Rosenstiel. 2015. Driver-Activity Recognition in the Context of Conditionally Autonomous Driving. In 2015 IEEE 18th International Conference on Intelligent Transportation Systems. 1652–1657, 2015.

9. Cabello, Frank, Julio León, YuzoIano, and Rangel Arthur. "Implementation of a fixed-point 2D Gaussian Filter for Image Processing based on FPGA." In Signal Processing: Algorithms, Architectures, Arrangements, and Applications (SPA), 2015, pp. 28-33. IEEE, 2015.

10. Canny J, "A computational approach to edge detection," IEEE Trans. Pattern Anal. and Mach. Intell., vol. 8, pp. 679-714, Nov. 1986.

11. ChenC., J. Ni, and J. Huang, "Blind detection of median filtering in digital images: A difference domain based approach," IEEE Trans. On Image Processing, vol. 22, no. 12, pp. 4699–4710, 2013.

12. Chen Y W and K. Kubo, ``A robust eye detection and tracking technique using gabor _lters," in Proc. 3rd Int. Conf. IEEE Intell. Inf. Hiding Multi-media Signal Process., vol. 1, pp. 109_112, Nov. 2007.

13. Choi I, and D. Kim, Eye Correction Using Correlation Information, Lecture Notes in Computer Science, Vol.4843, pp.698-707, 2007.

14. Chudasama D, T. Patel, S. Joshi, G. Prajapati "Survey on Various Edge Detection Techniques on Noisy Images" , IJERT International Journal of Engineering Research & Technology ISSN: 2278-0181 Vol. 3 Issue 10, October- 2014

15. DanWitzner, Hansen and Qiang Ji. In the eye of the beholder: A survey of models for eyes and gaze. IEEE Transactions on Pattern Analysis and Machine Intelligence, 32(3):478–500, March 2010

16. Daugman. How iris recognition works. In Proceedings of the International Conference on Image Processing, volume 1, pages 33–36, Rochester, NY, USA, December 2002.

17. Davies E. R, "Computer and machine vision: Theory, algorithms, practicalities," Academic Press, 2012.

18. De Oliveira, J., Soares, L., Costa, E., &Bampi, S. (2016, February). Exploiting approximate adder circuits for power-efficient Gaussian and Gradient filters for Canny edge detector algorithm. In Circuits & Systems (LASCAS), IEEE 7th Latin American Symposium on, pp. 379-382, 2016.

19. Dongheng Li, David Winfield , Starburst: A hybrid algorithm for video-based eye tracking combining feature-based and model-based approaches in Proceedings of the 2005 IEEE Computer Society Conference on Computer Vision and Pattern Recognition (CVPR'05)2005

20. Dongkyun Kim, Junhee Jung, An FPGA-based Parallel Hardware Architecture for Real-time Eye Detection in JOURNAL OF Semiconductor Technology And Science, Vol.12, No.2, June, 2012

21. Duchowski. A breadth-first survey of eye-tracking applications. Behavior Research Methods Instruments and Computers, 34(4):455 -470, 2002

22. Elhossini A, M. Moussa, A memory efficient FPGA implementation of Hough transform for line and circle detection, in: Proc. of the 25th Canadian Conference on Electrical and Computer Engineering, Montreal, QC, Canada, 29 April–2 May, 2012.

23. Er. Komal Sharma, Er. Navneet Kaur, "Comparative Analysis of Various Edge Detection Techniques", International Journal of Advanced Research in Computer Science and Software Engineering, Volume 3, Issue 12, December 2013.

24. Fahmy S. A, P. Y. K. Cheung and W. Luk, "Novel FPGA-based implementation of median and weighted median filters for image processing", in Proc. 2005 International Conference on Field Programmable Logic and Applications FPL, pp. 142-147, 2005.

25. Fahnestock J. D.and R. A. Schowengerdt, "Spatially variant contrast enhancement using local range modification," Opt. Eng., vol. 22, no. 3, pp. 378–381, 1983.

26. Flores, M. J., Armingol, M. J., &Esscalera, A. D. (2011). Driver Drowsiness Detection System under Infrared Illumination for the Intelligent vehicle. IET Intelligent Transport Systems, 5(4), 241-251, 2011.

27. Fu B and R. Yang, ``Display control based on eye gaze estimation," in Proc. 4th Int. CISP, vol. 1, pp. 399_403, 2011.

28. Faundez-Zanuy, “Biometric security technology,” IEEE Aerosp. Electron. Syst. Mag., vol. 21, no. 6, pp. 15–26, Jun. 2006.

29. Garg, Bharat, and G. K. Sharma "A quality-aware Energy-scalable Gaussian Smoothing Filter for image processing applications" Microprocessors and Microsystems (2016).

30. GipsJ., P. DiMattia, F. X. Curran, and P. Olivieri, ``Using EagleEyes_An electrodes based device for controlling the computer with your eyes to help people with special needs," in Proc. Interdisciplinary Aspects Comput. Help. People Special Needs, pp. 77_84, , 1996.

31. Gonzalez R. C and R. E. Woods, Digital Image Processing. New York: Addison-Wesley, 1992.

32. K. Grabowski and A. Napieralski, “Hardware architecture optimized for iris recognition,” IEEE Trans. Circuits Syst. Video Technol., vol. 21, no. 9, pp. 1293–1303, 2011.

33. HanumantharajuM. C, M. Ravishankar, D. R Rameshbabu, Design and FPGA Implementation of an 2D Gaussian Surround Function withReduced On-Chip Memory Utilization, IEEE International Conferenceon Advances in Computing, Communications and Informatics (ICACCI),Mysore, pp. 604 - 609, August 2013.

34. Hansen and Q. Ji, ``In the eye of the beholder: A survey of models for eyes and gaze," IEEE Trans. Pattern Anal. Mach. Intell., vol. 32, no. 3, pp. 478_500, Mar. 2010.

35. Harsh Prateek Singh, A. 2014. Noise Reduction in Images using Enhanced Average Filter.International Journal of Computer Applications, pp. 16 – 19, 2014.

36. Hasan and M. A. Amin, “Dual iris matching for biometric identification,” Signal, Image and Video Processing, vol. 8, no. 8, pp. 1605–1611, 2014.

37. Hotrakool W, P. Siritanawan, and T. Kondo, ``A real-time eye-tracking method using time-varying gradient orientation patterns," in Proc. Int. Conf. Electr. Eng., Electron. Comput. Telecommun. Inf. Technol., 2010, pp. 492_496.

38. Ibrahim M. T, T. M. Khan, S. A. Khan, M. A. Khan, and L. Guan, “Iris localization using local histogram and other image statistics,” Opt. Lasers Eng., vol. 50, no. 5, pp. 645–654, 2012.

39. Ivanov and T. Blanche, “Improving gaze accuracy and predicting fixation in real time with video based eye trackers,” Journal of Vision, vol. 11, no. 11, p. 505.

40. JacobR. Eye tracking in advanced interface design in virtual environments and advanced interface design. Oxford University Press, 1995.

41. Jan F, I. Usman, S. A. Khan, and S. A. Malik, “A dynamic non-circular iris localization technique for non-ideal data,” Computers and Electrical Engineering, vol. 40, no. 8, pp. 215–226, 2014.

42. Jain and A. Kumar, “Biometric recognition: An overview,” Second Gener. Biometrics Ethical, Leg. Soc. Context, pp. 49–79, 2012.

43. Jaspreet Kaur,Salt& Pepper Noise Removal using Fuzzy Based Adaptive Filter;International Journal of Science, Engineering and Technology Research (IJSETR) Volume 1, Issue 1, July 2012 .

44. Jun B, and D. Kim, Robust Real-Time FaceDetection Using Face Certainty Map, LectureNotes in Computer Science, Vol.4642, pp.29-38, 2007.

45. Karaman M, L. Onural and A. Atalar, “Design and implementation of a general-purpose median filter unit in CMOS VLSI,” IEEE Journal of Solid-State Circuits, Vol. 25, No. 2, pp. 505–13., , 1990.

46. S. Khalighi, F. Pak, P. Tirdad, and U. Nunes, “Iris recognition using robust localization and nonsubsampledcontourlet based features,” J. Sign. Process. Syst., vol. 81, no. 1, pp. 111-128, 2015.

47. Kass, A. Witkin, and D. Terzopoulos. “Snakes: Active contour models”, Int. Journal of Computer Vision, vol. 1, no. 4, pp. 321-331, 1987.

48. KatarzynaHarezlak, A, Pawel Kasprowski. 2014. Towards Accurate Eye Tracker and Calibration – Methods and Procedures.International

conference on Knowledge Based and Intelligent Information and Engineering Systems, pp. 1073 – 1081, 2014.

49. Kenneth Holmqvist, Marcus Nystrom, Richard Andersson, Richard Dewhurst, JarodzkaHalszka, and Joost van de Weijer. Eye tracking:A comprehensive guide to methods and measures. Oxford UniversityPress, 2011

50. Khairosfaizal W and A. Nor'aini, ``Eye detection in facial images using circular Hough transform," in Proc. 5th CSPA, pp. 238_242, Mar. 2009.

51. Kocejko T, A. Bujnowski, and J. Wtorek, ``Eye mouse for disabled," in Proc. IEEE Conf. Human Syst. Interact., May 2008, pp. 199_202

52. Kohei Arai and Makoto Yamaura, "Computer Input with Human Eyes-Only Using Two Purkinje Images Which Works in a Real-Time Basis without Calibration", International Journal of Human Computer Interaction (IJHCI), Volume(1): Issue (3), Japan.

53. Kothari, R. and Mitchell, J. Detection of eye locations in unconstrained visual images. In Proceedings of the IEEE ICIP, volume 3, pages 519–522. IEEE, (1996).

54. Kun Peng, Liming Chen, Su Ruan, Georgy Kukharev, "A Robust Algorithm for Eye Detection on Gray Intensity Face without Spectacles", JCS&T Vol. 5 No. 3, France, October 2005

55. Kuo, J. Lee, and S. Kao, ``Eye tracking in visible environment," in Proc. 5th Int. Conf. IIH-MSP, pp. 114_117, 2009.

56. Laine A, J. Fan, and W. Yang, "Wavelets for contrast enhancement of digital mammography," IEEE Eng. Med. Biol. Mag., vol. 14, no. 6, pp. 536–550, 1995.

57. Leng Donga, Yan Chena, Alastair Galea, Peter Phillipsb. 2016. Eye Tracking Method Compatible with Dual-Screen Mammography Workstation. International Conference on Medical Imaging Understanding and Analysis, pp. 206-211, 2016.

58. Li, D. Winfield, and D. J. Parkhurst. 2005. Starburst: A hybrid algorithm for video-based eye tracking combining feature-based and model-based approaches. In Computer Vision and Pattern Recognition-Workshops, 2005. CVPR Workshops. IEEE Computer Society Conference on. IEEE, 79–79, 2005.

59. Li, S. Wang, and X. Ding, “Eye/eyes tracking based on a unified deformable template and particle filtering,” Pattern Recognition Letters, vol. 31, pp. 1377–1387, 2010.

60. Lin K, J. Huang, J. Chen, and C. Zhou, Real-time Eye Detection in Video Streams, FourthInternational Conference on Natural Computation(ICNC'08), pp.193-197, Oct., 2008.

61. Liu H and Q. Liu, ``Robust real-time eye detection and tracking for rotated facial images under complex conditions," in Proc. 6th ICNC, vol. 4. 2010, vpp. 2028_2034, . 2010.

62. J. Liu-Jimenez, R. Sanchez-Reillo, and B. Fernandez-Saavedra, “Iris biometrics for embedded systems,” IEEE Trans. Very Large Scale Integr. Syst., vol. 19, no. 2, pp. 274–282, Feb. 2011.

63. LiX. andW. G.Wee, ``Anef_cient method for eye tracking and eye-gazed FOV estimation," in Proc. 16th IEEE Int. Conf. Image Process., Nov. 2009, pp. 2597_2600.

64. Loìpez, J. Daugman, and E. Cantoì, “Hardware–software co-design of an iris recognition algorithm,” IET Inf. Secur., vol. 5, no. 1, p. 60, 2011.

65. Maini, Raman, and Himanshu Aggarwal, "Study and comparison of various image edge detection techniques", International Journal of Image Processing (IJIP), Issue 3, no. 1, Pp. 1-11, 2009.

66. Marciniak, A. Dabrowski, A. Chmielewska, and A. A. Krzykowska, “Selection of parameters in iris recognition system,” Multimed. Tools Appl., vol. 68, no. 1, pp. 193–208, 2014.

67. Masek and P. Kovesi, “MATLAB source code for a biometric identification system based on iris patterns,” The School of Computer

Science and Software Engineering, the University of Western Australia, 2003.

68. Matey, Oleg Naroditsky, Keith Hanna, Ray Kolczynski, Dominick J. LoIacono, ShakuntalaMangru, Michael Tinker, Thomas M. Zappia, and Wenyi Y. Zhao, “Iris on the move: Acquisition of images for iris recognition in less constrained environments,” Proceedings of the IEEE, vol. 94, no. 11, pp. 1936–1947, 2006.

69. Mehrotra H, P.K. Sa, B. Majhi, Fast segmentation and adaptive SURF descriptor for iris recognition, Math. Comput. Model 58 (1–2) (2013) 132–146.

70. Mehrubeoglu M, L. M. Pham, H. T. Le, R. Muddu, and D. Ryu, ``Realtime eye tracking using a smart camera," in Proc.AIPR Workshop, 2011, pp. 1_7.

71. Md. Foisal Hossain, Mohammad Reza Alsharif, “Image Enhancement Based on Logarithmic TransformCoefficient and Adaptive Histogram Equalization”, 2007 International Conference on Convergence InformationTechnology, IEEE 2007

72. Muroò and J. Pospišil, “The human iris structure and its usages,” Physica, vol. 39, pp. 87–95, 2000.

73. NandhagopalN., S.Navaneethan“Implementation of the human eye pupil detection usingintensity values with edge detection” in Pramana Research Journal, Volume 9, Issue 1, 2019.ISSN NO: 2249-2976, Page No: 432 – 437.

74. Nascimento. J. C., Abrantes. A. J., Marques. J. S., “AN ALGORITHMFOR CENTROID -BASEDTRACKING OF MOVING OBJECT. ”, Lisboa,portugal, October 1994.

75. Netravali A. N and B. G. Haskeli, Digital Pictures: Representation and Compression. New York: Plenum, 1988.

76. ParkerJ.R. and A.Q. Duong. Gaze tracking: A sclera recognition approach. In Proceedings of the IEEE International Conference onSystems, Man and Cybernetics, pages 3836–3841, San Antonio, TX,USA, October 2009

77. Pedersen S.J.K, “Circular Hough transform”, Aalborg University, Vision, Graphics and Interactive Systems, 2007.

78. Pizer S. M, E. P. Amburn, J. D. Austin, R. Cromartie, A. Geselowitz, T. Greer, B. H. Romeny, J. B. Zimmerman, and K. Zuiderveld, “Adaptive histogram equalization and its variations,” Comput. Vision, Graphics, Image Processing, vol. 39, pp. 355–368, 1987

79. Pizer S. M, J. B. Zimmerman, and E. V. Staab, “Adaptive grey level assignment in CT scan display,” J. Comput. Assist. Tomogr., vol. 8, no. 2, pp. 300–305, 1984

80. H. Proença, “Iris recognition: On the segmentation of degraded images acquired in the visible wavelength,” IEEE Trans. Pattern Anal. Mach. Intell., vol. 32, no. 8, pp. 1502–1516, 2010.

81. Pranith A and C. R. Srikanth, ``Iris recognition using corner detection," in Proc. 2nd ICISE, 2010, pp. 2151_2154.

82. Qian W, L. P. Clarke, B. Zheng, M. Kallergi, and R. Clark, “Computer assisted diagnosis for digital mammography,” IEEE Eng. Med. Biol. Mag., vol. 14, no. 6, pp. 561–568, 1995

83. Qiong Wang, Jingyu Yang, “Eye Detection in Facial Images with Unconstrained Background”, Journal of Pattern Recognition Research 1 (2006) 55-62, China, September 2006.

84. Radman, K. Jumari, and N. Zainal, “Iris segmentation in visible wavelength environment,” Procedia Engineering 41 pp. 743-748, 2012.

85. Rakvic, B. J. Ulis, R. P. Broussard, R. W. Ives, and N. Steiner, “Parallelizing iris recognition,” IEEE Trans. Inf. Forensics Secur., vol. 4, no. 4, pp. 812–823, 2009.

86. Raudonis, R. Simutis, and G. Narvydas, ``Discrete eye tracking for medical applications," in Proc. 2nd ISABEL, 2009, pp. 1_6.

87. Ross, “Iris recognition: The path forward,” Computer (Long. Beach. Calif.), vol. 43, no. 2, pp. 30–35, 2010.

88. Russo F and G. Ramponi, “A fuzzy operator for the enhancement of blurred and noisy images,” IEEE Trans. Image Processing, vol. 4, pp. 1169–1174, Aug. 1995.

89. Richards D, “VLSI median filters”, IEEE Transaction on Acoustics, Speech and Signal Processing, Vol. 38, No. 1, pp. 145-153, , 1990.

90. RoigaA. B, M. Moralesb, J. Espinosaa, J. Pereza, D. Masa, and C. Illueca, “Pupil detection and tracking for analysis of fixational eye micromovements,” Optik, vol. 123, pp. 11–15, 2012.

91. Roy K, P. Bhattacharya, and C. Y. Suen, “Iris segmentation using variational level set method,” Opt. Lasers Eng., vol. 49, no. 4, pp. 578–588, Apr. 2011.

92. Ryo Takahashi , Hiromasa Suzuki, JouhYeong Chew, S. 2018. A system for three-dimensional gaze fixation analysis using eye tracking glasses. Journal of Computational Design and Engineering, pp. 27 - 42.

93. RyuZ. M., The Effect of Nonlinear Filtering on the Resolution of Calibrated Thermal Images. Ph.D. Dissertation, University of Texas at Austin, 1986

94. Rziza ,Alioua, A. Amine, , and D. Aboutajdine, ``Eye state analysis using iris detection based on circular houghtransform," in Proc. ICMCS, Apr. 2011, pp. 1_5.

95. S. Khorbotly, F. Hassan, A modified approximation of 2D Gaussian smoothing filters for fixed-point platforms, in: IEEE 43rd Southeastern Symposium on Sys- tem Theory (SSST), March 2011, pp. 151–159

96. Sankowski, K. Grabowski, M. Napieralska, M. Zubert, and A. Napieralski, “Reliable algorithm for iris segmentation in eye image,” Image Vis. Comput., vol. 28, no. 2, pp. 231–237, Feb. 2010.

97. Scott J, M. Pusateri, and M. U. Mushtaq, “Comparison of 2D median filter hardware implementations for real-time stereo video,” 2008 37th IEEE Appl. Imag. Pattern Recognit. Work., pp. 176–181, 2008.

98. Serra J, Image Analysis and Mathematical Morphology. New year Acadamic Press,1982.

99. Sherrir R. H and G. A. Johnson, “Regionally adaptive histogram equalization of the chest,” IEEE Trans. Med. Imag., vol. MI-6, pp. 1–7, Jan. 1987.

100. Sigut, J., &Sidha, S. A. (2011).Iris Center Corneal Re-flection Method for Gaze Tracking Using Visible Light. IEEE Transactions on Biomedical Engineering, 58(2), 411-419.

101. Su YeongGwon, Chul Woo Cho, Hyeon Chang Lee, Won Oh Lee ,and Kang Ryoung Park, “ Robust eye and pupil detection method for gaze tracking,” IntJAdv Robotic Sy. Vol.98, No.10, pp.1-7, 2013.

102. SundaramR , B. C. Dhara, and B. Chanda, ``A fast method for iris Localization," in Proc. 2nd Int. Conf. EAIT, 2011, pp. 89_92.

103. Swirski, L., Bulling, A., & Dodgson, N. (2012).Robust real-time pupil tracking in highly off-axis images. In: Proceedings of the Symposium on Eye Tracking Re-search and Applications (pp. 173-176). New York, NY, USA.

104. T. Ohno, ``One-point calibration gaze tracking method," in Proc. Symp. Eye Track. Res. Appl., 2006, p. 34.

105. Tang and J. Zhang, ``Eye tracking based on grey prediction," in Proc. 1st Int. Workshop Educ. Technol. Comput. Sci., 2009, pp. 861_864.

106. Timm and Bath. An eye tracking computer user interface. In IEEE Proceedings of Research Frontier in Virtual Reality Workshop, 2002.

107. T¨urkan, M., Pard`as, M., and C¸etin, A. E. (2007). Human eye localization using edge projections. In Proceedings of the 2nd VISAPP, pages 410–415. INSTICC

108. Vasanth, S. Karthik, S. Nirmal Raj, and P. PreethaMol, "FPGA implementation of optimized sorting network algorithm for median filters," in International Conference on "Emerging Trends in Robotics and Communication Technologies", INTERACT, pp. 224–229, 2010.

109. Villanueva A, V. Ponz, L. Sesma-Sanchez, M. Ariz, S. Porta, and R. Cabeza. 2013. Hybrid method based on topography for robust detection of iris center and eye corners. ACM Transactions on Multimedia Computing, Communications, and Applications (TOMM) 9, 4 (2013), 25.

110. Viola and M. Jones. 2001. Rapid object detection using a boosted cascade of simple features. In Computer Vision and Pattern Recognition, 2001. CVPR 2001. Proceedings of the 2001 IEEE Computer Society Conference on, Vol. 1. IEEE, I–511.

111. Wang Yuanji. Li Jianhua, Lu E, Fu Yao, Jiang Qinzhong, "Image Quality Evaluation Based On Image Weighted Separating Block Peak Signal To Noise Ratio", IEEE International Conference Neural Networks & Signal Processing, Nanjing, China, December 14-17, 2003.

112. Wang N, Q. Li, A.A.A. El-Latif, T. Zhang, X. Niu, Toward accurate localization and high recognition performance for noisy iris images, Multimedia Tools Appl. 71 (3) (2014) 1411–1430.

113. Wildes, R.P., Asmuth, J.C., Green, G.L., Hsu, S.C., Kolczynski, R.J., Matey, J., McBride, S.E.: A system for automated iris recognition. In: Applications of Computer Vision, 1994., Proceedings of the Second IEEE Workshop on, IEEE (1994) 121–128

114. Wyatt, "The human pupil and the use of video-based eyetrackers," Vision Research, vol. 50, pp. 1982–1988, 2010.

115. Wildes, "Iris recognition: an emerging biometric technology," Proc. IEEE, vol. 85, no. 9, pp. 1348–1363, 1997.

116. Yang, J. Sun, J. Liu, X. Yang, D. Wang, and W. Liu, ``A gray difference-based pre-processing for gaze tracking," in Proc. IEEE 10th ICSP, Oct. 2010, pp. 1293_1296.

117. Yang, J. Sun, J. Liu, J. Chu,W. Liu, andY. Gao, ``Agaze tracking scheme for eye-based intelligent control," in Proc. 8thWCICA, 2010, pp. 50_55.

118. Yoo D H, J. H. Kim, B. R. Lee, and M. J. Chung, ``Non-contact eye gaze tracking system by mapping of corneal reflections," in Proc. 5th IEEE Int. Conf. Autom. Face Gesture Recognit., May 2002, pp. 94_99.

119. Yoo and M. J. Chung, ``A novel nonintrusive eye gaze estimation using cross-ratio under large head motion," Special Issue on Eye Detection and Tracking, Computer Vision and Image Understanding, vol. 98, no. 1, pp. 25_51, 2005.

120. Yuan H.-D, "Blind forensics of median filtering in digital images," IEEE Trans. on Information Forensics and Security, vol. 6, no. 4, pp. 1335–1345, 2011.

121. Yuan Z and J. Kebin, ``A local and scale integrated feature descriptor in eye-gaze tracking," in Proc. 4th Int. CISP, vol. 1. 2011, pp. 465_468.

122. Young Land D. Sheena. Survey of eye movement recording methods. Behavior Research-Methods and Instrumentation, 7:397-429, 1975.

123. Zhaofeng He, Tieniu Tan, Zhenan Sun and XianchaoQiu "Boosting Ordinal Features for Accurate and Fast Iris Recognition". Proc. of the 26th IEEE Computer Society Conference on Computer Vision and Pattern Recognition (CVPR'08). pp. 1–8, (June 2008).

124. Zhou X, N. Tomagou, Y. Ito, and K. Nakano, "Efficient Hough transform on the FPGA using DSP slices and block RAMs", in Proc. of IEEE 27th International Symposium on Parallel & Distributed Processing Workshops and PhD Forum, Cambridge, MA, pp. 771 - 778, May 2013.

125. Zhu Z, Q. Ji, Robust real-time eye detection andtracking under variable lighting conditions andvarious face orientations, Computer Vision andImage Understanding, Vol.98, No.1, pp.124-154, Apr., 2005.

126. Zhu and Q. Ji, ``Novel eye gaze tracking techniques under natural head movement," IEEE Trans. Biomed. Eng., vol. 54, no. 12, pp. 2246_2260, Dec. 2007